THE ROLE OF RECEPTOR FOR ADVANCED GLYCATION END PRODUCTS (RAGE)– AMYLOID BETA AXIS IN RETINAL GANGLION CELL DEATH IN GLAUCOMA

Nafiseh A. S. Hosseini Fin

BSc., MSc. Biotechnology

A Thesis Submitted in Fulfilment of the Requirement for

the Degree of Master of Philosophy

University of Technology Sydney

August 2018

Declaration

I declare that:

This thesis presents work carried out by me and does not incorporate without acknowledgment any material previously submitted for a degree or diploma in any university.

To the best of my knowledge it does not contain any materials previously published or written by another person except where due reference is made in the text; and all substantive contributions by others to the work presented, including jointly authored publications, is clearly acknowledged.

Nafiseh A. S. Hosseini Fin

August 2018

Dedication

To My Beloveds

Acknowledgement

Completion of this thesis is not only because of my hard work, but also because of the support and assistance of many special people. One of the most important of these people is my principal supervisor, Dr. Mojtaba Golzan. Over the last two years, Dr. Golzan has spent countless hours discussing research, training me, troubleshooting scientific challenges, and proofreading this thesis.

I am also very grateful to my co-supervisors, Prof. Kathryn Rose and Dr. Maria Sukkar. They have been spent much time attending meetings with me and advising me. Although occupied with many commitments, Prof. Rose has been so kind and supportive to me. Her helpful advice encouraged me to confront problems and go through them.

In addition, many thanks to University of Technology Sydney for providing me with the full scholarship to complete my degree.

I would like to thank Ms. Dana Georgevsky from vision sciences research group, for her contribution to animal work particularly my second experiment. Dr. Hussein Mansour who worked in our group also assisted with preparation and optimization of used protocols, particularly molecular techniques. This thesis was copyedited by Dr. Laurel Mackinnon, PhD, ELS.

Finally, I dedicate my deepest gratitude to my lovely husband, parents and brother. Without their continued love and constant encouragement, I could not have reached this point in life.

Overview of Thesis

The current work is structured as a "thesis by compilation" and is presented in the following format. Chapter 1 provides a comprehensive review of the literature. This chapter discusses the role of RAGE and its ligand amyloid beta in Alzheimer's disease, the known epidemiological and pathological similarities between Alzheimer's disease and glaucoma, and the current evidence of the involvement of RAGE in retinal pathology and its potential role in glaucoma. A summarised version of this chapter will be submitted as an invited review paper to the Journal of Experimental Eye Research with the title 'Receptor for advanced glycation end product mediates retinal ganglion cell loss in glaucoma'.

Chapter 2 describes how $RAGE^{-/-}$ mice are protected against retinal ganglion cell loss and retinal dysfunction in experimental glaucoma. Chapter 3 reports how $RAGE^{-/-}$ mice are protected against retinal ganglion cell loss after exogenous amyloid beta oligomers injection into the vitreous. Finally, Chapter 4 summarises the findings and discusses how RAGE and its ligand amyloid beta may mediate retinal ganglion cell loss in glaucoma. This thesis also includes two separate supplementary sections of figures and details of the protocols used in the thesis, which have been added to the Appendix.

List of Publications

1. Hosseini N, Sukkar M, Golzan SM, "Receptor for advanced glycation end product (RAGE) mediates retinal ganglion cell loss in experimental glaucoma", Investigative Ophthalmology and Visual Science, 59(9), 3726; 2018 (Conference abstract).

Contribution of authors

1. Nafiseh A.S. Hosseini Fin
Ethics application preparation, experimental setup and implementation, data acquisition and analysis

2. Maria Sukkar
Experiment Design, data analysis, manuscript preparation

3. Mojtaba Golzan
Overview of ethics approval, experiment Design, data acquisition and analysis, manuscript preparation

Table of Contents

List of figures

List of tables

List of abbreviations

AD	Alzheimer's Disease
AGE	Advanced Glycation End products
AMD	Age-related Macular Degeneration
AOH	Acute Ocular Hypertension
APP	Amyloid Precursor Protein
Aβ	Amyloid Beta
BBB	Blood-Brain Barrier
BRB	Blood-Retinal Barrier
CAMs	Cell Adhesion Molecules
CNS	Central Nervous System
DMSO	Dimethylsulfoxide
DR	Diabetic Retinopathy
ECM	Extracellular Matrix
ERG	Electroretinogram
GAPDH	Glyceraldehyde 3-Phosphate Dehydrogenase
GCL	Ganglion Cell layer
HFIP	1,1,1,3,3,3-Hexafluoro-2-Propanol
HMGB1	High Mobility Group Box 1
IOP	Intra Ocular Pressure
IPL	Inner Plexiform Layer
LBP	Lycium Barbarum Polysaccharides
LGN	Lateral Geniculate Nucleus
MAPK	Mitogen Activated Protein Kinase
MHC	Major Histocompatibility Complex
MMP	Matrix Metalloprotease
NADPH	Nicotinamide Adenine Dinucleotide Phosphate-oxidase
NF-κB	Nuclear Factor-kappaB
NFL	Nerve Fiber Layer
OCT	Optical Coherence Tomography
OHT	Ocular Hypertension
ONH	Optic Nerve Head
pSTR	Positive Scotopic Threshold Response
RAGE	Receptor for Advanced Glycation End products
RGC	Retinal Ganglion Cell
ROS	Reactive Oxygen Species
RPE	Retinal Pigment Epithelium
SAPK	Stress Activated Protein Kinase
SDS-PAGE	Sodium Dodecyl Sulfate Polyacrylamide
TGF	Transforming Growth Factor
TNF	Tumor Necrosis Factor
TRT	Total Retinal Thickness
WT	Wild Type

ABSTRACT

Glaucoma encompasses a heterogeneous group of neurodegenerative processes associated with progressive damage to the resident neurons within the retina known as retinal ganglion cells (RGCs). The early stages of glaucoma are not associated with any symptoms, pain or change in sight. As a result, up to 40% of RGC loss occurs before a clinical diagnosis is made. Current treatments are effective at reducing intraocular pressure (IOP), the major risk factor for the disease, but a significant proportion of patients still experience vision loss despite treatment. Identifying new treatments that prevent RGC death caused by glaucomatous pathology is a major unmet need.

The receptor for advanced glycation end products (RAGE) is implicated in the pathogenesis of many chronic diseases, particularly neurodegenerative diseases such as Alzheimer's disease (AD) in which RAGE and its ligand, amyloid beta (Aβ), have been shown to mediate neuronal loss. Interestingly, higher RAGE expression and Aβ deposits have also been identified in the RGC layer in glaucoma. Given the current evidence for the involvement of similar underlying pathophysiological mechanisms in AD and glaucoma and that both RAGE and Aβ are linked to cell death pathways, I hypothesised that RAGE–Aβ signalling underlies RGC loss in glaucoma.

To address this hypothesis, RAGE knockout ($RAGE^{-/-}$) mice and wild-type (WT) control mice were exposed to acute IOP elevation. Further, the time-dependent effects of intravitreal injection of Aβ on RGC loss, retinal dysfunction and structural damage in $RAGE^{-/-}$ and WT mice were also investigated. In this study, $RAGE^{-/-}$ mice were protected against RGC loss in experimental glaucoma compared with WT mice. The potent effects of Aβ on RGC loss was significantly diminished in $RAGE^{-/-}$ mice compared with WT mice.

These findings suggest that RAGE–Aβ is involved in RGC loss in an acute model of glaucoma. Similar experiments in other animal models of glaucoma are needed to confirm whether inhibition of RAGE–Aβ binding helps to slow the development of glaucoma.

Introduction

Glaucoma is a neurodegenerative disease with no significant symptoms or signs indicative of disease activity. It is a leading cause of preventable blindness that currently affects 300,000 Australians. Studies suggest that over 50% of people with glaucoma are unaware [1] of their disease and more than 72% of new cases are detected incidentally during examination for another reason unrelated to glaucoma [2], [3]. Despite numerous pharmacological attempts to lower intraocular pressure (IOP), the single most significant risk factor for the disease, glaucoma can continue to progress and eventually lead to retinal ganglion cell (RGC) loss and subsequent vision loss.

During normal vision, light passes through the cornea and lens before reaching the retina, the light-sensitive layer of the eye. The retina is divided into two main structures: the *outer* and *inner* retina. The outer retina houses the photoreceptors, the cells that receive light and transmit it through electrical signals, which are then transmitted to RGCs located within the inner retina. RGCs are responsible for relaying visual signal from the inner retina to the brain. The cell body of RGCs is located within the inner layer of the retina, and their axons extend to the brain via the optic nerve.

In glaucoma, it is believed that elevated IOP induces haemodynamic stress at the optic nerve head, which leads to optical nerve axonal compression and subsequent RGC loss via apoptosis [4]. As a progressive neurodegenerative disease, glaucoma affects peripheral vision in its early stages and can cause central visual dysfunction later in the disease process (Figure 1).

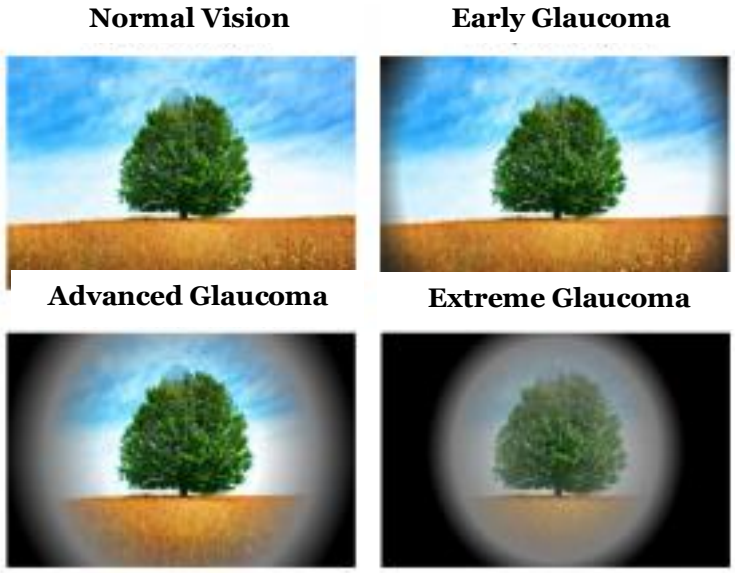

Figure 1. Alterations in normal vision with glaucoma [4]. The loss of sight in glaucoma is generally continuous and peripheral vision might be lost without any symptoms.

Statement of the problem

Elevated IOP is considered to be a prime factor for glaucomatous damage to the optic nerve head, which leads to RGC loss. Management of IOP, the sole modifiable risk factor, is at the centre of most pharmacological interventions targeted at halting disease progression. However, a significant proportion of patients experience some degree of vision loss despite the therapeutic management [5]. As a result, the focus of recent research has shifted from IOP management to devising strategies that delay or halt RGC loss as potentially the most beneficial approach to preserve vision in glaucoma.

A variety of molecular signalling pathways have been investigated to understand better the mechanisms that mediate RGC loss. The receptor for advanced glycation end products (RAGE) is a pattern recognition receptor that binds many molecules involved in tissue injury and is involved in various chronic diseases associated with aging. RAGE binds a number of ligands and is highly expressed in RGCs. Prominent among the various

ligands amyloid beta (Aβ), the central player in Alzheimer's disease (AD), has a potent neurotoxic effect on RGCs [6]–[8]. Although RAGE–Aβ-mediated neuronal cell death has been widely studied in AD, its potential role in RGC death in glaucoma has not been investigated.

Hypothesis

That in glaucoma, 1) RAGE takes part in RGC loss and 2) the RAGE–Aβ axis is involved in RGC loss.

Research aims

To address this hypothesis, IOP was increased in $RAGE^{-/-}$ and wild-type (WT) control mice to replicate a model of retinal ischaemia–reperfusion injury and experimental glaucoma. Following on from the results of the first experiment, in the second experiment, the RAGE ligand, Aβ, was intravitreally injected in to the vitreous of $RAGE^{-/-}$ and WT control mice. The specific aims of the project were as follows.

AIM 1: Determine whether RAGE mediates RGC loss and retinal dysfunction in a model of acute retinal ischaemia.

AIM 2: Determine whether RAGE–Aβ activation exacerbates RGC loss.

1. Chapter 1—Review of the literature

1.1. The eye and the retina

The eye, an organ of the visual system, comprises several biological structures including the retina, optic nerve, vitreous, sclera, lens, iris, pupil and cornea (Figure 2).

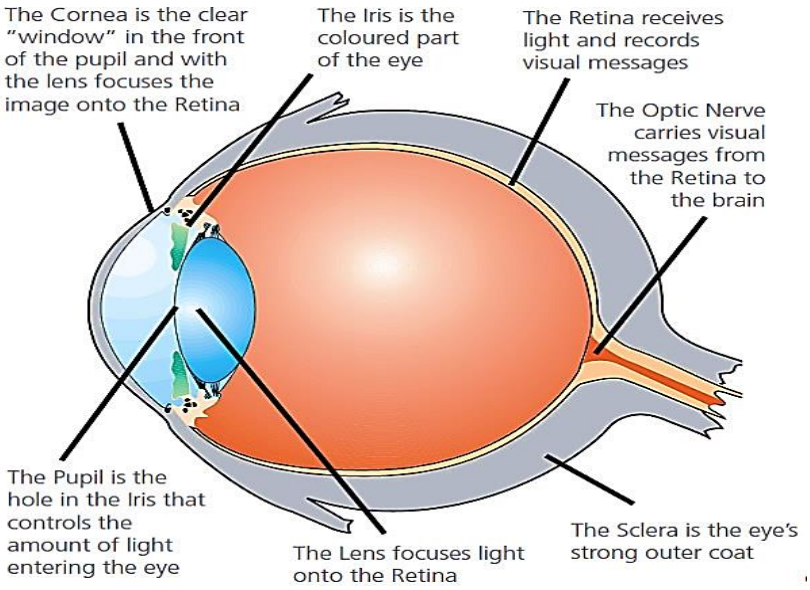

Figure 2. Eye components and their role in vision[1]

The retina is located at the posterior section of the eye. It comprises 10 different layers, of which the nerve fiber layer (NFL) is the innermost layer closest to the lens (Figure 3). Photoreceptors including the rods and cones are located in the outermost neighbouring epithelium pigment layer and choroid. The middle retinal layers house the neuron cell bodies and their synapses, and the outer nuclear layer contains the somata of photoreceptors. The inner nuclear layer (INL) houses the cell body of bipolar, amacrine

[1] https://www.glaucoma.org.au/about-glaucoma/what-is-glaucoma/

and horizontal cells, and the inner plexiform layer (IPL) contains the synapses of RGCs and bipolar cells [9].

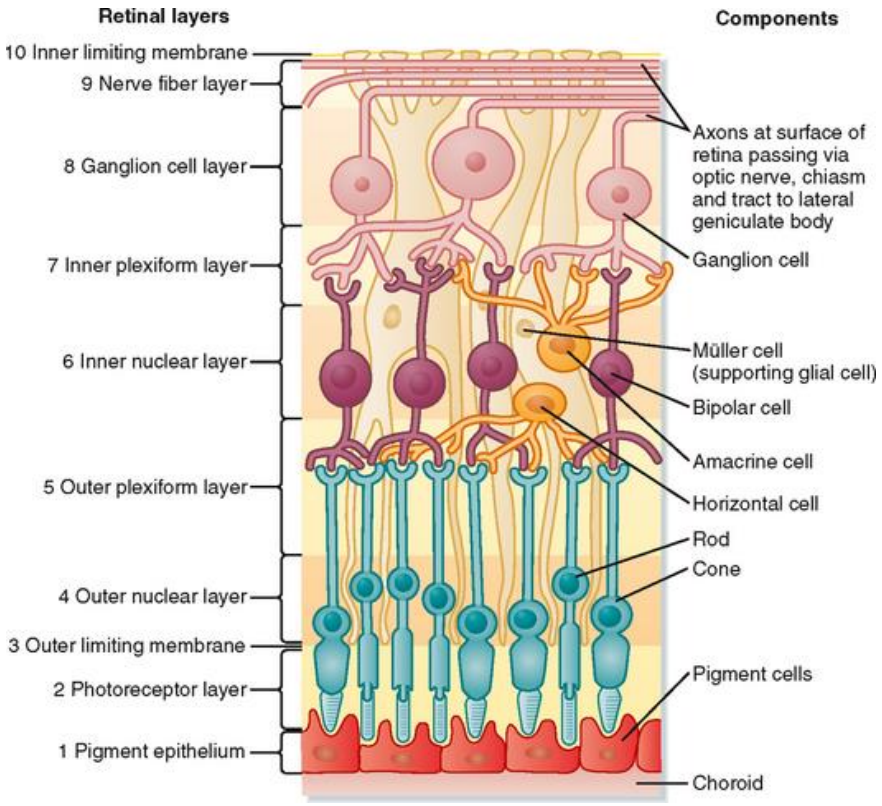

Figure 3. Retina layers and cells[2]

1.2. Glaucoma

Glaucoma remains one of the three major causes of blind registrations in Australia; an estimated 2.4% of the Australian population over the age of 50 will develop the disease[10]. It is a chronic progressive optic neuropathy involving characteristic loss of optic nerve fibres (disc cupping) and corresponding visual field defects. The pathogenic mechanisms remain controversial. IOP is clearly associated, but up to one-third of

[2] https://basicmedicalkey.com/the-special-senses-2/

glaucoma patients with normal tension glaucoma never manifest elevated IOP. Ocular hypertension (OHT) is a far more frequent finding in the community than glaucoma. In Japan the incidence of glaucoma increases with age, although, in contrast to Western countries, the mean IOP decreases with age [11]. Several studies have concluded that lowering IOP has a beneficial effect [12]–[16]. However, not all patients respond to pressure reduction, and some progress to a stage involving a significant amount of RGC degeneration, which predisposes to vision loss[17]. RGC degeneration can begin decades before clinical symptoms of the disease are apparent. This time-dependent process is the key to helping researchers to understand, and clinicians to prevent, RGC loss in the very early stages of glaucoma. Therefore, the focus of current research is to identify the molecular mechanism(s) involved in RGC loss in glaucoma.

1.2.1. Glaucoma risk factors

Glaucoma is a multifactorial disease, and several genetic and environmental factors are involved in both the early and progressive stages of the disease. Although increased IOP is the predominant risk factor for glaucoma, not all patients show increased IOP [18]. Moreover, a limited proportion of people with normal IOP develop glaucoma [19].

Other risk factors for glaucoma are as follows;

- advanced age (over 40 years for people of African ethnicity and over 60 years for the general population) [20]
- African or Asian ethnicity [20]
- family history of glaucoma [21]
- history of diabetes, high or low blood pressure, or migraine headache [21]

- history of systematic corticosteroid drug use [22], [23].

1.2.2. Glaucoma pathophysiology

Although the underlying cause of glaucoma is not understood completely, the rate of RGC loss is linked to IOP level. The drainage pathway of the eye's anterior chamber is responsible for regulating IOP by maintaining the balance between aqueous humour production and its drainage through the trabecular meshwork (Figure 4). In glaucoma, an increased resistance to aqueous outflow leads to increased IOP and subsequent mechanical strain and stress on the posterior structure of the eye, notably the optic nerve head and lamina cribrosa [24]. The chronic mechanical stress causes compression and deformation of the lamina cribrosa, the weakest structure exposed to the pressurised intraocular space. Deformation of the lamina cribrosa then leads to remodelling of its structure and disruption of axonal transport. This interrupts the retrograde delivery of tropical factors to RGCs from the relay neurons of the lateral geniculate nucleus (LGN) in the brain and ultimately results in loss of vision [25], [26].

1.2.3. Clinical presentation

Following RGC and optic nerve fibre loss in glaucoma, structural changes in the appearance of the optic nerve head become apparent. In the early stages, structural alterations caused by axon degeneration leads to excessive *optic disc cupping*, a characteristic shape of the optic disc and visual loss (Figure 4). While normal people have a small cup to disc ratio, this ratio tends to increase in glaucoma patients leading to a greater cup to disc ratio [27] This progressive structural damage leads to further fibre loss that can be picked up on an optical coherence tomography (OCT) scan. In the advanced stages of the disease, progressive RGC loss continues leading to accelerated deterioration

of visual fields, the total area in which objects can be seen in the side (peripheral) vision as one focuses on a central point.

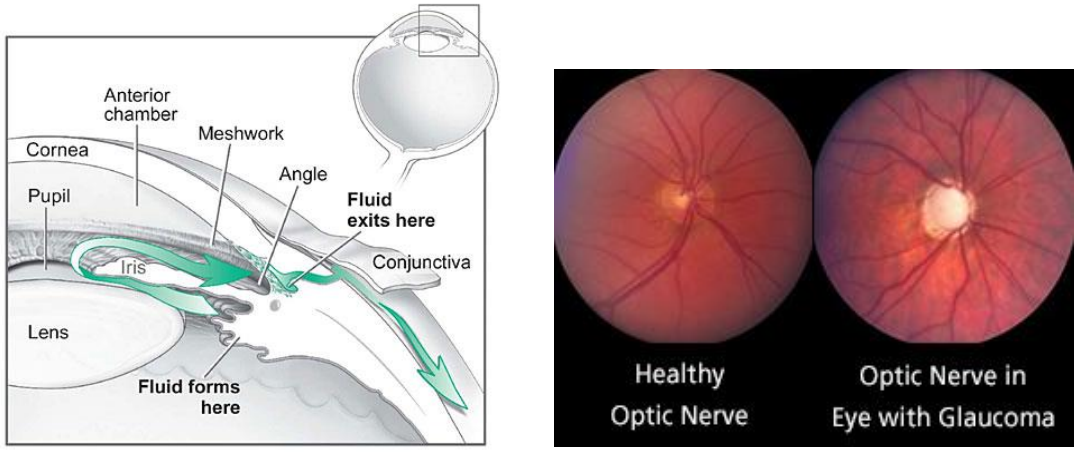

Figure 4. Left) The eye-drainage pathway that regulates IOP[3], Right) Increase in the cup-to-disc ratio in glaucoma patients[4]. The "cup" forms a small portion of the disc in the normal optic nerve, but this portion increases in the optic nerve of glaucoma patients.

1.2.4. Glaucoma as a neurodegenerative disorder

Given the many key similarities between glaucoma and the central nervous system (CNS) disorders, glaucoma is often considered a chronic retinal neurodegenerative disorder. First, despite its peripheral location, the retina is considered as a part of the CNS [28] because embryonic development of the retina derives from the out-pocketing of the diencephalon, a portion of the brain comprising the thalamus and hypothalamus. The brain and the eye are connected through adjacent vasculatures, the blood–brain barrier (BBB) and the blood–retina barrier (BRB) [29]–[31]. Second, neurodegeneration is typically a progressive process, which may have no prior symptoms, and is mainly accompanied by loss of specific neuronal cells and, in the case of glaucoma, RGC loss.

[3] https://nei.nih.gov/health/glaucoma/glaucoma_facts
[4] https://www.glaucoma.org/treatment/optic-nerve-cupping.php

Third, structural alterations in the LGN region of the brain of glaucoma patients have also been reported [32], [33]. This suggests a connection of neuronal cells between the retina and the brain, and provides further evidence that glaucoma is a neurodegenerative disease of the visual system.

1.3. Similarities between glaucoma and AD

Epidemiological studies suggest that glaucoma occurs in about 25% of people with AD [34], [35]. A recent longitudinal study reported that people with glaucoma were four times more likely to develop dementia (odds ratio=3.9; CI 1.5–10.4, $p<0.001$) after adjusting for age, sex, education, family history of glaucoma, vascular risk factors and apolipoprotein ε4, a major genetic determinant of AD risk [36]. This finding suggests that a common underlying mechanism contributes to the pathogenesis of both diseases. Among many possibilities, deposition of Aβ plaques appears to be the single major driving factor for both diseases. Accumulation of extracellular Aβ is a key hallmark of AD and, interestingly, Aβ is highly deposited in the retina, optic nerve and RGCs of people with acute ocular hypertension (AOH), glaucoma and AD [37]–[39]. Although the functions of Aβ are not fully understood, some researchers have suggested a physiological role in synaptic physiology and as an anti-microbial molecule [40]–[44]. Some studies have indicated that the Aβ isoform, $A\beta_{1-42}$, and to a lesser extent $A\beta_{1-40}$, are cytotoxic for CNS neurons and microvascular endothelial cells [45]–[47].

Aβ is formed by cleavage of the amyloid precursor protein (APP). A transmembrane protein is expressed throughout the brain and the eye, including in RGCs. APP plays a major role in the normal nervous system where it regulates synaptic plasticity [48]. APP

is processed through various enzymes through two distinct pathways: amyloidogenic and non-amyloidogenic. It is through the amyloidogenic pathway, through which APP is initially cleaved by the enzyme β-secretase and then by γ-secretase, yielding Aβ [49], [50] (Figure 5). Dysfunction in Aβ metabolism results in accumulation of $A\beta_{1-42}$, which aggregates to produce oligomers that are thought to trigger AD pathogenesis [51], [106]. The accumulation of Aβ plaques in the AD brain is also attributed to an imbalance in the in–out flux of Aβ. The influx of Aβ across the BBB is mediated through RAGE and the out flux is mediated through lipoprotein-related receptor 1 [52].

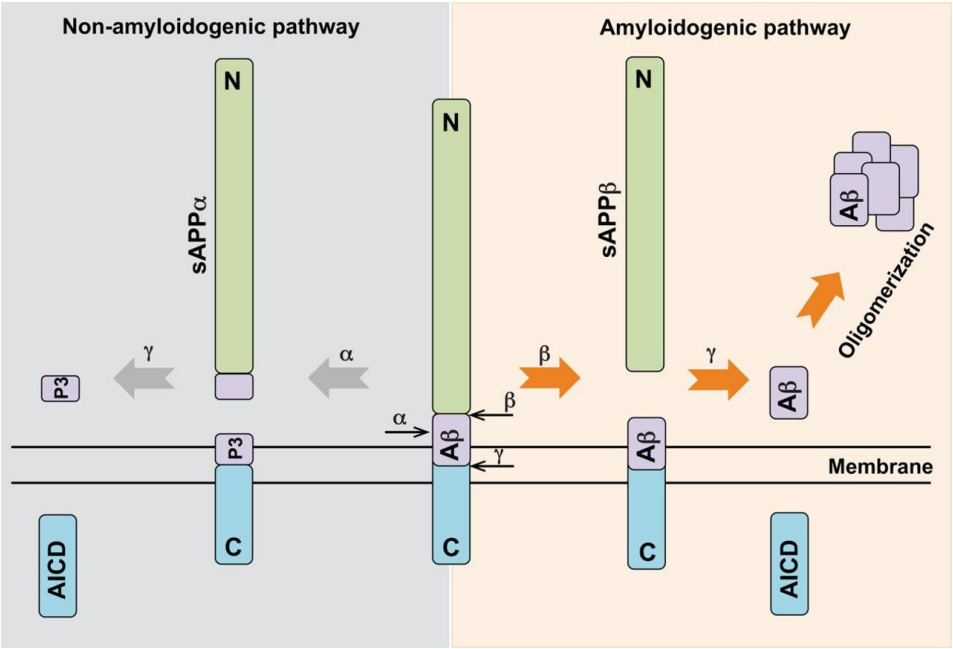

Figure 5. The proteolytic processing of APP [47]. APP is processed in two distinctive amyloidogenic and non-amyloidogenic pathways. Though, Aβ is generated in amyloidogenic pathway by successive action of β- and γ-secretase, its production is prevented in non-amyloidogenic pathway.

There is evidence that increased Aβ level induces neuronal apoptosis [53]. Co-localisation of caspase-3 and Aβ plaques has also been reported in the brain of AD patients

[53]. A similar concept has been reported in a rat glaucoma model [53]. Increased retinal levels of APP fragments, Aβ and caspase-3 were detected in hypertensive eyes compared with control eyes. Accumulation of Aβ deposits have been reported in the RGC layer of an animal model of AD [8]. Similarly, accumulation of retinal Aβ in OHT and glaucomatous eyes has been also reported [54], [55]. Guo et al. reported that targeting the Aβ pathways can reduce RGC loss during glaucoma [6], [18]. More recently, it has been shown that *Lycium barbarum* polysaccharides (LBP) is protective against Aβ-mediated neurotoxicity of RGC during AOH via downregulation of RAGE [56]. This implies that RAGE–Aβ binding may mediate RGC loss by transferring Aβ from the blood circulation via upregulation of vascular RAGE. The following sections explore this mechanism further and review the literature on RAGE, its structure, ligands and involvement in AD and, possibly, glaucoma.

1.4. RAGE

The RAGE locus is located on chromosome 6 between Class 2 and 3 major histocompatibility complex (MHC) and produces a 55 kDa protein of 404 amino acids [57], [58]. RAGE is found on the membrane of different cell types such as glial cells and neurons [59]–[63]. Initially, RAGE was shown to interact only with advanced glycation end products (AGE), the products of non-enzymatic glycation and oxidation of proteins and lipids caused by normal ageing and accumulation of stress stimuli [58]. RAGE was later shown to be a multi-ligand receptor that binds to a diverse repertoire of ligands including AGE, Aβ, beta-sheet fibrils, high-mobility group box 1 (HMGB1), S100, Mac-1 and phosphatidylserine [64]–[66]. Activation of RAGE–ligand activation has various effects on proinflammatory and cellular stress cascades, which can lead to cell loss [67].

1.4.1. RAGE structure and function

RAGE is structurally correlated with the superfamily of cell adhesion molecules [68]. This receptor comprises three extracellular domains of 332 amino acids including the Ig-like variable type domain (V) at the N-terminus and two constant-type domains C1 and C2, a transmembrane domain, and a cytosolic tail of 43 highly charged amino acids [58]. The cytosolic domain is required for prompting signal transduction [57], [58], [68], [69]. RAGE ligands typically interact with its V domain [58]. RAGE typically has three isoforms including a full-length membrane-bound form (mRAGE) and soluble form of RAGE (sRAGE), which lacks transmembrane and cytosolic domains. Both sRAGE and mRAGE share similar ligands, and there is evident that sRAGE acts as a decoy and neutralises mRAGE ligands [70] (Figure 6).

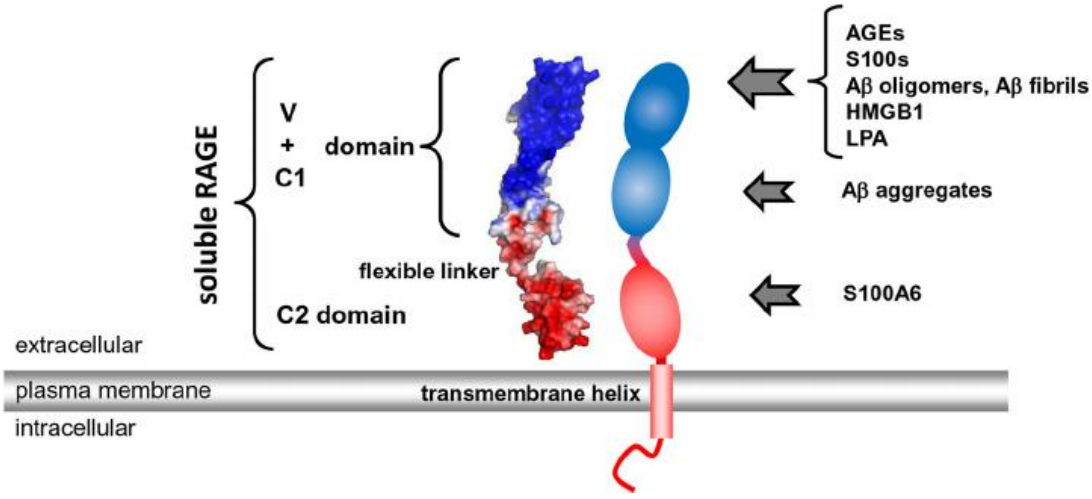

Figure 6. Schematic depiction of RAGE structure and model of sRAGE [61]. RAGE is composed of three extracellular domains of C1, C2 and V all of which participate in RAGE-ligand interactions. The receptor is also anchored in the cell membrane by its transmembrane alpha helical domain and extended to an attached cytosolic domain which takes part in signal transduction.

The RAGE promoter is recognised as a binding site for nuclear factor-kappaB (NF-κB), interferon-γ response element, Sp1 binding site, and interleukin 6 DNA binding motif [71], [72]. These binding sites control RAGE expression [71]. RAGE is minimally expressed across the various organs of the body with the exception of the lungs in which RAGE is highly expressed [65], [71], [58]. Nonetheless, accumulation of its ligands upregulate RAGE expression in positive-feedback activation to initiate an inflammatory response and stress signalling [74].

1.4.2. RAGE and Aβ in AD

RAGE–ligand signalling is involved in synaptic dysfunction, neuroinflammation, accumulation of toxic reactive oxygen species (ROS) and oxidative stress, all of which are known contributors to progressive AD [37], [67], [75]–[77]. Higher levels of RAGE have been identified in endothelial cells, neurons and microglia surrounding amyloid plaques [78]. In AD, influx of circulating Aβ across the BBB into the brain is increased by RAGE via transcytosis [79], and within the brain, RAGE is likely to internalise Aβ oligomers into the neuronal and glial cells via endocytosis [80]. RAGE–Aβ activation is believed to disrupt the tight junction proteins, the basic structure of the BBB, thereby perpetuating the deleterious effects of neurotoxic Aβ via disrupting the Aβ production–clearance homeostasis [52]. This phenomenon has been confirmed by a recent study that showed the coexistence of Aβ, elevated RAGE and matrix metalloproteases (MMPs), and disrupted microvessels in the brains of transgenic 5xFAD mice [81]. RAGE–Aβ interaction has also been shown to activate multiple intracellular signalling pathways. Onyango [82] reported the activation of the p38 mitogen-activated protein kinase (MAPK), stress-activated protein kinase/c-Jun N-terminal kinase (JNK), and NF-κB

pathways as a result of RAGE–Aβ binding. The activation of p38 MAPK particularly has been shown to be a RAGE-dependent pathway in which Aβ production [83] and internalisation occur, leading to intraneuronal Aβ cytotoxicity [84].

In AD, RAGE–Aβ interaction mediates oxidative stress and increases ROS generation in cerebral endothelial cells and astrocytes [62], [85]. Aβ is a known oxidising agent [86], [87] that can exert cellular effects upon binding to RAGE on the cell surface. RAGE–Aβ binding activates nicotinamide adenine dinucleotide phosphate oxidases (NADPH) [88] in primary astrocytes, leading to ROS generation [89]. An increase in Aβ levels at sites of inflammation can promote RAGE-dependent oxidative stress[90]. Aβ peptides activate NF-κB in rat primary microglia, as well as in human monocytes [91]. This suggests a possible feedback loop in which RAGE–Aβ binding leads to NF-κB activation, which increases RAGE expression in neurons and further RAGE–Aβ interaction, ultimately leading to accelerated Aβ cytotoxicity [78]. This continuous NF-κB activation, increases the expression of proinflammatory cytokines resulting in prolonged activation of cell damage, including apoptosis [92].

The mounting evidence of how RAGE expression plays a significant role in the underlying pathology of AD suggests that it is a potential target for the treatment of this disease. A high-affinity RAGE-specific inhibitor, FPS-ZM1, which binds specifically to the V domain of RAGE and crosses the BBB, has been shown to reduce Aβ levels in the brain of transgenic *APPsw/0* mice, which overexpress human Aβ-precursor protein [93]. Another inhibitor of RAGE–Aβ interaction, PF-04494700, is currently in a clinical trial for AD [91]. In preclinical studies, the compound has been shown to slow cognitive decline on behavioural assays and decrease Aβ load in the brain [90]. The soluble isoform of

RAGE, sRAGE, has been shown to act as a decoy, by sequestering Aβ and preventing RAGE–Aβ activation [52]. This observation has prompted studies investigating sRAGE as a diagnostic and therapeutic agent in AD. Plasma sRAGE level is significantly lower in AD patients [94], [95], which suggests the possibility of using this biomarker in screening for the disease. In a mouse model of AD, administration of sRAGE increased cerebral blood flow and reduced inflammation and Aβ levels [52]. Collectively, these results suggest that RAGE inhibitors and/or sRAGE promotion may be used to regulate RAGE–Aβ interaction, which in turn may prevent or delay the onset of AD. However, further studies are required to investigate its specificity and sensitivity.

In summary, the current data suggest that RAGE–Aβ interaction initiates a cascade of several signalling pathways (e.g., ROS generation, NF-κB) in AD, which ultimately leads to neuronal apoptosis. Given the evidence discussed earlier of the common underlying pathophysiological role of Aβ in AD and glaucoma, we postulate a new hypothesis that RAGE–Aβ binding, similar to AD, may play a significant role in glaucoma pathogenesis and retinal neurodegeneration.

1.5. RAGE and Aβ in retinal pathology

Within the eye, and specifically the retina, RAGE is expressed in a number of cells including Muller cells, retinal pigment epithelium (RPE) cells and RGCs [96]–[98]. The implications of RAGE expression in the retina through binding with its ligands and activating a cascade of intracellular transduction pathways have been studied in numerous eye conditions including glaucoma [96], age-related macular degeneration (AMD)[99] and diabetic retinopathy [75]. The RPE and RGC layer are known to express and secrete Aβ [100], [101]. Aβ accumulation has been shown to play a role in the

pathogenesis of various retinal abnormalities including AMD and glaucoma [100], [102]–[104]. Aβ expression increases during ageing and exacerbates the underlying pathology of AMD [101]. Studies of oligomeric Aβ, have reported a correlation between soluble Aβ levels and the progress of AMD caused by disrupted neurotransmission and neuronal death [105]–[107]. The presence of drusen, yellow deposits of lipids and fatty proteins, increases an individual's risk of developing AMD. Aβ has been identified as a common substructural component of drusen[108]. Interestingly, drusen displays intense staining for RAGE [98], [109]. As discussed earlier, RAGE-mediated endocytosis is also active in the retina, and this process translocates Aβ into the intracellular space of RPEs in cases of breakdown of the outer BRB axis [110].

RAGE–ligand interaction increases intracellular oxidative stress, as indicated by increased activity of NADPH oxidase (Figure 7), a key mediator of superoxide radical production in the retina, and ROS overproduction [62], [85], [88]. Oxidative stress is a hallmark of retinal abnormalities including diabetic retinopathy (DR), AMD and glaucoma; AGE accumulation has been reported in all of these diseases [96], [98], [110]. RAGE–ligand signalling plays a crucial role in inducing and perpetuating oxidative stress in the retina, which leads to inflammation and subsequent retinal cell loss. Oxidative stress upregulates NF-κB activation, which stimulates the production of inflammatory cytokines and chemokines and triggers an inflammatory response and death of retinal cells, including RPEs and RGCs in AMD and glaucoma, respectively [111].

RAGE–ligand binding also activates vascular endothelial growth factor, a pathological feature of both DR and AMD, via the RAGE–AGE–JNK signalling pathway, which leads to increased vascular permeability and new blood vessel formation [112].

These findings suggest that RAGE–ligand interactions perpetuate the vicious cycle between oxidative stress, inflammation and cell apoptosis in retinal degenerative disorders.

1.6. Role of RAGE in glaucoma

RAGE has been detected in RGCs of human glaucomatous eye tissues; higher levels have been detected in glial cells particularly Muller cells [96]. By inducing the overexpression of immune and neurotoxic compounds, RAGE upregulation interferes with regular function in glial cells involved in RGC survival [96], [113], [114]. These immune neurotoxic compounds include tumour necrosis factor (TNF) (Figure 7) [115], nitric oxide synthase[116] and surface antigens of glial cells [117]. Some evidence shows RAGE activation accounts for this response in glaucoma [96] and that glial cell activation precedes RGC alterations. For example, elevation of IOP in rats increased glial activity and density in the retina and optic nerve, predominantly in the laminar cribrosa [118] before RGC loss [119]. In other words, glial activation is followed by secondary alterations that lead to RGC loss [120], [121]. This suggests the involvement of glial cells in the pathogenesis of glaucoma. Upon glial activation and proliferation, secretion of neuroinflammatory compounds, such as cytokines, increases, and the increased cytokine release perpetuates cellular stress, which contributes to RGC loss during glaucoma. Among the RAGE-mediated upregulated proinflammatory cytokines, TNF-α has been reported to trigger the pro-apoptotic caspase cascade in RGCs in glaucoma. RGC loss has been shown to decrease by 66% after TNF-α inhibition [113], [122].

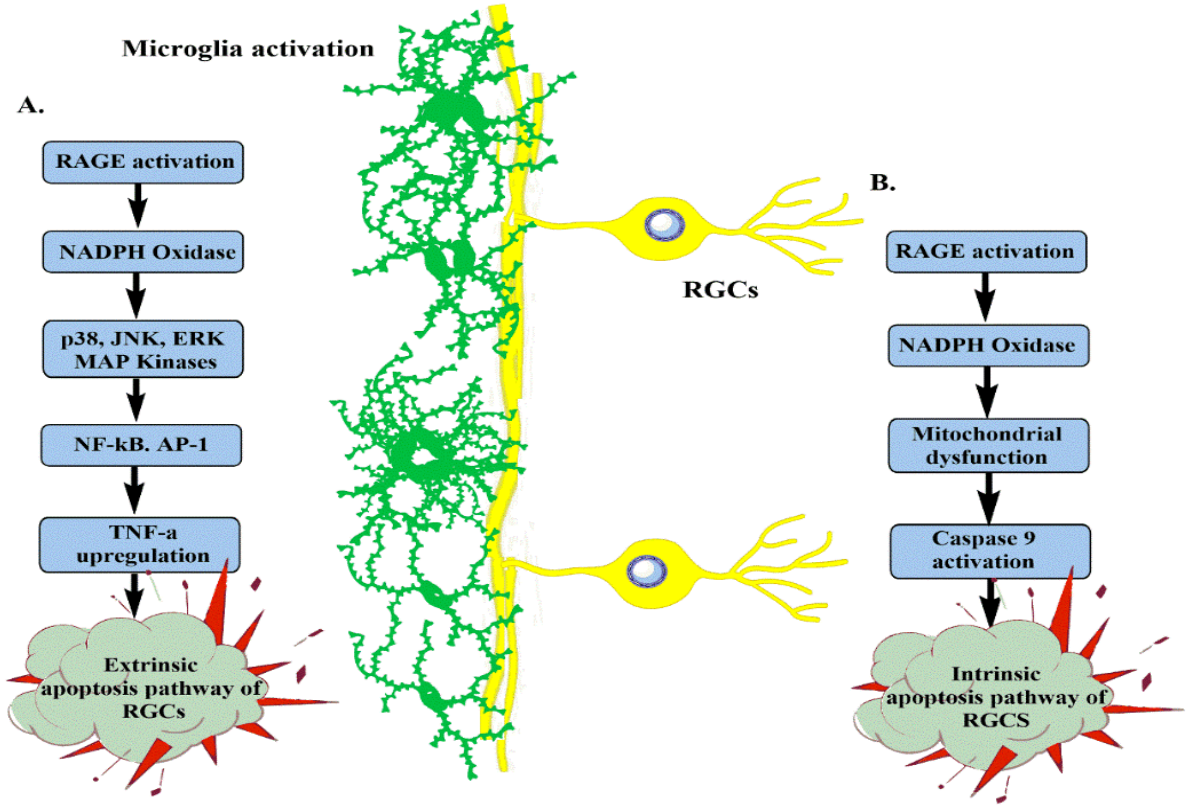

Figure 7. Trigger of the extrinsic and intrinsic apoptotic pathways by RAGE activation, which leads to RGC loss

RAGE–ligand activation accounts for the underlying glaucomatous pathology following AOH [96]. In one study, increased Hmgb1 level induced an inflammatory response, which contributed to neurotoxicity via RAGE signalling 7 days after AOH [123]. The co-localisation of AGE, RAGE and RGC loss in human glaucoma has been reported [96]. In that study, AGE accumulation was noted in the optic nerve head, although RGC and glial cells showed intracellular AGE; these findings suggest a role of the RAGE–AGE mediated signalling pathways in retinal degeneration. RAGE-neutralising antibody significantly suppresses AGE-mediated apoptosis and cytotoxicity [113], [122]. AGE

pathogenesis follows the cross-linking and trapping of extracellular and intracellular proteins, which lead to remodelling and rigidity of the extracellular matrix (ECM) [124].

Upregulation of MMPs caused by RAGE–Aβ binding in endothelial cells is also associated with changes in aqueous humour outflow. These changes in outflow because of remodelling of the ECM in the trabecular meshwork may contribute to IOP elevation. Elevation of IOP is a key factor in the irreversible RGC apoptosis in glaucoma [125], [126]. A disruption in aqueous humour homeostasis can elevate IOP, which increases the mechanical stress in ocular structures, particularly the lamina cribrosa, and ultimately results in optic nerve damage [24], [127]. It has been suggested that overexpression of transforming growth factor-β (TGF-β) results from the overproduction of ECM molecules such as elastin, collagen and fibronectin via the canonical Smad and non-canonical MAPK pathways and that the increase in TGF-β signalling may be linked to IOP elevation in glaucoma patients [128]–[130]. RAGE–TGF-β signalling has not been studied in the ECM of the eye to date, although there is evidence that RAGE plays a significant role in ECM deposition [131]. RAGE–Aβ ligation in endothelial cells has been shown to upregulate MMP production via the RAGE–Aβ–CaN–MMP signalling pathway, which leads to disruption of the BBB in AD [81] (Figure 8).

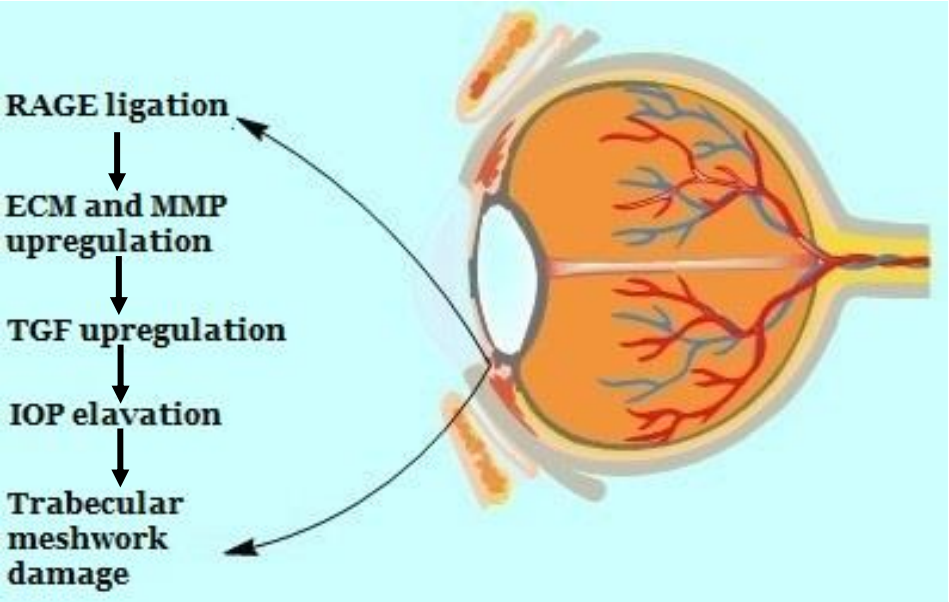

Figure 8. Effect of TGF upregulation on IOP. RAGE activation is presumed to cause trabecular meshwork damage via upregulation of ECM/MMP which is followed by TGF over expression leading to IOP elevation. Trabecular meshwork damage is linked to the pathogenesis of glaucoma.

In summary, these studies suggest that RAGE–ligand binding is actively involved in RGC loss in glaucoma through various signalling pathways. It appears RAGE expression promotes Aβ production and **e**xtracellular Aβ translocation into the intracellular space via endocytosis. RAGE–AGE binding mediates oxidative stress and RAGE–HMGB1 activation is responsible for an inflammatory response and subsequent neurotoxicity in glaucoma (Table 1).

Table 1. RAGE ligands and their presence in glaucoma patients and animal models of glaucoma

RAGE ligand	Experiment	Reference
AGE	Human glaucoma	Tezel *et al.* [96]
Aβ	Animal model of glaucoma	Mi *et al.* [56] Guo *et al.* [6]
HMGB1	Animal model of glaucoma	Dvoriantchikova *et al.* [123]
S100	Animal model of glaucoma	Casola *et al.* [132]

1.7. The role of the RAGE– Aβ axis in glaucoma: potential hypothesis

Current evidence on the involvement of RAGE in the pathophysiological mechanisms of several chronic diseases (e.g., diabetes, AD, AMD) suggests that RAGE plays a pivotal role in the pathophysiology of these diseases. Both RAGE and Aβ, have been established as mediators of the cellular perturbation leading to neural dysfunction in AD. The increased expression of RAGE in various cell types including microglia, neurons and astrocytes together with the elevated Aβ level in AD confirms the neurodestructive role of RAGE–Aβ binding in neurodegeneration. Given that RAGE is overexpressed in various cells of the retina and that Aβ deposits increase in the GCL during glaucomatous neurodegeneration, it can be postulated that RAGE–Aβ binding is actively involved in mediating RGC loss. More specifically, based on striking similarities between glaucoma and AD, we speculate that a similar cascade of pathophysiological events, by which RAGE mediates neuronal apoptosis in AD, may occur during the

glaucomatous pathogenesis leading to RGC loss. Given that RAGE and Aβ are highly expressed in the optic nerve head in AD patients [108], we hypothesise that RAGE–Aβ binding initiates a cascade of signal transductions that lead to oxidative stress and ROS production. Further, we hypothesise that RAGE is actively involved in transporting extracellular Aβ and influx across the BRB and into RGCs through endocytosis, which eventually contributes to RGC loss. If indeed RAGE mediates Aβ uptake in glaucoma, RAGE inhibitors may prevent or reduce the intracellular accumulation of Aβ and subsequent RGC loss, a similar treatment strategy currently in clinical trials for AD.

Current evidence of the involvement of RAGE in the pathophysiological mechanisms of several chronic diseases (e.g., diabetes, AD, AMD) suggests that RAGE plays a pivotal role in the pathophysiology of these diseases. More specifically, both RAGE and Aβ, have been established as mediators of the cellular perturbation leading to neural dysfunction in AD. The increased expression of RAGE in various cell types including microglia, neurons and astrocytes together with the elevated Aβ level in AD confirms the neurodestructive role of RAGE–Aβ binding in neurodegeneration. Given that RAGE is overexpressed in various cells of the retina and that Aβ deposits increase in the GCL during glaucomatous neurodegeneration, it can be postulated that RAGE–Aβ binding, similar to that observed in AD, is actively involved in mediating RGC loss.

2. Chapter 2— Methods

2.1. Sodium dodecyl sulfate polyacrylamide (SDS-PAGE) and western blotting protocols

The western blotting is a widely used analytical technique in molecular biology to detect specific proteins in a sample of tissue homogenate or extract. We used the iBind western system (Life Technologies) in our experiments which will be explained step by step in this section. This has allowed us to save time and reagents mainly due to a less antibody incubation time compared with conventional methods. We were also able to use a mixture of antibodies simultaneously.

2.1.1. Preparation of protein sample and protein concentration assay

1. Enucleated eyes were stored in -80°C immediately after collection.
2. Cell lysis buffer from stock solution was prepared per table 2. This reagent buffer was used for tissue extract homogenization and BSA assay to determine protein concentration and preparation of the sample gel load.

Table 2. Lysis buffer preparation recipe for homogenising tissues

Reagent	Volume
5 × Tris EDTA-buffer: 250mM Tris HCl, pH 7.5, 5 mM EDTA	200 µL
5 × NaCl: 750mM NaCl	200µL
5 × SDS: 0.5% sodium dodecyl sulphate	200µL
5 × DOC: 2.5% deoxycholic acid, sodium salt	200µL
5 × Igepal CA-630: 5% Igepal CA-630	200µL

*10 µl Protease inhibitor cocktail: containing 4-(2-aminomethyl), benzenesulfonyl fluoride (ABESF), pepstatin A, bestatin, leupeptin, aprotinin, and trans-epoxy-succinyl-L-leucyl-amido (4-guanidino)-butane (E-64)

3. Tissues were placed in a clean 1.5 mL Eppendorf tube and 25 μL of cell lysis buffer (Table 2) was added. Samples were homogenized using a micropestle to ensure protein is in a lysate form.
4. The sample protein was centrifuged at 10–15,000 rpm for 5 min to resuspend the pellet of tissue debris. This was repeated 3 times and then finally clear protein supernatant was removed into a clean 0.6ml Eppendorf tube. For storage, the protein supernatant was placed in -80°C freezer.
5. BCA assay (triplicates) including BSA standards (Table 3) was prepared to determine the protein concentration of the unknown sample (Unknown sample dilute 1 in 25 μL of lysis buffer). 20 μL of sample (BSA standards and unknown) + 250 μL of working reagent (Micro BCA kit) were added.

Table 3. Concentration of solutions used for the standard curve of the BCA assay

Vial	BSA (μL)	Diluent lysis buffer (μL)	Required volume (μL)
A	50	450	60
B	40	460	60
C	25	475	60
D	12.5	487.5	60
E	6.25	493.75	60
F	3.125	496.875	60
G	1.5625	498.4375	60
H	0.78125	499.21875	60
I (blank)	0	500	60

6. Meanwhile, the protein sample was chilled on ice for immediate use, otherwise stored at -80°C freezer for long-term storage.

7. Protein concentration was determined using TECAN microplate reader (Life Sciences, Zurich, Switzerland).
8. TECAN microplate reader and PC were turned on to run i-control software program.
9. BCA Assay icon was selected (562 nm).
10. Reading plate was configured using "Falcon 96 well transparent/black" plate in the software.
11. Edit layout for entire plate was selected.
12. The positions of blanks, standards, and samples were entered. Triplicate blanks, standards and samples (vertical) were indicated.
13. In the basic parameter menu table: No. of flashes (20), Settle timing (500 millisecs). Excitation filter (562nm) were chosen.
14. When the run cycle was completed, an excel sheet was generated as raw data.
15. The raw data was copied and prepared in the "standard curve" template and automatically the results were generated to create standard curve graph and the volume load was calculated for each protein sample.
16. Once the protein concentration was determined the sample buffer was added (Table 4).

Table 4. Sample buffer preparation recipe for SDS-PAGE

Reagent	Volume
Tris-HCL pH 6.8	63 mM
Glycerol	10%(w/v)
SDS	2%(w/v)
Bromophenol Blue	0.0025%

* storage in 4°C for 6 months.

17. Protein samples were briefly vortexed.

2.1.2. Gel Electrophoresis

We used ready-made 4–20% Tris-glycine mini gels (located in 4°C fridge) for western blotting apparatus as it has been optimized for 20-200 kDa protein separation.

18. Ready-made precast gel was removed from plastic pack and the plastic gel cassette was rinsed in Milli Q water.
19. The plastic comb was removed, and the gel cassette was placed onto the electrode assembly and thoroughly rinsed the with 1× SDS-tank buffer.
20. 5 µL of pre-stained protein standard and all the sample protein were loaded using gel loading pipette tips.
21. Further fill front and back chamber of the mini tank with the 1 × SDS-TANK buffer (Table 5)

Table 5. 1× Tank buffer preparation recipe for SDS-PAGE

Reagent	Amount
15.4mM Tris base	1.875 g
0.12M Glycine	9 g
2.2mM SDS	0.625 g
dH2O	Make up to 1 L

22. Lid was placed on mini Tank (Life Technologies)

Note: Make sure to align the color-coded banana plugs and jacks. The correction orientation is made by matching the jacks on the lid with the banana plugs on the

electrode assembly. Insert the electrical leads into a suitable power supply with the proper polarity (Voltage 120 V, 1.5 h)

23. Power was applied to the mini Gel Tank to run electrophoresis

2.2. Gel Removal and Preparation of Protein Transfer

24. After electrophoresis was complete, the power supply was turned off and the lead was disconnected.
25. The tank lid was removed and carefully lifted to remove the gel cassette.
26. The gel cassettes were thoroughly rinsed in Milli Q water.
27. A gel releaser was used to gently remove the plates apart.
28. iBlot stack (Life technologies) was opened and placed on the dry iBlot2 device.
29. The gel was prepared and placed on the membrane within the dry iBlot2 device.
30. Filter paper was removed and immersed in Milli Q water and placed directly on the gel.
31. Blotting roller was used to remove any air bubbles between the gel and the membrane.
32. The filter pad was directly placed on top of the stack.
33. Once the filter pad, filter paper, the gel and the membrane were directly aligned the iBlot2 device was immediately closed and locked.
34. The “P0” method was selected to transfer proteins to the membrane.
35. Using tweezers, the membrane was removed, and a small diagonal incision was made on the top right corner of the membrane as an indication for protein position.
36. The membrane was then placed in a plastic blot tray and rinsed in Milli Q water (2x).

Note. After the gels were transferred, you may also pre-stain gel by equilibrating in 100ml Milli Q water in a large plastic gel container and thereafter apply simply blue Safe Stain microwave method. This ensures whether all the proteins were transferred onto the membrane and therefore you may proceed to blocking and antibody incubation of the membrane

2.3. Membrane Blocking

37. After the transfer was completed, the power supply was turned off and the iBlot stack was removed.
38. The membrane was washed and equilibrated in Milli Q water.

Note. Ensure the protein of the blot is facing up.

39. The membrane was immersed in 5 mL of 1× FD solution buffer in plastic blot tray.

2.4. Antibody Incubation

Note. Ensure both primary and secondary antibodies were prepared earlier.

40. The membrane was placed in the middle of the iBind card (protein is facing up).
41. The blotting roller was used to remove any air bubbles.
42. The iBind lid was closed and antibodies and solutions were sequentially added to the iBind well.

Note: Ensure that the wells are not positioned over the membrane when the lid is closed. Don't move device or open the lid until incubation is complete.

43. Antibodies were incubated for 2.5 to 3 h.

44. After incubation was complete, the membrane was removed and rinsed in Milli Q water 3 times prior to protein detection.

2.5. Odyssey Protein Detection System

45. Using the infrared (IR)-dye imaging system, dry membrane blot (protein facing-down) was placed in the Licor Odyssey machine for imaging.
46. The Image Studio software, and Odyssey CLX was selected.
47. Name and work areas selected.
48. Settings (membrane, western, Auto exposure, channel = 700/800, resolution = 169um, quality = Medium, focus = 0mm) was set up to obtain ideal image for protein band detection.
49. Image was captured and saved.
50. ImageJ software was then used for densitometry analysis.

2.6. Histology

2.6.1. Tissue Fixation

Eyes were fixed in 4% PFA (Table 6) overnight immediately after collection. The following day, tissues were rinsed 3 times -each time 5 minutes- in PBS 0.1 M and submerged in 70% ethanol for an extra day.

Table 6. Recipe for preparation of 4 % PFA

Ingredient	Amount
4g Paraformaldehyde	4 g
50mL dH20	50 mL
PBS	0.2 M up to 100 mL
NaOH	1 M (to be added until solution is clear)

* filter solution after preparation and keep it at -20°C for long term storage.

2.6.2. Tissue Processing, embedding and sectioning

Tissue processing involves the steps required to take animal tissues from fixation to a state where they are infiltrated with histological wax and can be embedded ready for sectioning on the microtome. In our experiments processing was done automatically with a tissue processor (ThermoFisher). Eye tissues were processed in subsequent cycles and with different reagents for fixation, dehydration and wax infiltration.

Afterwards, the specimens were embedded into a "block" to be clamped into a microtome for section cutting. The eyes orientation in paraffin was considered carefully in order to have efficient sections on slides. A cassette was placed on top of the mould, topped up with more wax and the whole thing was placed on a cold plate to solidify. When this was completed- at least 10 minutes was required- the block with its attached cassette were removed from the mould for microtomy.

In all experiments, 10µm radial sections of eyes were cut using the microtome (ThermoFisher).

2.7. Tissue staining

2.7.1. H&E staining

H&E staining is a popular staining method in histology. It is the most widely used stain in medical diagnosis. The staining method involves application of hemalum, which

is a complex formed from aluminium ions and oxidized hematoxylin. This colours nucleus of cells (and a few other objects, such as keratohyalin granules) blue. Materials coloured blue by hemalum are often said to be basophilic. The nuclear staining is followed by counterstaining with an aqueous or alcoholic solution of eosin Y, which colours eosinophilic other structures in various shades of red, pink and orange. Eosin is a fluorescent red dye resulting from the action of bromine on fluorescein. It can be used to stain cytoplasm for examination under the microscope. Structures that stain readily with eosin are termed eosinophilic. Eosin is most often used as a counterstain to hematoxylin in H&E staining.

RGCs were manually counted in 300 μm increments of the GCL. To objectively count RGC numbers, the measurement was repeated 3 times and the average count of RGCs for each retina section was used for statistical analysis. Cover-slipped slides were imaged using a BX51 upright EPI fluorescence microscope (Olympus, Tokyo, Japan) (20× objective).

2.7.1.1. H&E staining protocol

All H&E procedures were performed using an automatic slide staining device (ThermoFisher). All sections were;

1. Heated prior staining for deparaffinization at 65° C for 30 min.
2. Treated with Xylene for two 10 min intervals.
3. Treated with 100% Ethanol (EtOH) for two 5 min intervals.
4. Stained with filtered 0.1% Hematoxylin for 10 min in jar.
5. Rinsed in cool running ddH2O for 5 min.
6. Stained with 0.5% Eosin (1.5 g dissolved in 300ml of 95% EtOH) for 5 min.
7. Dipped in distilled H2O until the eosin stops streaking for 2 minutes.

8. Dipped in 50% EtOH
9. Dipped in 70% EtOH.
10. Equilibrated in 95% EtOH for 30 sec.
11. Equilibrated in 100% EtOH for 1 minute.
12. Dipped in Xylene.
13. Cleaned with a kimwipe.
14. Mounted, and cover slipped with DPX mountant.

2.7.2. Immunostaining

Immunostaining is a widely used technique in biological research and clinical diagnostics. Immunostaining utilizes fluorescent-labelled antibodies in order to detect specific target antigens (Figure 9).

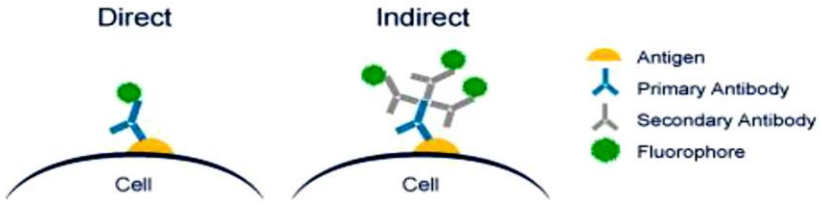

Figure 9. Schematic showing the principle of immunostaining. In direct immunostaining (left image), the fluorophore is attached to the primary antibody, and the secondary antibody is not required. In indirect immunostaining (right image), the secondary antibody.

2.7.2.1. Immunostaining protocol

DAY 1

1. Tissues were permeabilized in 1% Triton X-100/PBS for 30 min at room temperature.

2. Sections were washed in 0.1M PBS for three 5 min intervals.
3. Sections were blocked with 1% BSA/PBS for 30 min.
4. Sections were labeled with primary antibody (diluted in blocking solution).
5. Sections were incubated overnight at 4°C in fridge, in covered tray with parafilm.

DAY 2

6. Sections were washed with 0.1 % Triton X-100/PBS for two 5 min intervals.
7. Sections were washed with 0.1 M PBS for 5 min interval.
8. Sections were labeled with secondary antibody (diluted in blocking solution).
9. Sections were incubated 2 h at room temperature in dark.
10. Sections were washed with 0.1 % Triton X-100/PBS for two 5 min intervals.
11. Sections were washed with 0.1 M PBS for 5 min interval.

2.7.3. Thioflavin S staining

Thioflavin S is a valid stain used to detect any form of Aβ. This dye binds to the characteristic β-pleated sheet conformation of amyloid [133].

2.7.3.1. Thioflavin S protocol

In our experiments we used double staining on tissues. Thioflavin S staining was done after immunostaining in order to visualise Aβ alongside other antigens used in the experiment.

1. 1% Thioflavin S in 80 % EtOH prepared and filtered.
2. Sections were stained with thioflavin S for 12 min at room temperature.
3. Sections were washed with 80 % EtOH two 5 min interval.
4. Sections were washed with 0.1 M PBS 5 min interval.

5. Tissues were labelled with DAPI mounting medium (Sigma).
6. Sections were washed with 0.1 M PBS for two 5 min interval.
7. Slides were cover slipped for imaging.

2.8. Induction of experimental glaucoma

Elevated intraocular pressure known as ocular hypertension is the most important risk factor in glaucoma. AOH is an ischemic condition found in acute glaucoma [56]. AOH mouse model has been considered as suitable models to study RGC ischemia in glaucoma. Therefore, AOH was induced in one eye of each mouse in our experiments.

A total of 24 mice were used (12 WT, 12 $RAGE^{-/-}$). Animals arrived at animal house when they were 10 weeks old. After a week of acclimatization, at week 11, all animals were anaesthetised with isoflurane (initially inducted with 5% isoflurane but then maintained at 2%), a drop of proparacaine hydrochloride 1% (for topical eye anaesthesia) (Alcon) and 1% Tropicamide (for pupil dilation) (Alcon) were instilled and the anterior chamber of the right eye was cannulated using a 33-gauge needle (Precise Medical Supplies) connected to an elevated reservoir of sterile balanced salt solution generating a pressure of more than 90 mmHg. This was maintained for 45 minutes before allowing reperfusion to commence (Figure 10). The state of AOH was verified by checking the whitening of the anterior segment of the globe including the iris and blanching of episcleral veins and retinal artery under the surgical microscopy. A drop of Chlorsig 0.5% (as antibiotic) (Aspen Pharmacare) was also administered after pressure elevation. Carprofen 5 mg/kg (as analgesia) (Zoetis) was also administered subcutaneously following the eye injections. The fellow eye was injected but not pressurized, acting as a control. At seven days post AOH, animals were euthanized, and tissues collected.

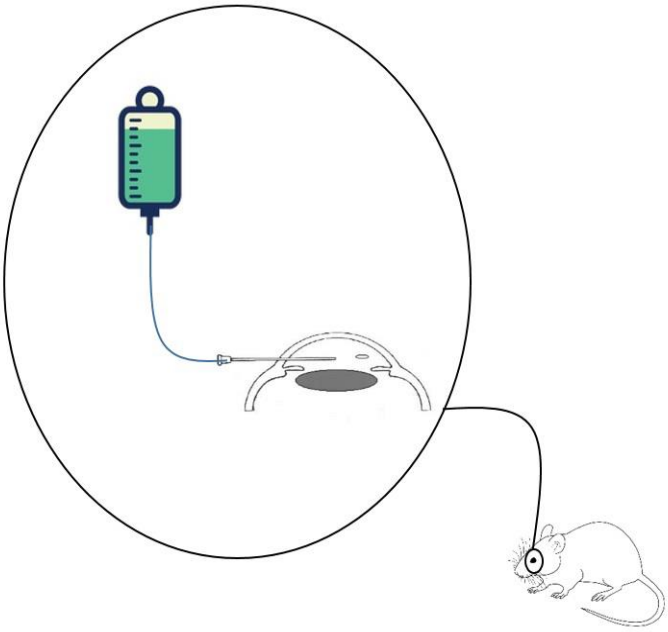

Figure 10. Schematic design of AOH induction

2.9. Aβ injection

The oligomeric subform of Aβ (Aβ1-42) was used to investigate the effects of RAGE-Aβ activation on RGC loss in RAGE–/– and WT control mice. Aβ1-42 has shown to be less soluble and more prone to aggregation and therefore, more neurotoxic [133]. Synthetic oligomeric Aβ was prepared and injected into the vitreous. 72 h and 1 week post-injections, the structure and function of the retina were evaluated. 12 animals (6 WT, 6 RAGE–/–) were culled at each time point.

2.9.1. Preparation of oligomeric $A\beta_{1-42}$

1. Oligomeric Aβ1-42 was prepared using the protocol described by Fa. *et al.* method [134].
2. Lyophilized $A\beta_{1-42}$ was equilibrated at room temperature for 30 min.

3. $A\beta_{1-42}$ peptide was resuspended in ice cold HFIP to obtain a 1 mM solution and was vortexed for 30 sec.
4. $A\beta_{1-42}$/HFIP solution was aliquoted into three polypropylene Eppendorf's and tightly sealed.
5. The Eppendorf's were the incubated for 2 h at room temperature to allow for Aβ monomerization. Next, the Eppendorf's were opened and $A\beta_{1-42}$/HFIP solution was concentrated by using a SpeedVac centrifuge (800 g, room temperature) for 1 h.
6. The Eppendorf's were sealed and stored at -80°C.
7. Prior to the animal experiment, the solution was resuspended using 5% DMSO anhydrous in 0.1M PBS solution to obtain a concentration up to 5mM $A\beta_{1-42}$. Solutions were sonicated in the water bath for 10 minutes to ensure complete resuspension.
8. 5mM $A\beta_{1-42}$ solutions were aliquoted into polypropylene vials and stored at -20°C.
9. The night before using Aβ injections, 5mM $A\beta_{1-42}$/DMSO aliquot was resuspended with PBS to a final $A\beta_{1-42}$ solution of 2.3 μg /2μL.
10. The diluted solution was vortexed for 30 seconds and then incubated for 12 h at 4°C to allow for oligomerization.

2.9.2. Intravitreal injection of Aβ

The vitreous of the right eye was injected with 2 μL of 0.25 mM Aβ (Hamilton syringe 10 μL) using a 33- gauge needle (Precise Medical Supplies). Subsequently, left eye was injected with 2 microliters of PBS serving as the control eye (Figure 11).

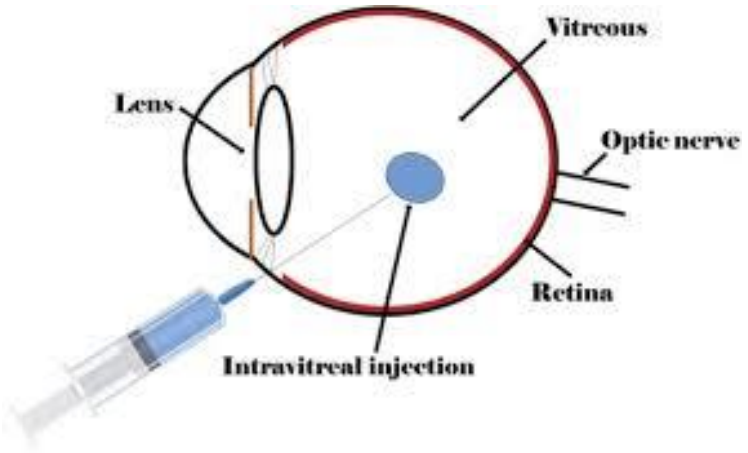

Figure 11. Intravitreal injection method [159]

2.10. Scotopic Threshold Response (STR)

STR is a non-invasive in vivo eye scan used to assess the function and integrity of the inner retina. In fact, the most sensitive response portion of the dark adapted Electroretinogram is the positive STR [135]. During the test, dark adapted mice were anaesthetised, and an electrode placed on the cornea (at the front of the eye) to measure the electrical responses to light stimuli of the cells that sense light in the retina.

In our experiment, the Handheld Multi-species ElectroRetinoGraph (Ocuscience) instrument was used for pSTR measurements. The results of pSTR was recorded on display panel which can be saved for later analysis. STR measurement requires a very weak stimulus compared with other components of ERG. Therefore, pSTR should be measured in dark adapted mice before other measurements in ERG. pSTR trace is known to originate from proximal neurons either amacrine cells or RGCs (depending on species). In rodents STR is known to originate from integrity of RGCs [136].

2.10.1. pSTR protocol

1. The day before doing performing pSTR, the mice were kept in darkness overnight (minimum 10 hours).
2. Animals were anaesthetised using mixture of ketamine (75 mg/kg) and xylazine (10 mg/kg)

Note: reversal should be done using atipamezole (as antisedan) 1mg/kg.

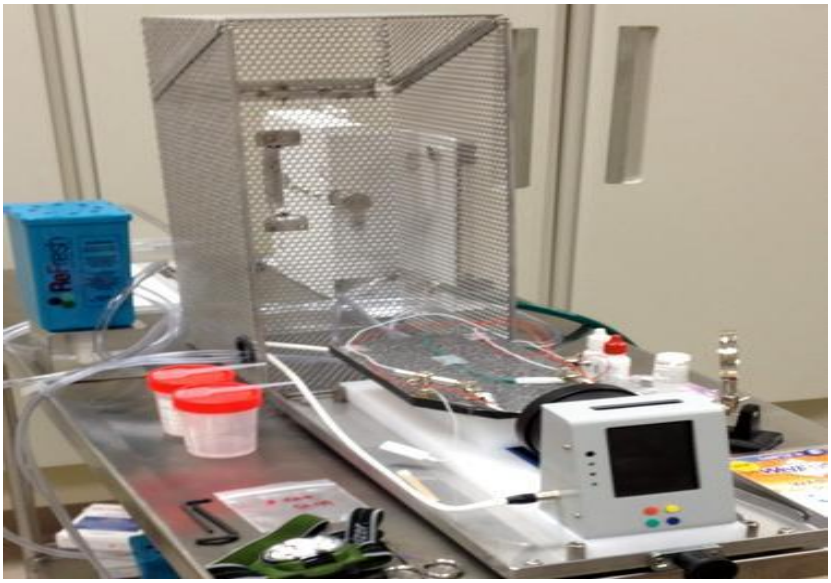

Figure 12. STR equipments [166]

3. Animals were placed on a warm stage (Figure 12).
4. The pupils were dilated by applying a drop of 1% tropicamide (Alcon).
5. Ground electrode (green wire) was subcutaneously inserted under the skin above the tail. Reference electrodes (red wires) were subcutaneously inserted under the cheek.
6. Corneal electrodes (contact lens based) were placed on the centre of the cornea to record pSTR signals.

2.11. Optical Coherence Tomography (OCT)

OCT is a noninvasive eye scan which uses a weakly coherent infrared laser to take 3-dimensional (3D) cross sectional image of retina [137]. Using OCT, retinal pathology and structure can be observed and analyzed [138]. Using OCT, different layers of retina can be visualised, and therefore thickness of retinal layers can be measured. In our experiments we used spectral domain (SD)-OCT instrument (Wasatch Photonics) for imaging retinal structure.

2.11.1. OCT protocol

1. Animals were induced with 5% Isoflurane in oxygen flowrate of 2L/min and then maintained on 2% of isoflurane in 100% oxygen flowrate of 2 L/min.
2. Animals were placed on warm stage while the anesthetic gas was delivered via the nose cone.
3. 1% Tropicamide (pupil dilation) (Alcon) was applied on mice eye.
4. OCT scanner head was moved towards the eye inasmuch as the corneal surface was sensed with the camera and the retinal structure appeared on the screen.

The image was adjusted to position the optic nerve centrally.

3. Chapter 3— RAGE Knockout mice are protected against RGC loss in glaucoma[5]

3.1. Introduction

Glaucoma is a progressive neurodegenerative disease that leads to RGC loss and irreversible blindness. Given the multifactorial nature of glaucoma, several genetic and environmental factors are believed to be involved in its pathogenesis. Chronic IOP elevation is considered to be the main risk factor for ischaemia and its subsequent contribution to glaucoma. However, the exact molecular mechanisms to link increased IOP to RGC loss remain unclear.

Previous studies have established a role for RAGE in neurodegeneration [139]. RAGE is a cell surface receptor that binds a repertoire of ligands such as Aβ, HMGB1 and AGEs. RAGE ligand binding is associated with activation of the pathogenic processes leading to progressive perturbation of normal cellular homeostasis. RAGE expression is upregulated in an Aβ-rich environment such as AD [140], [141]. RAGE has also been shown to act as a transporter of Aβ across the BBB into the brain via transcytosis [79]. Transcytosis is defined as the receptor-mediated transport of ligands from one side of the cell to the other. There is evidence that RAGE upregulation actively mediates the neurotoxic effects of Aβ in the central nervous system [84]. RAGE also activates signalling pathways related to the neuroinflammatory response [142], oxidative stress [96] and neuron cell loss [142],

[5] The current chapter is prepared in research article format and will be submitted to a peer-reviewed journal.

[143]. RAGE is believed to be actively involved in the various processes of neurodegeneration.

The role of RAGE and its ligands in neuronal loss during neurodegeneration including AD has been widely investigated; however, little is known about the role of the RAGE–ligand axis in glaucoma. There is evidence that RAGE is upregulated in the eyes of people with glaucoma [96]. Tezel *et al.* reported that the RAGE ligand, AGE, and TNF-α are involved in the extrinsic apoptotic pathway in the retina of glaucoma patients. They also demonstrated that oxidative stress is a major underlying cause of glaucoma in the aging retina [96]. RAGE and Aβ have both been detected in the GCL in experimental glaucoma [6], [56]. Mi *et al.* administered a natural neuroprotective agent, LBP, to an experimental mouse model of glaucoma and observed RGC protection via downregulation of RAGE [56]. In a separate study, RAGE-mediated HMGB1 was also upregulated in an ocular hypertensive mouse model [123]. This study found that neutralising HMGB1 reduced the extent of retinal disruption in experimental glaucoma [123]. In light of these findings, the present study included the hypothesis that RAGE and Aβ are involved in RGC loss in glaucoma. To address this hypothesis, AOH was induced in $RAGE^{-/-}$ and WT mice to explore the role of RAGE and Aβ in RGC loss in experimental glaucoma.

3.2. Materials and Methods

3.2.1. Animals

Male $RAGE^{-/-}$ mice (aged 10–12 weeks, 22±3 g) and C57BL/6 WT control mice (aged 10–12 weeks, 23±3 g) were used in this study. C57Bl/6 WT animals were purchased from the Animal Resources Centre (Perth, Australia). $RAGE^{-/-}$ mice which were kindly provided by Professor Ann Marie Schmidt (New York University Langone Medical Centre,

New York, NY, USA) were derived from C57Bl/6 mice. All animals were kept on a cyclic light (12 h on; 12 h off; ~300 lx), air-conditioned room (21±2°C) with water and food available *ad libitum*. The study was approved by the Animal Care and Ethics Committee, University of Technology Sydney (ETH16-0549). All procedures involving animals were conducted in accordance with the Australian code for the care and use of animals for scientific purposes and the guidelines of the association for research in vision and ophthalmology (ARVO) statement for the use of animals in vision research.

3.2.2. Animal model of AOH and histology work

AOH was induced in mice eye following the protocol which was explained in chapter two. Animals were euthanised 7 days after induction of AOH. All experiments including sample processing, H&E staining, immunostaining and imaging, thioflavin S staining, western blotting, STR and OCT eye scans were also explained in chapter two in detail. The used antibodies are shown below in table 7 and 8.

Table 7. List of primary antibodies

Primary antibody (dilution)	Target	Supplier
Brn3a (1:1000) for immunostaining and (1:500) for western blotting	Rabbit polyclonal antibody exclusively stains RGCs by binding to an RGC-specific nuclear epitope; used in immunostaining and western blotting.	Sigma, B9684
Aβ (1:100)	Rabbit monoclonal antibody detects several isoforms of Aβ, such as such as $Aβ_{1-37}$, $Aβ_{1-38}$, $Aβ_{1-39}$, $Aβ_{1-40}$, and $Aβ_{1-42}$; used in immunostaining.	Cell Signalling Technology, Danvers, MA, USA, D54D2
Caspase 3 (1:1000)	Rabbit polyclonal antibody detects both pro- and active (cleaved) forms of enzyme; used in immunostaining and western blotting.	Novus Biologicals, Littleton, CO, USA NB100-56112
RAGE (1:1000)	Rabbit polyclonal antibody detects a specific epitope in mouse RAGE; used in immunostaining.	Sigma, R5278

Aβ (1:1000)	Mouse monoclonal antibody detects IgG1 epitope of oligomeric Aβ-42; used in western blotting.	Life Technologies, VIC, Australia, 13-0100Z
GAPDH (1:1000)	Chicken polyclonal antibody used as a control in western blotting.	Millipore, Burlington, MA, USA, AB2302

Table 8. List of secondary antibodies

Secondary antibody (dilution)	Target	Supplier
IRDye 800CW (0.5:2000)	Chicken polyclonal antibody; used in western blotting.	Millennium Science, Mulgrave VIC, Australia, LCR-925-32218
IRDye 800CW (0.5:2000)	Mouse monoclonal antibody; used in western blotting.	Millennium Science, LCR-925-32210
IRDye 680RD (0.5:2000)	Rabbit polyclonal antibody; used in western blotting.	Millennium Science, LCR-925-68071
Cy3 (1:1000)	Rabbit polyclonal antibody; used in immunostaining.	Jackson ImmunoResearch, West Grove, PA, USA, 111-165-003

3.2.3. Statistics

All statistical tests were performed using GraphPad Prism 7 (GraphPad Software Inc., San Diego, CA, USA). The data are presented as mean ± standard error of the mean (SEM). Unpaired Student's *t* tests were used to compare groups. Statistical differences were considered to be significant at p-values <0.05.

3.3. Results

The current experiment was performed with the aim of investigating whether RAGE mediates RGC loss in experimental glaucoma. Based on the available evidence

which was comprehensively discussed in the literature review, we expect to see an upregulation of RAGE in mice following AOH. Further, we explore upregulation of RAGE and its ligand, Aβ, in AOH mice model to examine whether RAGE-Aβ are involved in RGC loss in experimental glaucoma.

3.3.1. RAGE$^{-/-}$ mice are protected against RGC loss after AOH

Radial cross-sectional images from the optic nerve head (experimental glaucoma and control eye) stained with H&E were used to count RGCs manually in 300 μm increments of the GCL. H&E staining showed a significant reduction in RGC counts per 300 μm linear retina in both RAGE$^{-/-}$ and WT mice with experimental glaucoma. However, the decrease in RGC counts was larger in WT mice (17±1, $p<0.0001$, n=8) than in RAGE$^{-/-}$ mice (26±1, n=8, $p=0.01$, n=8) (Figure 13, A–E).

Analysis of OCT scans from the same retinas showed a significant thinning of TRT was observed in the eye with glaucoma in both WT (178.9 ± 1.687 μm vs. 163 ± 2.3 μm, $p<0.0001$, n=9) and RAGE$^{-/-}$ mice (172.2 ± 0.9679 μm vs. 168 ± 1.1 μm, $p=0.03$, n=12) compared with their control. Comparison of WT AOH and RAGE$^{-/-}$ AOH also showed a significant reduction in TRT in WT AOH (Figure 13, F–K). By contrast, non-significant reduction in GCL/IPL complex thickness was observed in WT AOH and RAGE$^{-/-}$ AOH compared with their controls (41±2 μm vs. 34±2 μm, $p=0.09$ in WT and 40±2 μm vs. 37±2 μm in RAGE$^{-/-}$, $p=0.2$, n=8) (Figure 13, F–L).

The non-significant thinning of the GCL/IPL complex shown in the OCT scans of the retinas with glaucoma may be attributed to either a lack of sufficient RGC loss to affect the overall layer thickness or to insufficient image resolution to demonstrate GCL thinning effectively. To confirm RGC loss, Brn3a immunostaining and immunoblotting

were used to quantify RGC numbers objectively. Brn3a exclusively stains RGCs by binding to an RGC-specific nuclear epitope and, therefore, can be used as a marker to quantify cell survival rate. The results of Brn3a staining confirmed the histology findings. The RGC counts were significantly lower in WT mice (79±2 vs. 47±5, p=0.003, n=3) compared with a non-significant reduction in RGC counts in RAGE$^{-/-}$ mice (81±4, vs. 66±5, p=0.07, n=3). RGC counts were also significantly lower in WT AOH than in RAGE$^{-/-}$ AOH (Figure 13, L–P). Western blotting showed significant lower Brn3a expression in WT AOH than in WT control (1±0, vs. 0.2±0.06, p<0.001, n=3). The change in Brn3a expression was not significant in RAGE$^{-/-}$ AOH (1.3±0.4 vs. 0.9±0.2, n=3, p=0.4) (Figure 13, Q–R).

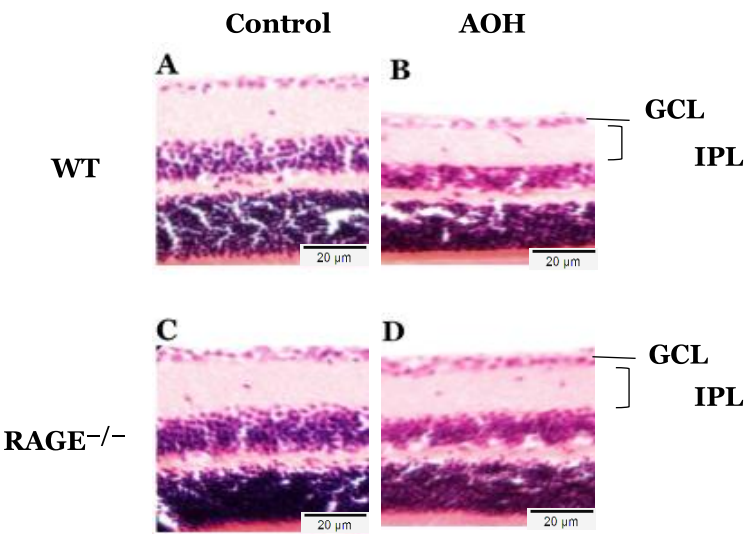

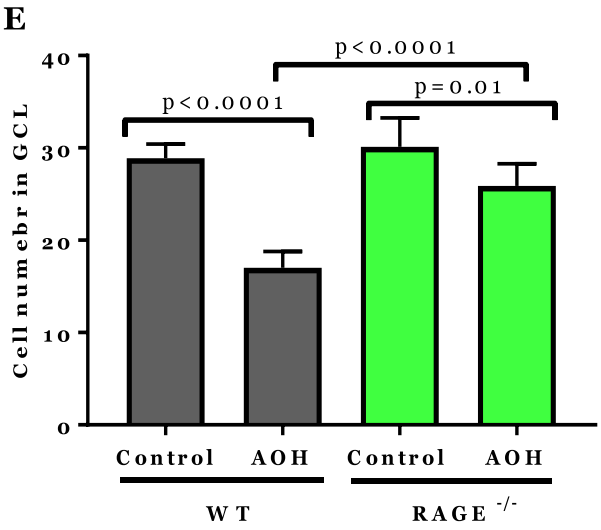

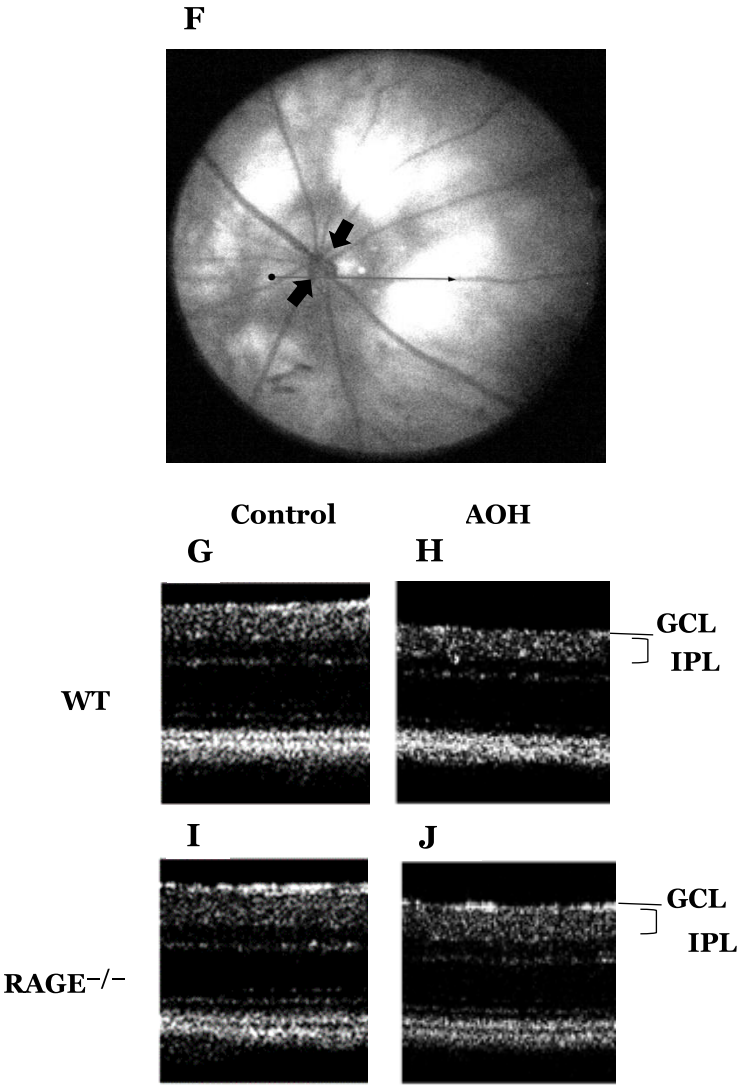
F
Control
AOH
G
H
WT
GCL
IPL
I
J
RAGE−/−
GCL
IPL

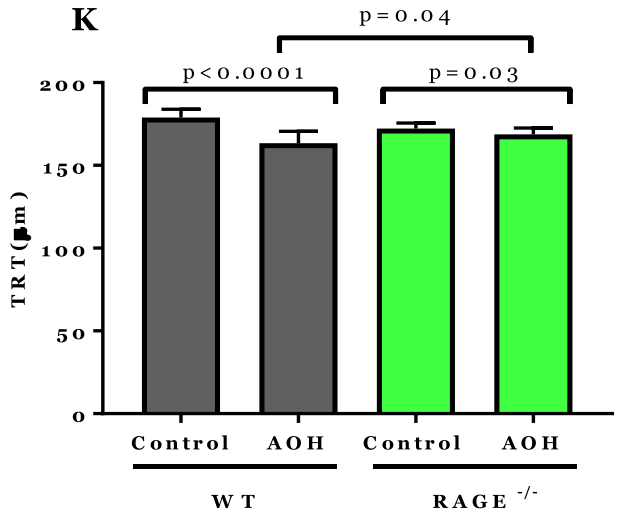
K
p = 0.04
p < 0.0001
p = 0.03
TRT(μm)
200
150
100
50
0
Control
AOH
Control
AOH
WT
RAGE -/-

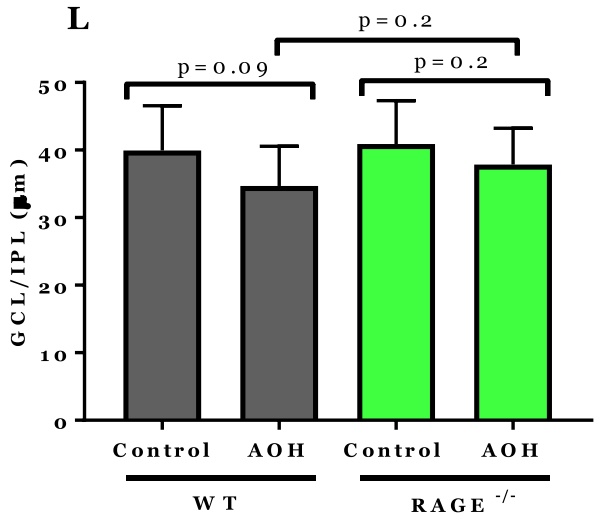
L
p = 0.2
p = 0.09
p = 0.2
GCL/IPL (μm)
50
40
30
20
10
0
Control
AOH
Control
AOH
WT
RAGE -/-

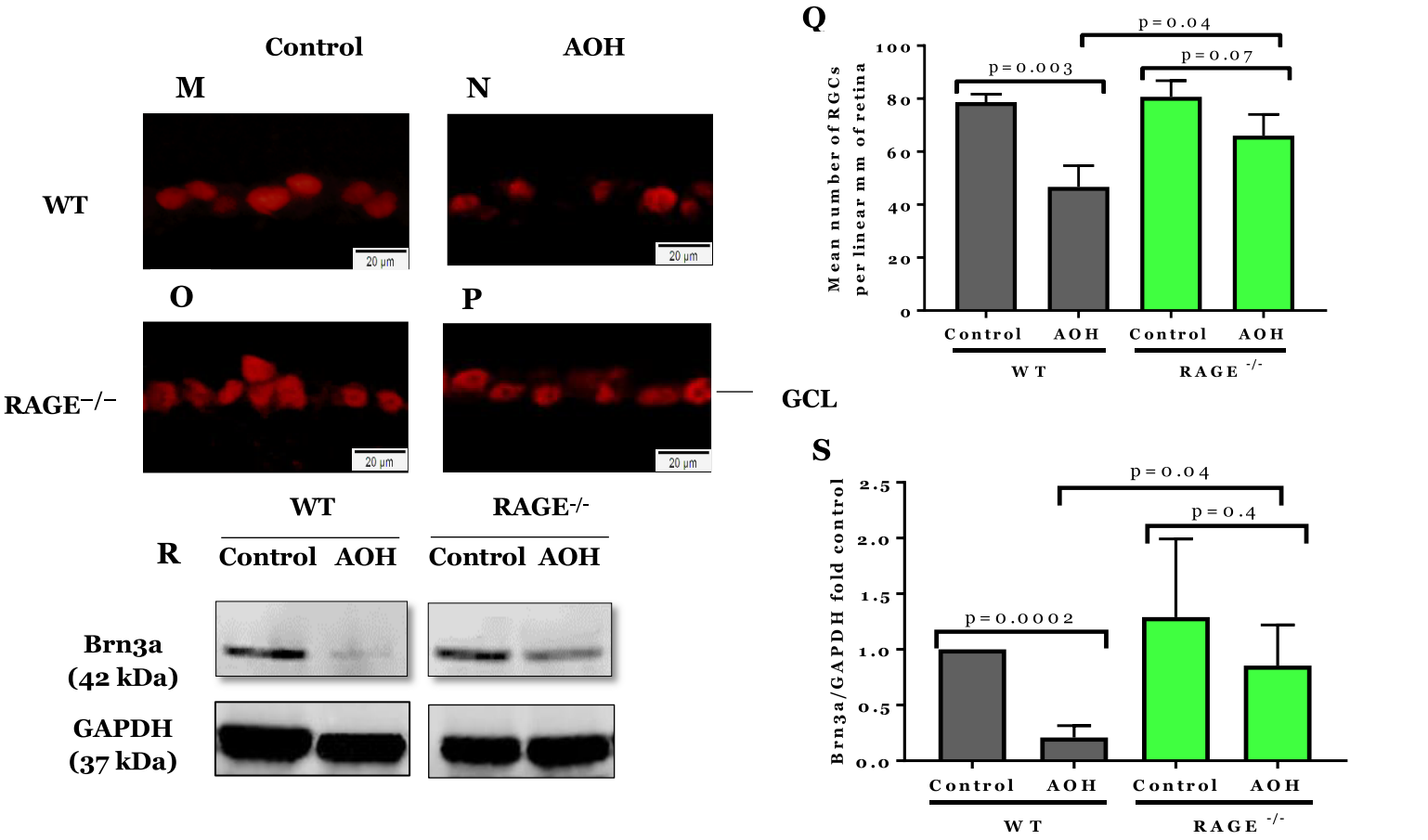

Figure 13. Investigation of RGC loss and alterations in retina structure after AOH. (A–E) H&E staining of RAGE$^{-/-}$ and WT retinal sections at 10 µm thickness; A. WT control; B. WT AOH (glaucoma); C. RAGE$^{-/-}$ control; D. RAGE$^{-/-}$ AOH (glaucoma); E. Graph representing quantitative measure of RGCs per 300 µm linear retina and their alterations after AOH (n=8); (F–L) SD-OCT of mouse retina; F. Representative example of enface eye scan which shows optic nerve head in WT control using SD-OCT devise. Optic nerve head has been shown by arrows. G. WT; H. WT AOH; I. RAGE$^{-/-}$ (control); J. RAGE$^{-/-}$ AOH; K. Quantitative comparison of TRT alteration using in vivo OCT imaging (n=8); L. Quantitative comparison of GCL/IPL alteration using in vivo OCT imaging (n=8); (M–Q) Brn3a immunostaining to label RGCs (red); M. WT control; N. WT AOH; O. RAGE$^{-/-}$ control; P. RAGE$^{-/-}$ AOH; Q. Number of Brn3a+ RGCs in a 1 mm linear region of the GCL layer from the optic nerve head (n=3); R. Western blotting of WT and RAGE$^{-/-}$ mice using Brn3a antibody showing the Brn3a band around 42 kDa. GAPDH was used as a control; S. Densitometric analysis was performed using ImageJ software (n=3). Data are represented as the Brn3a/GAPDH fold change. There ratio of Brn3a expression in all tissue samples was compared with WT Control.

3.3.2. Aβ deposition increases in the GCL after AOH

Retinal Aβ was visualised in WT and RAGE$^{-/-}$ mice following AOH. Double staining for Aβ using an Aβ antibody was also performed to confirm the findings of thioflavin S staining. Aβ was detected in the WT AOH retina but not in the RAGE$^{-/-}$ AOH (Figure 14, A, Figures 26 and 28, Appendix). Western blotting was used to quantify Aβ,

and showed significant upregulation of Aβ in WT AOH (Figure 14, B and C). Aβ levels were 1.8-fold higher in WT AOH retinas than in WT retinas (Figure 14, C).

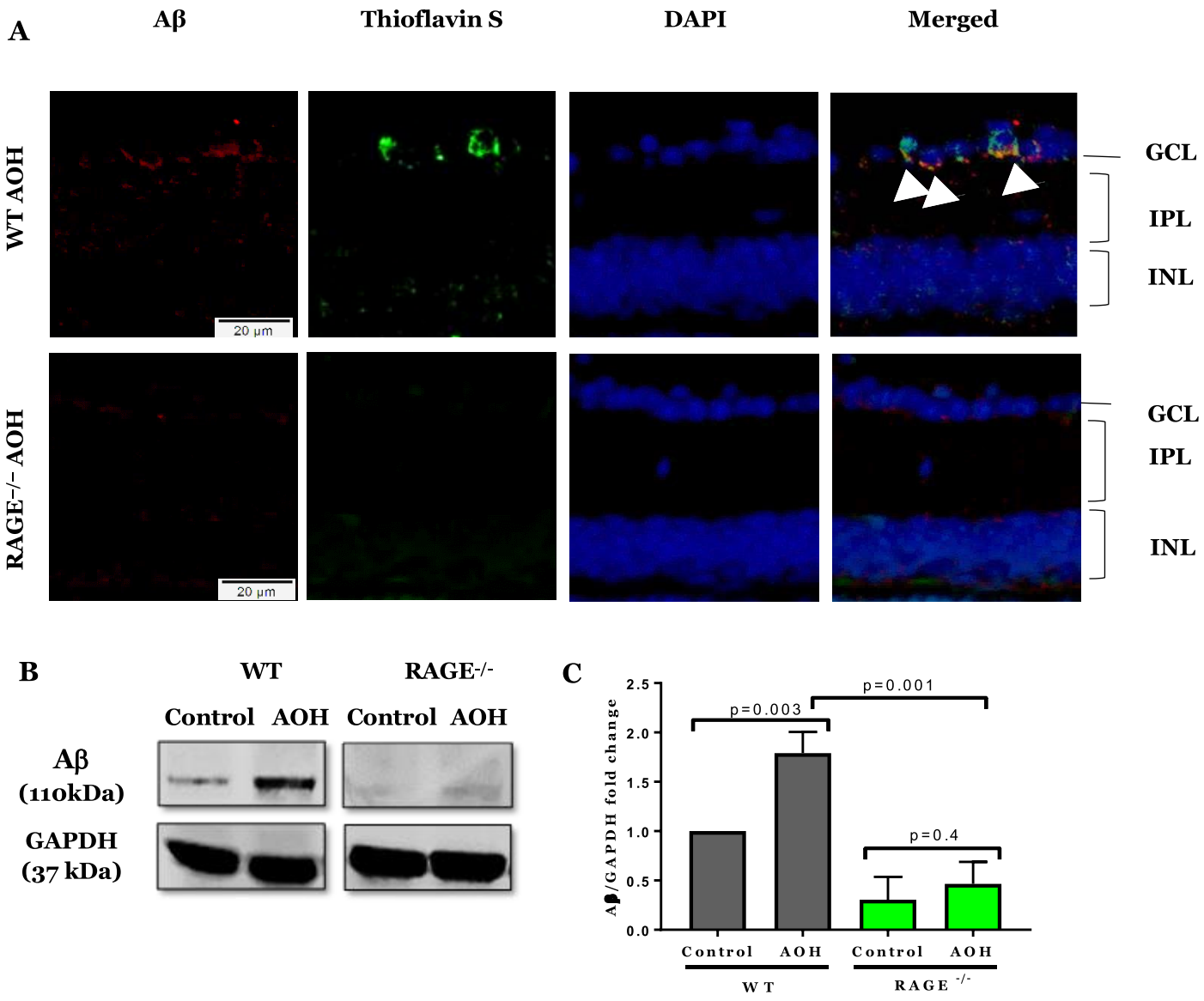

Figure 14. Investigation of Aβ deposition in mouse retina after AOH. A. Immunostaining of WT AOH and RAGE$^{-/-}$ AOH retina using Aβ antibody (red), DAPI (blue), and thioflavin S staining (green) (n=3) B. Western blotting of Aβ antibody in WT and RAGE$^{-/-}$ retinas show the Aβ band at 110 kDa. GAPDH was used as a control; C. Densitometric analysis of Aβ alteration after AOH in WT and RAGE$^{-/-}$ was performed using ImageJ software. Data are represented as Aβ/GAPDH fold change (n=3). The ratio of Aβ expression in all tissue samples was compared with WT Control.

3.3.3. RAGE and Aβ co-localise in the GCL after AOH

Following on from the previous finding and to determine the role of RAGE in binding retinal Aβ, the next experiment was performed with the following aims: 1) whether RAGE expression is increased and 2) whether RAGE and Aβ co-localise, following AOH. Immunostaining for RAGE confirmed greater RAGE expression in the GCL of WT AOH retina than in the WT control (Figure 15 to Figure 27, Appendix which shows no RAGE expression in RAGE$^{-/-}$ mice). The same retinas were then double stained for Aβ. RAGE and Aβ co-localised in the WT AOH retina, which suggests that RAGE–Aβ binding follows AOH.

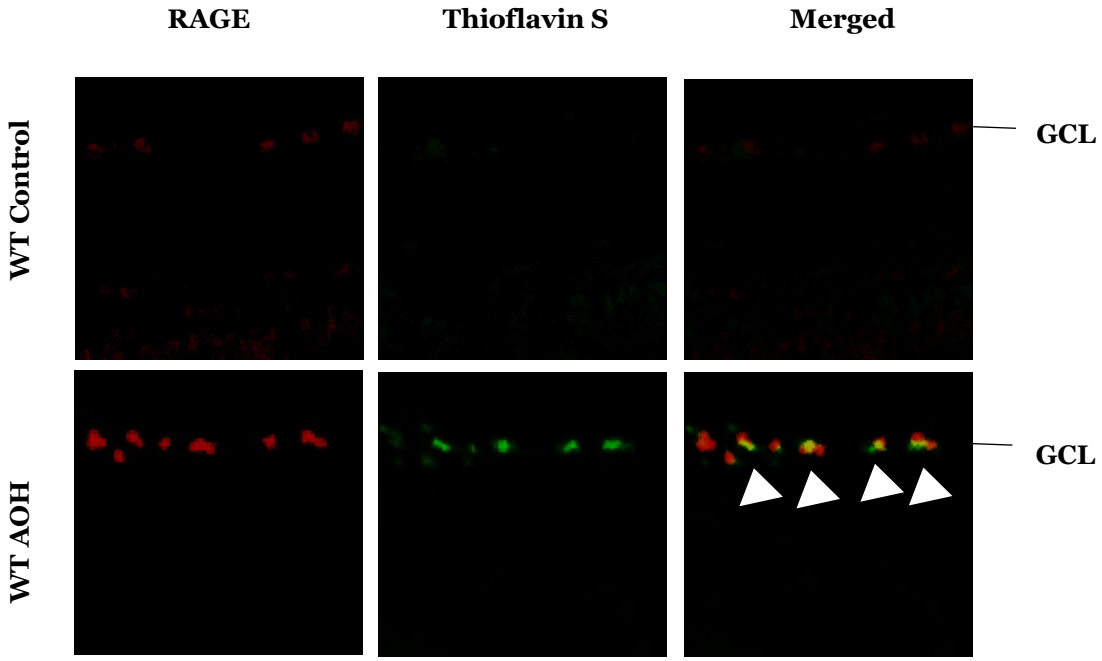

Figure 15. Immunostaining of WT retinas using RAGE antibody. Immunostaining was performed on WT Control and WT AOH retinas at 10 μm thickness using RAGE antibody (red) followed by thioflavin S dyeing for Aβ labelling. Arrows show RAGE and Aβ colocalization in the GCL 1 week following AOH (n=3).

3.3.4. RGC loss occurs because of apoptosis

To investigate the molecular mechanism(s) involved in RGC loss, caspase 3 immunostaining was used as a biomarker of apoptosis to determine whether RGC loss is linked to upregulation of Aβ as shown in the preceding section. Immunostaining showed an increased fluorescence signal intensity of caspase 3 in the GCL of both WT AOH and $RAGE^{-/-}$ AOH (Figure 16, A and B to Figure 29, Appendix). Interestingly, caspase 3 co-localised with Aβ in the immunostaining, which indicates that both caspase 3 and Aβ were upregulated following AOH (Figure 16, A). The caspase 3 signal intensity was 2.3-fold higher in WT AOH than in $RAGE^{-/-}$ AOH retinas (Figure 16, B). The immunoblotting confirmed this by showing 1.8-fold higher cleaved caspase 3 levels in WT AOH than in WT control (Figure 17, A–C).

RGC loss also occurs due to the cell necrosis which is a type of caspase independent RGC loss [144]. There is evidence that necrosis which can be a programmed mechanism known as necroptosis occurs in ischaemia injury [145]. It has been illustrated which RGC loss in ischaemia injury can initiate by activation of several key molecules including RAGE [146]. Therefore, RAGE inhibition can reduce RGC loss after AOH due to both apoptosis and necropsis. However, the exact mechanisms by which RAGE mediates RGC necropsis is not fully understood.

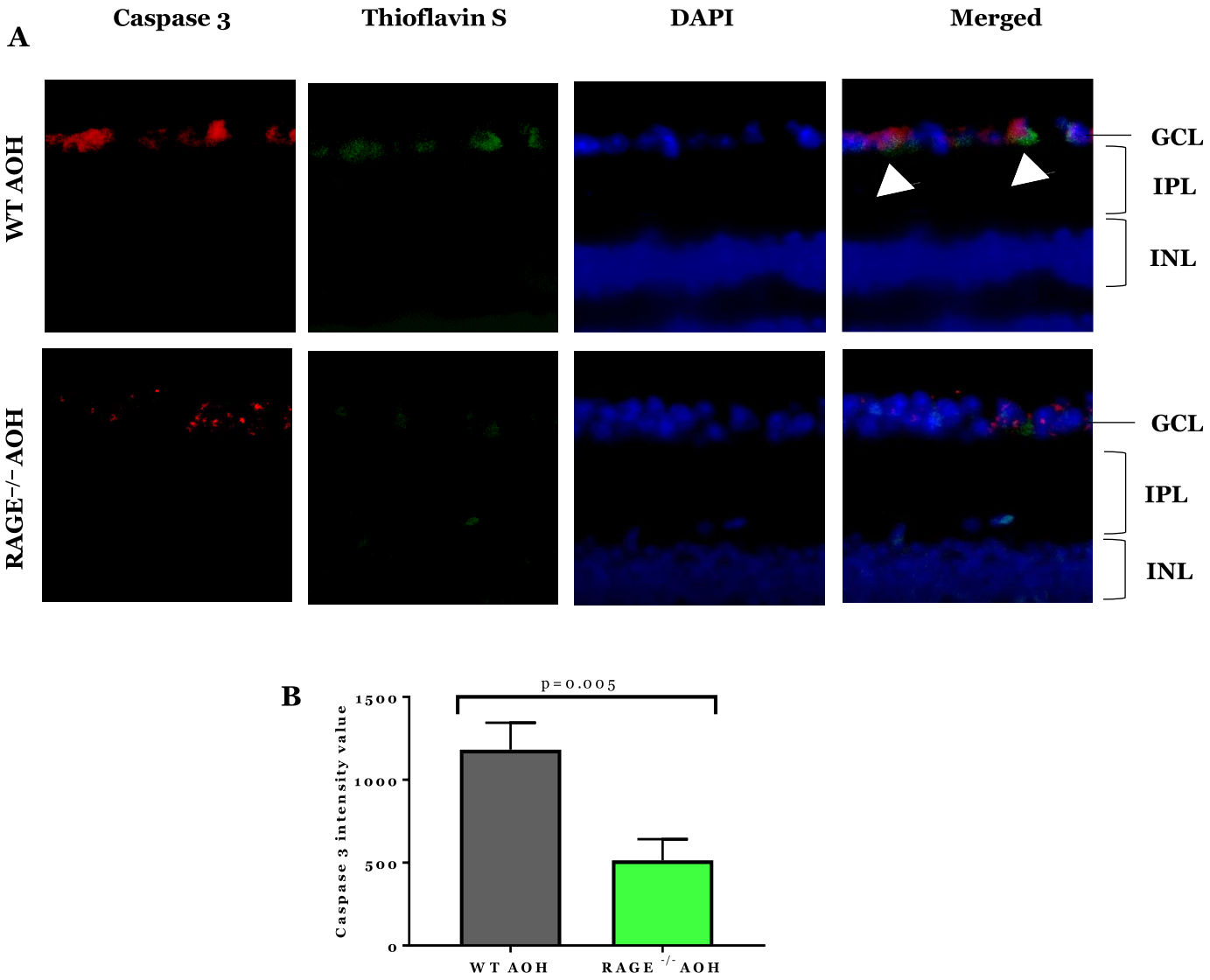

Figure 16. Immunostaining of WT retinas using caspase 3 antibody. A. Immunostaining of retina sections in WT AOH and RAGE$^{-/-}$ AOH at 10 μm thickness using caspase 3 antibody (red) and DAPI (blue). Later Aβ deposits were detected in the GCL with thioflavin S (green); B. Intensity of the caspase 3 (red) signal was quantified using ImageJ software (n=3).

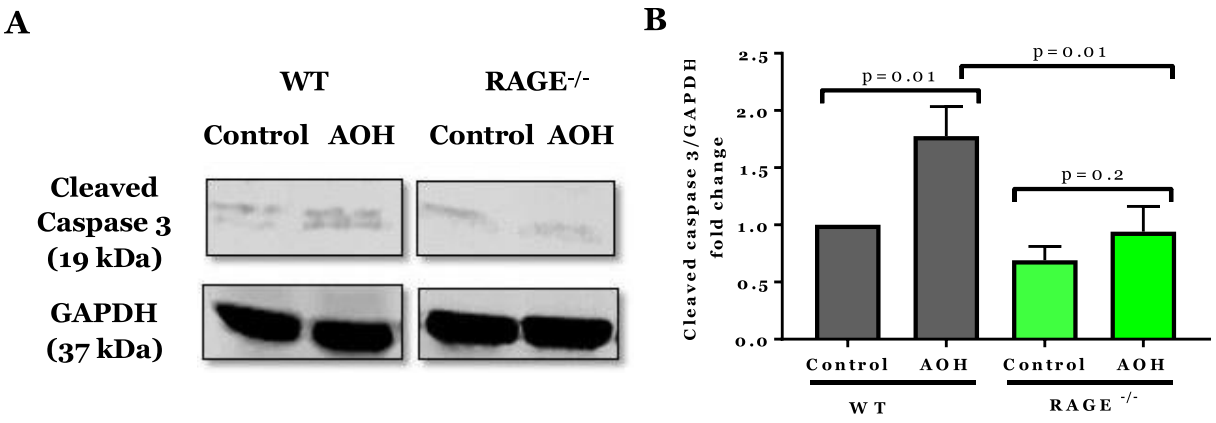

Figure 17. Western blotting of WT and RAGE−/− retinas using caspase 3 antibody. A. Immunoblotting of tissues from mice using caspase 3 antibody shows cleaved caspase 3 band around 19 kDa. GAPDH was used as control (n=3); B. Graph representing densitometric analysis of cleaved caspase 3 expression in WT and RAGE−/− mice (n=3). Data are represented as cleaved caspase 3/GAPDH fold change. The ratio of cleaved caspase3 expression in all tissue samples was compared with WT Control.

3.3.5. Retinal function is partially preserved in RAGE$^{-/-}$ after AOH

The pSTR of the ERG was used to evaluate whether the inner retinal function is preserved in RAGE$^{-/-}$ mice following AOH. The amplitude of the pSTR was lower in both WT and RAGE$^{-/-}$ mice, compared to their respective controls. However, following AOH, the pSTR amplitude was significantly reduced in WT (107±5 µV vs. 73±5 µV, $p<0.01$, n=3) compared with RAGE$^{-/-}$ mice (103±6 µV vs. 94±4 µV, p=0.3, n=3) (Table 9, Figure 18).

Table 9. pSTR alterations in WT and RAGE$^{-/-}$ mice after AOH. pSTR was measured in dark-adapted mice using very dim light that was sufficient to stimulate inner retinal cells including RGCs (n=3).

	Control (µV)	AOH (µV)	p value
WT	107 ± 5, n=3	73 ± 5, n=3	p=0.01
RAGE$^{-/-}$	103± 6, n=3	93 ± 4, n=3	P=0.3

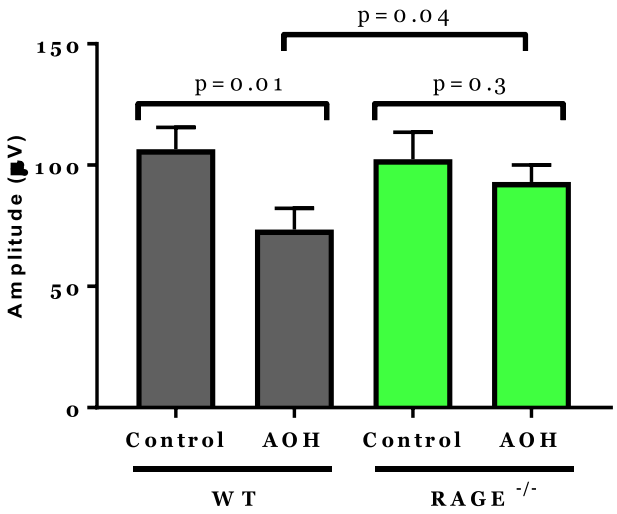

Figure 18. Data analysis of pSTR raw traces in WT and RAGE$^{-/-}$ mice after AOH. Graph representing the comparison of the pSTR amplitude in WT and RAGE$^{-/-}$ mice (n=3). A significant decrease in pSTR amplitude was occurred in WT AOH compared with WT control and RAGE$^{-/-}$ AOH.

3.4. Discussion

This study investigated whether RAGE knockout mice are protected against RGC loss when exposed to an acute IOP elevation in excess of 90 mmHg for a prolonged period (i.e., 45 min). Although AOH led to RGC loss because of apoptosis in both RAGE$^{-/-}$ and WT mice, the RGC loss was significantly greater in WT mice than in RAGE$^{-/-}$ mice. This observation was confirmed by the functional assessment of the retina, which showed partial inner retinal dysfunction in RAGE$^{-/-}$ mice. RAGE and Aβ upregulation were observed in WT mice after AOH. The AOH ischaemic model was used to study RGC loss because it is a well-established model of retinal ischaemia–reperfusion injury in mice [147], [148], which closely mimics glaucomatous pathogenesis. The ischaemic mouse model has been used widely to study RGC loss [123], [149] because it exhibits several similarities with mechanisms that lead to RGC loss in glaucoma [56].

Previous studies have shown a significant loss of RGCs as early as 3 days after AOH [56], [147]. Consistent with previous studies, the histological analysis in this thesis showed significant RGC loss in both RAGE$^{-/-}$ and WT mice, 7 days after AOH. However, RGC loss was more extensive in WT than in RAGE$^{-/-}$ mice, which suggests that RGCs were protected in the RAGE$^{-/-}$ mice. Dvoriantchikova *et al.* also investigated neuronal loss in following AOH. Using Neu-N, as a specific marker of neurons, they reported up to 95% neuronal protection in RAGE$^{-/-}$ mice compared with control mice 1 week after AOH [123]. The experiment presented here used a specific marker for RGCs, Brn3a, to quantify RGC loss. Brn3a is a transcription factor that is important to the development and differentiation of RGCs. Confirming the histology findings, the results from immunoblotting also showed significant loss of Brn3a expression in WT AOH mice.

TRT changes were also evaluated after AOH using images from OCT scans. OCT is used widely to study the retina *in vivo*, and any alterations in the retinal layers can be observed and analysed in real time using this method [150]. TRT thinning was observed in mice 7 days following AOH. Despite this thinning, partial protection of the retinal structure was observed in RAGE$^{-/-}$AOH compared with WT AOH mice. Axonal degeneration precedes RGC soma death in AOH [151]. The nerve fibre layer (NFL) comprises axons of RGCs. It is possible that the NFL layer bore most of the degenerative changes within the retina.

In addition to TRT thinning, analysis of pSTR amplitudes showed inner retinal dysfunction in both types of mice following AOH. pSTR is a sensitive component of the ERG because dark adaption stimulates the inner retina cells at a point near the behavioural threshold [152]. It is believed that the pSTR arises from the inner retina and

depends particularly on the integrity of RGCs [135], [153]. Fortune et al. demonstrated that pSTR is the most sensitive ERG component in experimental glaucoma [146]. Perez de Lara *et al.* reported a significant correlation between a reduction in pSTR amplitude and RGC loss in the DBA/2J transgenic mouse model of glaucoma[154]. In this thesis research, RGC function was significantly lower in WT AOH mice than in $RAGE^{-/-}$ AOH mice.

Previous studies have shown that RGC dysfunction precedes RGC loss [155]–[157]. However, in this thesis research, inner retina dysfunction did not exceed RGC loss and there was no 1:1 correlation of these two alterations. One possibility is that different subtypes of RGCs have different functional susceptibility after injury [158], [159]. There are almost 20 subtypes of RGCs in the eye, and each contributes a specific responsibility to visual function [160]–[162]. Unsurprisingly, the resilience to cellular stress can vary depending on the subtype. Further, some subtypes of RGC recover better than others [163]. Alarcon-Martinez *et al.* showed that the decline in pSTR could be recovered after optic nerve transection, which suggests that RGC dysfunction is reversible [163]. Another possibility is that the STR reflects more than RGC function and is also affected by other cells within the retina. Saszik *et al.* suggested that the pSTR trace can be affected by amacrine cells [135]. The exact origin of the pSTR is not clearly understood [152] and therefore this hypothesis is also likely to affect STR trace.

Current evidence suggests that apoptosis plays a main role in RGC loss in glaucoma [126]. The studies in this thesis research showed caspase 3 upregulation, which suggested that cell loss had occurred because of apoptosis. Activation of caspase cascades occurs in the process of apoptosis, and caspase 3 is activated downstream of this process.

Therefore, caspase 3 antibody was chosen as a marker of apoptosis in RGCs in these studies. Immunostaining and immunoblotting showed upregulation of caspase 3 in WT AOH and RAGE$^{-/-}$ AOH mice. However, the expression of caspase 3 and cleaved caspase 3 was 1.6% and 2% higher in WT AOH than in RAGE$^{-/-}$ AOH, respectively. This implies that inhibition of RAGE may reduce the activation of apoptosis.

Interestingly, caspase 3 has been shown to mediate APP cleavage to Aβ in rat OHT [53]. The histology results showing co-localisation of caspase 3 and Aβ are consistent with this observation. This finding suggests that caspase 3 upregulation directly contributes to apoptosis and increases Aβ production, which eventually leads to further RGC loss. Western blotting showed cleaved caspase 3 upregulation in RAGE$^{-/-}$ AOH mice. However, the amount of cleaved caspase 3 was not higher in RAGE$^{-/-}$ AOH compared with WT AOH, which suggests that RAGE activation may be involved in the initial stages of apoptosis. This suggestion is supported by the visualisation of RAGE upregulation in the GCL layer using immunostaining, which showed a strong RAGE signal in WT AOH. This finding indicates RAGE and caspase activation are linked and that both take part in apoptosis of RGCs. RAGE–ligand signalling has been shown to mediate upregulation of MAPKs and TNF, which are involved in apoptosis of RGCs [77], [164]. The fact that RAGE inhibition did not completely prevent RGC apoptosis provides evidence that a combination of molecular mechanisms is involved in RGC loss [164]. Therefore, it appears that RAGE suppression along with other therapeutic approaches may be more efficient in alleviating RGC loss caused by glaucomatous pathology.

Among the various RAGE ligands, Aβ was studied here because previous studies have established its neurotoxic role in several neurodegenerative disorders including AD.

Tezel *et al.* was the first to report the upregulation of RAGE and its ligand AGE in glaucoma [96]. Since then, other RAGE ligands, including HMGB1 [123] and S100 [132], have been investigated to determine their potential role in RGC loss in glaucoma. Among different ligands, Aβ uptake is shown to be mediated by RAGE from peripheral into CNS via endocytosis and transcytosis [79]. RAGE–Aβ interactions leads to activation of downstream p38 MAPK signalling which contributes to the uptake Aβ to RPE via endo-lysosomal compartments [165]. RAGE further mediates Aβ transport among various brain cells, and within the brain via endocytosis [80]. Therefore, RAGE is involved in Aβ neurotoxicity in disease condition. Current evidence for RAGE upregulation [6], [53], [55] and Aβ accumulation in the retina of experimental and human glaucoma led to the hypothesis that RAGE–Aβ may be involved in RGC loss in glaucoma. Consistent with previous studies, this thesis research observed Aβ in the GCL following AOH and that the strongest signal for Aβ was observed WT AOH mice. The present study has, for the first time, visualised Aβ in the GCL of AOH mice using thioflavin S staining.

The current literature shows that Aβ deposition increases following chronic ocular hypertension. The results of this thesis study are consistent with those of Mi *et al.*, who reported $A\beta_{1-42}$ overexpression in the GCL of AOH mice as indicated by immunostaining [56]. Aβ is produced by the consecutive cleavage of APP, which is expressed in RGCs of the retina in the human, mouse, rat, monkey and rabbit [166]–[169]. It is believed retinal APP plays a physiological role [170]. Besides, enzymes that contribute to the amyloidogenic processing of APP have been detected in retina [171]–[173]. This suggests

that retinal neurons are capable of switching APP processing to the amyloidogenic pathway under cellular stress.

Double staining for RAGE and thioflavin S showed co-localisation of RAGE and Aβ in the GCL of WT AOH mice but not WT control mice. RAGE is a known transporter of Aβ [170] and, regardless of whether Aβ has an intrinsic or extrinsic source, RAGE exacerbates the neurotoxic effects of Aβ via facilitating endocytosis and activating the cell death signalling pathways. The results of this study suggest that RAGE is also involved in Aβ-mediated apoptosis of RGCs in AOH.

In conclusion, results from the present study demonstrate that RAGE activation is one pathway which is involved in RGC loss in AOH. While we detected upregulation of Aβ and caspase 3 activation, further studies are required to confirm the exact underlying mechanism by which RAGE–Aβ axis mediates RGC apoptosis.

4. Chapter 4— RAGE–Aβ signalling mediates RGC loss in glaucoma[6]

4.1. Introduction

RGC loss resulting from chronic exposure to IOP is the main cause of blindness in glaucoma. Numerous efforts have been made to identify the molecular pathways associated with RGC loss in glaucoma, and all have concluded that a combination of several pathways are involved in the underlying molecular pathogenesis of RGC-related neurodegeneration in glaucoma [164].

Glaucoma has evolved over the past few years to be classified as a neurodegenerative disease. Aβ is at the epicentre of major neurodegenerative diseases such as AD [174] and, interestingly, glaucoma [6]. Aβ is produced by the enzymatic cleavage of APP [49], which is produced continually in RGCs [100], [167]. APP upregulation leads to accumulation of Aβs within the retina and has been shown in experimental glaucoma [6], [56]. Recent studies have shown that RAGE mediates the deleterious effects of Aβ in AD by translocating circulating Aβ across the BBB into the brain, which leads to neuronal loss [79]. This process is known as transcytosis [79]. RAGE is also associated with internalisation of Aβ within neurons in the AD brain via endocytosis[79]. Interestingly, RAGE upregulation has been reported in separate studies of experimental and human glaucoma. However, the effects of RAGE–Aβ activation has not been studied in glaucoma. In our previous related study (chapter 2), upregulation of

[6] The current chapter is prepared in research article format and will be submitted to a peer-reviewed journal.

Aβ and RAGE were observed in the GCL of experimental glaucoma, which suggested that RGCs are exposed to the deleterious effects of Aβ. That study also found that RAGE$^{-/-}$ mice are protected against RGC loss following AOH, which supports the notion that RAGE inhibition reduces the devastating effects of Aβ on RGCs. These results are in agreement with those of an earlier study by Guo *et al.*, who showed that targeting Aβ could reduce RGC loss in glaucoma [6]. Mi *et al.* also reported that upregulation of RAGE and Aβ leads to RGC loss in experimental glaucoma [56]. Collectively, these observations prompted the investigation of the effects of the role of the RAGE–Aβ axis in RGC loss.

In the current study reported in this chapter, exogenous Aβ was injected into the vitreous of RAGE$^{-/-}$ and WT mice, and the effects of the RAGE–Aβ axis on RGC loss was assessed at two separate time points.

4.2. Materials and Methods

All methods including preparation of oligomeric Aβ, intravitreal injection of Aβ, sample processing, H&E staining, immunostaining and imaging, thioflavin S staining, SDS-PAGE and western blotting, pSTR, OCT were all performed exactly as explained in chapter 2.

4.3. Results

The current experiment was performed with the aim of investigating whether RAGE mediates RGC loss following exogenous injection of oligomeric Aβ in to the vitreous. Based on the observed results in chapter 3, I expect to see an accelerated and time-dependent RGC loss, following intravitreal injection of Aβ, in WT mice compared with RAGE-/- mice. Further, I explore whether RGC loss occurs due to apoptosis.

4.3.1. Intravitreal injection of Aβ leads to RGC loss

RGC counts on radial H&E sections in 300 μm increments of the optic nerve head showed a non-significant reduction in the extent of RGC loss in WT mice compared with RAGE$^{-/-}$ (28±9% vs. 19± 2%, p=0.4, n=3) 72 h after Aβ injection. However, 1 week after Aβ injection, the decrease in RGC numbers was significantly larger in WT compared with RAGE$^{-/-}$ mice (55±4% vs. 24±1%, p<0.01, n=3) (Figure 19). The percentage of RGCs loss increased significantly from 72 h to 1 week after Aβ injection in WT mice but this increase was non-significant in RAGE$^{-/-}$ mice during this time (Figure 19). These findings suggest that RAGE$^{-/-}$ mice were protected against the neurotoxic effects of injected Aβ and that the neurotoxicity of Aβ is time dependent.

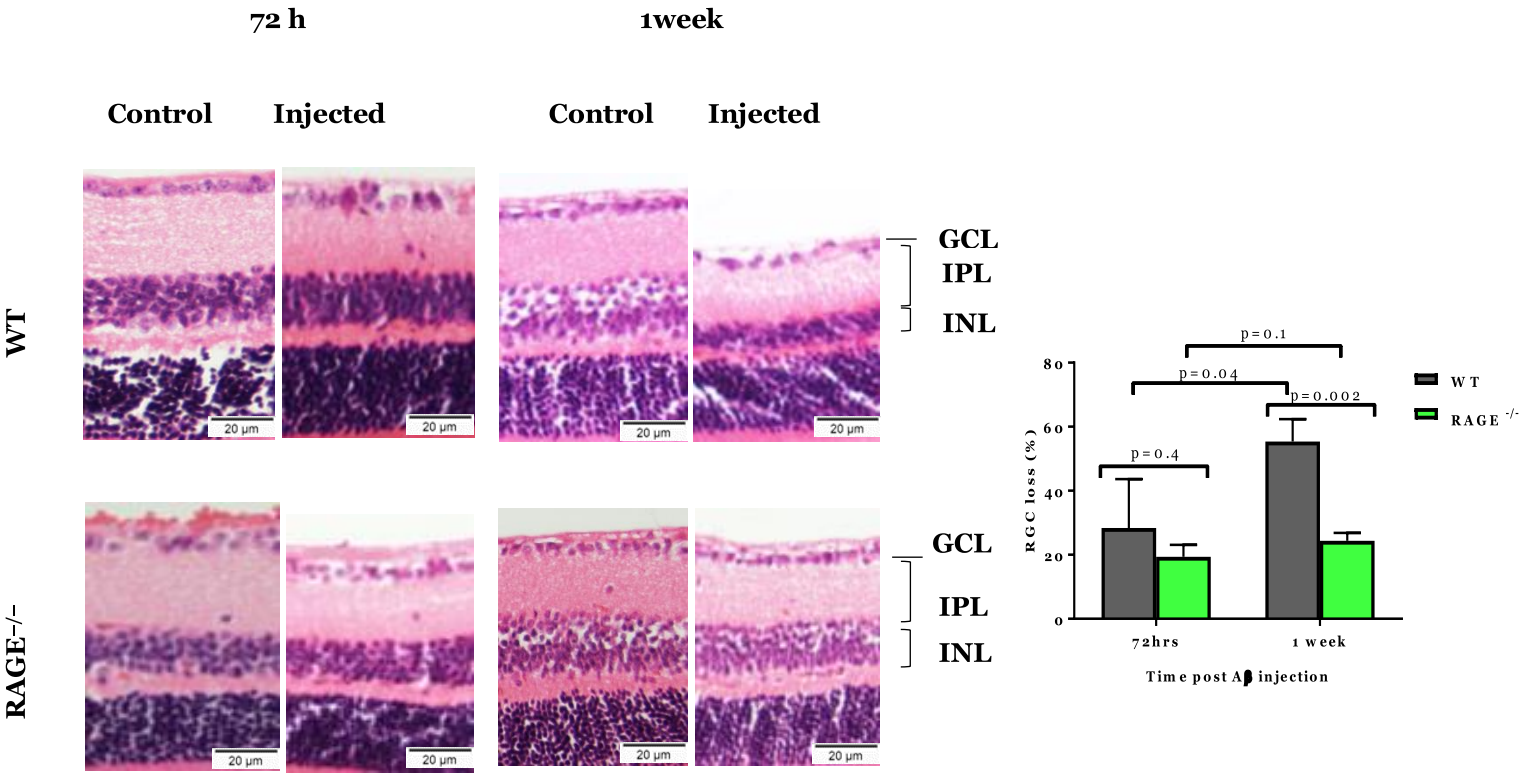

Figure 19. H&E staining of WT and RAGE$^{-/-}$ retina. H&E staining was performed on paraffin-embedded retina sections of WT and RAGE$^{-/-}$ mice at 10 μm thickness 72 h and 1 week after Aβ injection (n=3). RGCs were measured manually around the optic nerve head in increments of 300μm. RGC numbers in Aβ injected eyes of each mice were normalized to that of the saline injected eye and presented as percentage loss. Significant RGC loss was observed in WT at 1 week after Aβ injection compared with RAGE$^{-/-}$ mice. This suggested that RGCs in the retina of RAGE$^{-/-}$ mice were protected against neurotoxicity induced by the injected Aβ.

Retinal structure was also evaluated using OCT scans. TRT thinning was not significant 72 h after Aβ injection in WT mice compared with RAGE$^{-/-}$ mice (7±2% vs. 2±0.7%, p=0.09, n=4) (Figure 20-B). However, the OCT results showed significant thinning of the TRT in WT mice compared with RAGE$^{-/-}$ mice 1 week after Aβ injection (15±1% vs. 4±1%, p<0.01, n=4). Comparison of GCL/IPL thinning between WT and RAGE$^{-/-}$ mice did not show a significant decline 72 h post Aβ injection (15±4% vs. 6±2%, p=0.1, n=4) (Figure 20-C). However, the difference in the GCL/IPL complex between the two groups was significant (28±3% vs. 13 ± 0.7%, p<0.01, n=4) at 1 week after Aβ injection (Figure 20-C). Of note, OCT results showed disruption of the outer retina 72 h after Aβ injection in WT mice. Despite these changes at 72 h, no changes were observed at 1 week, which suggests that the outer retina injury has recovered by 1 week after Aβ injection.

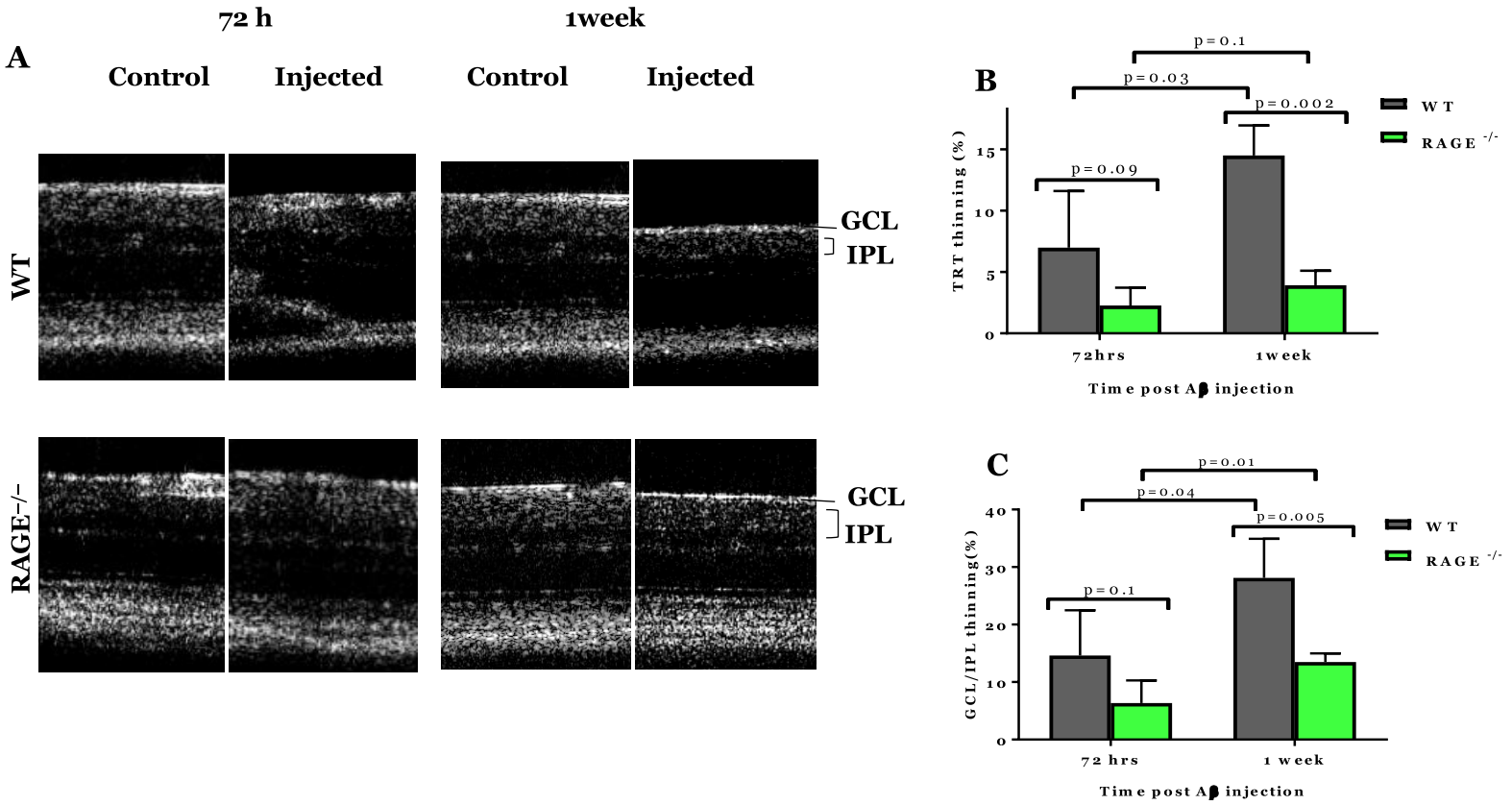

Figure 20. OCT in vivo imaging of WT and RAGE$^{-/-}$ mice. OCT imaging was performed in both the Aβ-injected and vehicle-injected eye (as control). Quantification of TRT and GCL/IPL using octseg.exe software showed significant TRT and GCL/IPL thinning in the WT 1 week after Aβ injection compared with RAGE$^{-/-}$ mice (n=4). TRT and GCL/IPL thinning in Aβ injected eyes of each mice were normalized to that of the saline injected eye and presented as the percentage.

4.3.2. Aβ is internalised in RGCs of WT mice but not in RAGE$^{-/-}$ mice

To examine the possible link between RGC loss and Aβ neurotoxicity, Aβ and RGCs were visualised using thioflavin S and Brn3a immunostaining. Brn3a and Thioflavin S co-localised in the GCL of both WT and RAGE$^{-/-}$ mice. The strongest signal was observed in WT mice 1 week after Aβ injection. A stronger signal for Aβ was observed within the RGCs of WT mice compared with RAGE$^{-/-}$ mice 1 week after Aβ injection. These findings suggest that Aβ was internalised within the RGCs of WT mice (Figure 21, Figure 30-Appendix).

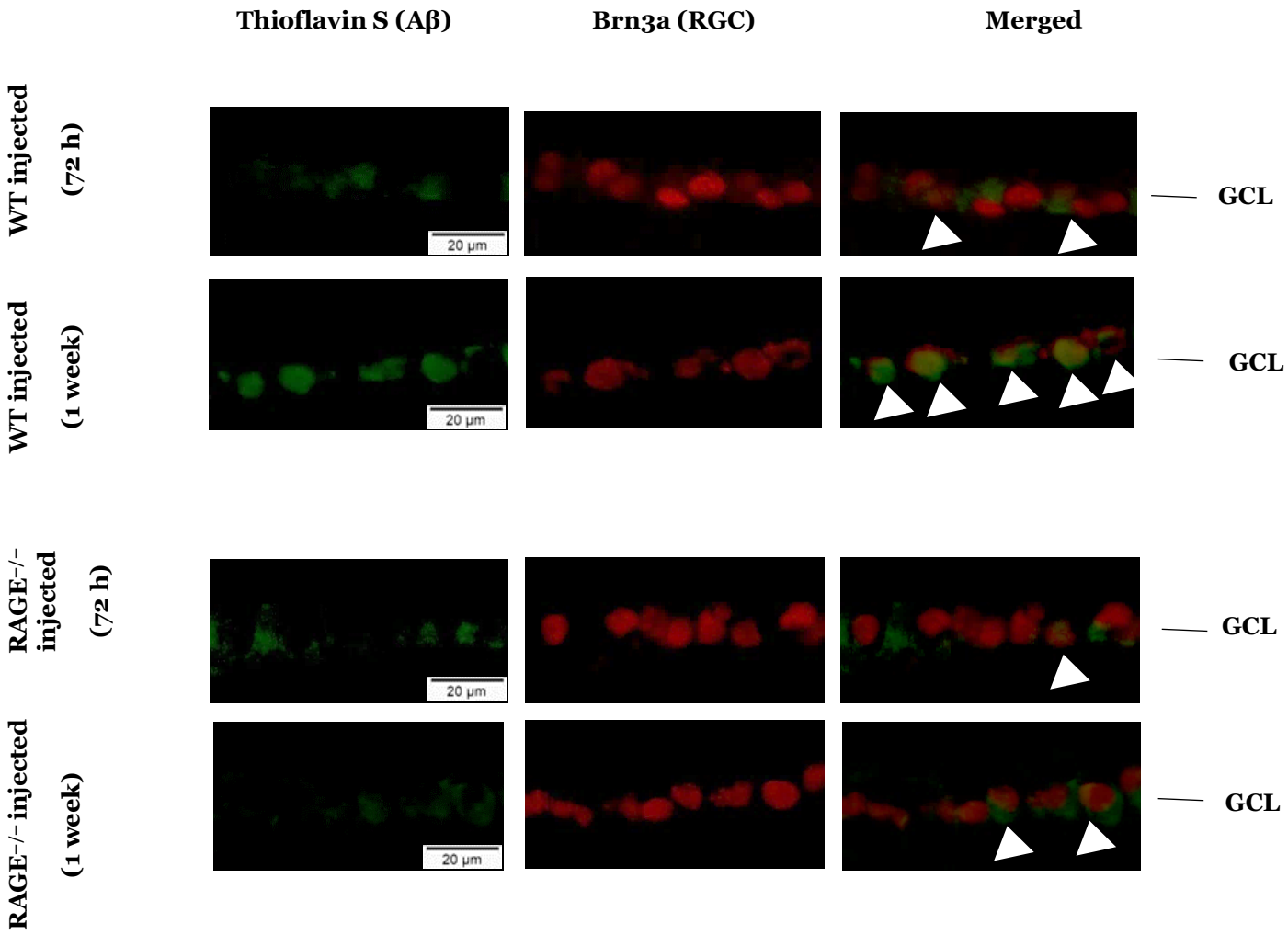

Figure 21. Immunostaining of WT and RAGE$^{-/-}$ mice. Brn3a (red) was used to label RGCs. Thioflavin S (green) was used to stain Aβ. Arrows indicate the strong colocalization of Brn3a and Aβ in WT retina 1 week after Aβ injection (n=3).

To confirm whether RAGE is involved in this internalisation, RAGE expression was assessed in WT mice. A similar trend to that for Aβ deposition was observed: a mild signal for RAGE 72 h after Aβ injection and a strong RAGE signal 1 week after Aβ injection in the GCL of WT mice. RAGE and Aβ co-localised in the GCL, which suggests the activation of the RAGE–Aβ axis in WT mice 1 week after Aβ injection (Figures 22 and 31- Appendix).

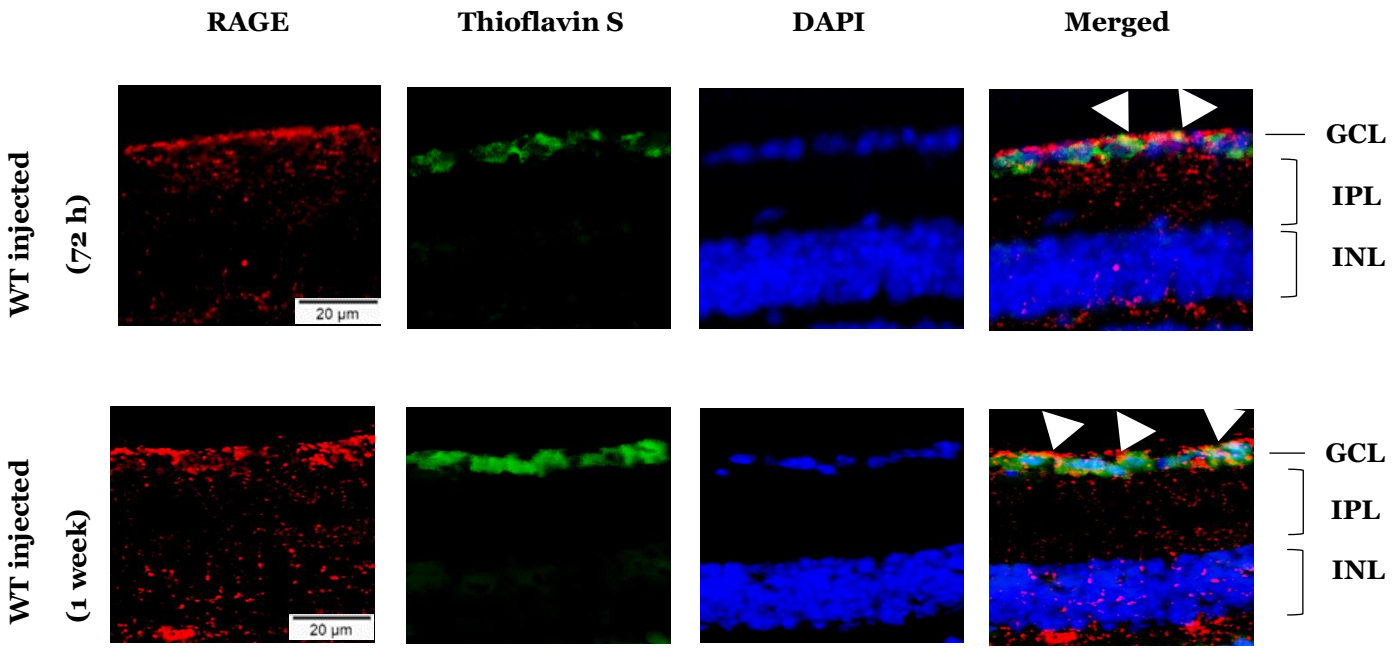

Figure 22. Immunostaining of WT mice using RAGE antibody. Immunostaining was performed on paraffin-embedded retinas of WT mice at 10 µm thickness. Strong RAGE upregulation (red) was observed in the GCL of WT mice 1 week after Aβ injection. Thioflavin S (green) was also used to stain Aβ and DAPI was used for nuclei immunostaining (blue). Colocalization of RAGE, thioflavin S and DAPI (shown by arrows) was observed in the GCL of WT retina 1 week after Aβ injection (n=3).

4.3.3. Aβ mediates RGC loss via apoptosis

To investigate whether Aβ mediates RGC loss via apoptosis, caspase 3 activation was studied as a biomarker of apoptosis. Parallel to the significant reduction in Brn3a levels shown in western blotting 1 week after Aβ injection, strong upregulation of caspase 3 was also detected. This confirmed the suggestion that the higher rate of RGC loss may be related to apoptosis in WT mice. This contrasts with the finding in RAGE$^{-/-}$ mice, which was a non-significant upregulation of caspase 3. These findings suggest that RGCs were protected against apoptosis in RAGE$^{-/-}$ mice (Figure 23).

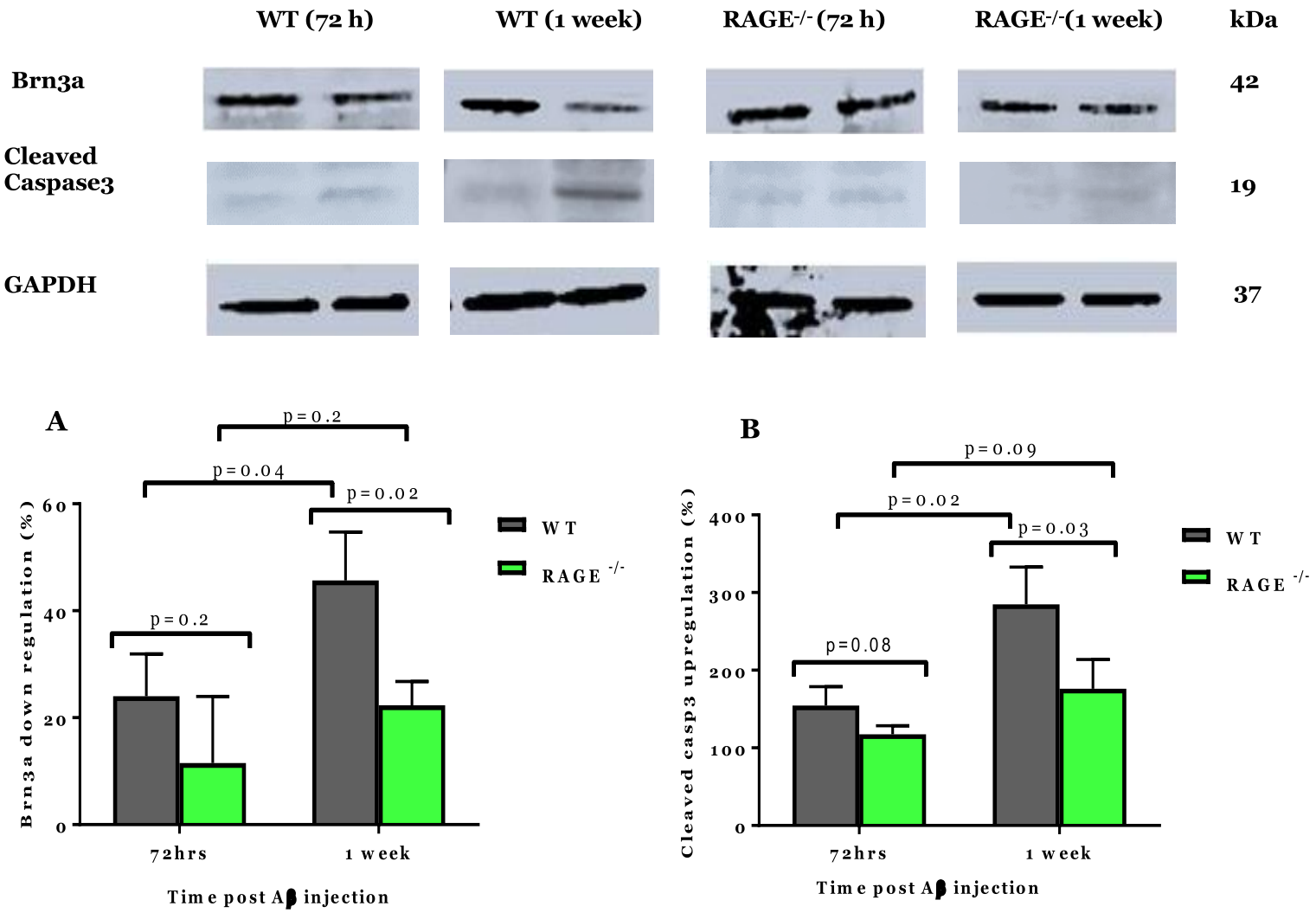

Figure 23. Western blotting of WT and RAGE$^{-/-}$ retinas. Brn3a and caspase 3 antibodies were used in western blotting of retinas; GAPHD was used as a control (n=3). A. Significant loss of RGCs was observed in WT 1 week after Aβ injection compared with RAGE$^{-/-}$ mice; B. In contrast to the significant Brn3a downregulation in WT 1 week after Aβ injection, cleaved caspase 3 were significantly upregulated, which suggested activation of apoptosis in RGCs following Aβ injection (n=3). Brn3q downregulation and cleaved caspase 3 upregulation in Aβ injected eyes of each mice were normalized to that of the saline injected eye and presented as percentage decrease/increase.

Immunostaining results also showed upregulation of caspase 3 upon intravitreal injection of Aβ. Although the co-localisation of caspase 3 and Aβ was observed in WT mice, a moderate caspase 3 signal was also detected in RAGE$^{-/-}$ mice 1 week after Aβ injection. However, caspase 3 and Aβ co-localisation was observed mainly in WT Aβ-injected mice (Figure 24, Figure 32-Appendix).

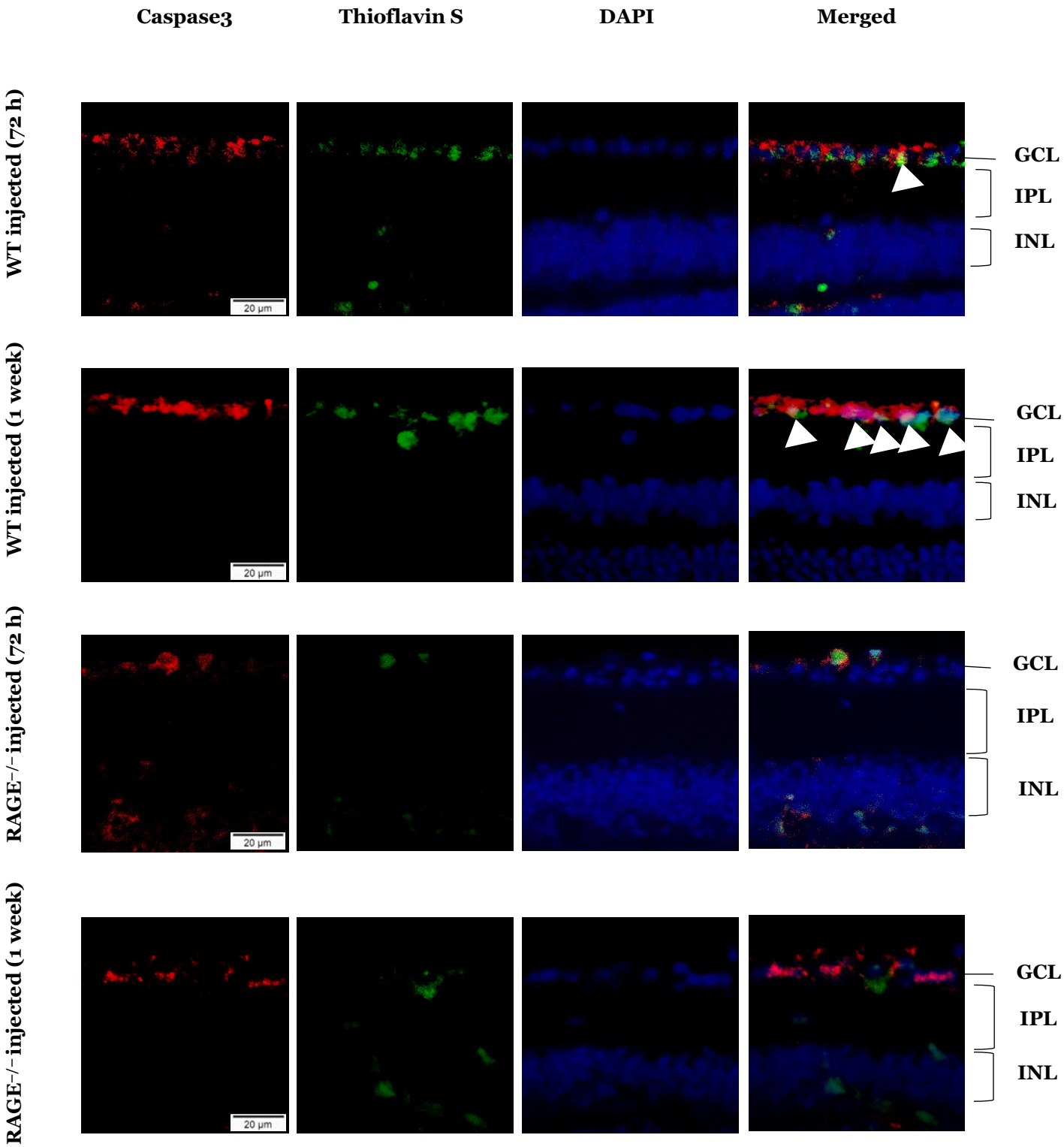

Figure 24. Immunostaining of WT and RAGE−/− retinas using caspase 3 antibody. Immunostaining was performed on paraffin-embedded retinas of WT mice at 10 µm thickness. Strong co-localization of caspase 3 and thioflavin S (indicator of Aβ) was observed mainly in the GCL of WT mice. Nuclei were labelled using DAPI (n=3).

4.3.4. Exogenous Aβ disrupts inner retinal function

Finally, the pSTR was assessed to evaluate whether the inner retinal function is preserved in RAGE$^{-/-}$ mice following exogenous Aβ injection. The amplitude of pSTR declined in both WT and RAGE$^{-/-}$ mice, and this reduction was larger at 1 week compared with 72 h. A significant decline in pSTR amplitude was observed only in the WT mice 1 week after Aβ injection (Table 10, Figure 25).

Table 10. pSTR measurements in WT and RAGE$^{-/-}$ mice. Vehicle-injected eye was used as a control. Animals were dark adapted overnight. pSTR traces were obtained using the Multi-species ElectroRetinoGraph. pSTR traces in both WT and RAGE$^{-/-}$ mice showed a significant decline in WT 1 week after intravitreal Aβ injection (n=3).

	Control (μv)	Injected (μv)	p value
WT 72 h	84± 10	71 ± 9	p=0.4
WT 1 week	101 ± 12	64 ± 5	p=0.04
RAGE$^{-/-}$72 h	93 ± 15	83 ± 12	p=0.6
RAGE$^{-/-}$ 1 week	96± 13	79 ±7	p=0.3

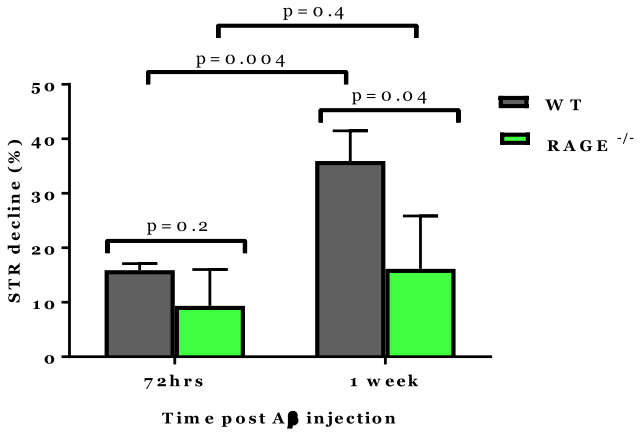

Figure 25. pSTR analysis of dark-adapted WT and RAGE$^{-/-}$ mice. Graph representing pSTR analysis of WT and RAGE$^{-/-}$ mice retinas showed a significant decline of the pSTR in WT mice 1 week after Aβ injection compared with RAGE$^{-/-}$ mice. WT mice also showed a significant decline of pSTR compared with WT mice 72 h after Aβ injection. This suggested an increase in inner retinal disruption including RGCs 1 week after Aβ injection.

4.4. Discussion

This study demonstrates, for the first time, that RAGE regulates Aβ-mediated RGC loss leading to apoptosis. The intravitreal injection of exogenous Aβ oligomers led to progressive damage to the retinal structure and function. Collectively, these results suggest that RAGE– Aβ activation is actively involved in RGC survival and loss.

Previous studies have shown that Aβ has a neurotoxic effect on RGCs [7]. Aβ accumulation impairs normal intra- and intercellular functions, and progressively leads to neuronal death and release of various forms of Aβ into the extracellular microenvironment. In its oligomeric form, Aβ is a highly penetrative molecule because of its amphipathic structure [175]. Further, the Aβ cell surface receptor, RAGE, facilitates the extracellular uptake of Aβ by brain neurons via endocytosis [84]. The results

presented here confirm this effect on the extracellular uptake because more intracellular Aβ signals were detected within RGC neurons in WT mice compared with RAGE$^{-/-}$ mice. Oligomeric Aβ which is not present in normal physiological conditions was injected in mice eye. Oligomeric Aβ is known to be highly toxic and is capable to bind to RAGE [140], [176]. This finding suggests that RAGE is actively involved in transporting extracellular Aβ into RGCs from the vitreous via endocytosis. However, Aβ internalisation was not completely inhibited, which indicates that other pathways that are involved in Aβ translocation. Lana *et al.* showed that internalisation of Aβ was reduced by up to 55% following RAGE blockage [177]. Taken together, these findings suggest that RAGE regulates at least one of the pathways associated with Aβ endocytosis.

RAGE–Aβ activation not only takes part in Aβ endocytosis but also activates signalling pathways such as p38 MAPK [84]. Activation of MAPK pathways has been shown to be one molecular mechanism involved in RGC apoptosis [164] in glaucoma. Interestingly, Kheiri *et al.* reported that targeting the p38 MAPK pathway can efficiently suppress the neurotoxicity of Aβ in AD[178]. This confirms that RGC loss does mimic cerebral neuronal loss in AD and that inhibiting RAGE–Aβ binding may be a useful and effective way to protect RGCs in glaucoma. Unfortunately, this thesis did not investigate whether a similar signalling pathway such as p38 MAPK mediates RGC loss, and further studies are currently underway to investigate this notion. However, caspase 3 upregulation was observed in the GCL following Aβ injection. This was consistent with a previous finding presented in Chapter 2 showing caspase 3 overexpression following AOH. Ji *et al.* observed activated caspase 3 and positive TUNEL staining signal 2 weeks after AOH [179]. Other studies, also using the ocular hypertension model, have shown

activation of caspase 3 in the initial stages of glaucoma [180], [181]. McKinnon *et al.* reported that activation of caspase 3 leads to RGC apoptosis and alters the normal processing of APP, which result in increased deposition of Aβ [180]. This indicates a link between caspase 3 activation and increased Aβ deposition in experimental glaucoma, a phenomenon that was also observed in the studies reported in this chapter.

These results lead to a new hypothesis that RAGE–Aβ is involved in RGC apoptosis probably via activation of caspase cascades. This hypothesis proposes that the internalisation of Aβ within RGCs through RAGE–Aβ activation (as explained earlier) initiates a cascade of events that ultimately leads to RGC apoptosis. It is also likely that RAGE–Aβ-mediated signalling pathways activate apoptosis via upregulation of intermediates leading to caspase 3 activation and, eventually, to RGC apoptosis. However further investigations are needed to test this hypothesis.

5. Chapter 5— Conclusion and Future Directions

5.1. Conclusion

The molecular mechanisms that mediate RGC loss in glaucoma have been reviewed in the literature and studied experimentally in both animal models and cell lines. There is uncertainty in the literature regarding the underlying pathophysiological mechanisms that disturb RGC function in glaucomatous pathology. The new evidence from experimental studies in a transgenic mouse model that lacks RAGE ($RAGE^{-/-}$) provided in this thesis builds upon and supports evidence from the literature that RAGE and its ligand, Aβ, are actively involved in neuronal cell loss following ischaemic insult, a phenomenon demonstrated in neurodegenerative diseases such as AD and glaucoma. These findings explain the potential pathophysiological role that RAGE and Aβ may play in mediating RGC loss in glaucoma.

Elevated IOP is a major risk factor for glaucoma. In the appropriate asymptomatic patient, a range of pharmacological interventions including prostaglandin analogues, beta-blockers, carbonic anhydrase inhibitors, sympathomimetics and miotics can be used to maintain IOP at the physiological level (i.e., 10–20 mmHg). In the non-responding patient, laser-based treatments can be applied to the trabecular meshwork to restore aqueous fluid drainage but carries a risk of developing acute angle-closure glaucoma. Successful management of glaucoma requires a detailed knowledge of the risks and benefits of pharmacological interventions and laser treatment. However, the major challenge in the field is the progressive loss of RGCs in a significant proportion of patients who do not respond to therapeutic or laser treatment. This progressive cell damage ultimately leads to vision loss and blindness.

RGCs in the GCL form the axons of the optic nerve that synapse in various locations of the brain including the superior colliculus, later geniculate nucleus and hypothalamus. The inner (neural) retina, the residence of RGCs, is classified as an outgrowth of the CNS and, not surprisingly, most pathways associated with disease pathogenesis in the brain can be applied to the retina. Evidence from the current literature indicates that apoptosis appears to be the common pathway for RGC loss in glaucoma. Aβ, the major component of senile plaques in AD and drusen components in AMD [172], is known to initiate various types of toxic mechanisms that contribute to neuronal death via apoptosis. Similarly, recent studies have suggested that Aβ is implicated in RGC apoptosis in glaucoma [53], [182]. Reports from animal models of glaucoma have provided evidence that caspase 3 mediates an abnormal processing of APP, which leads to increased expression of Aβ in RGCs. This supports the idea that Aβ has potent neurotoxic effects on RGCs in glaucoma.

Targeting pathways that promote Aβ in glaucoma may significantly delay and attenuate RGC apoptosis. Previous studies have shown that targeting the Aβ pathway can reduce RGC apoptosis by up to 80% [6]. Most low-concentration physiological and pathological mediators exert their effects by actively engaging receptors to assemble molecules at the cell surface and use signal transduction to increase their effects. This has already been demonstrated in AD. For example, it has been suggested that RAGE, a cell surface and Aβ receptor, acts as a carrier in transmembrane Aβ transport and mediates Aβ internalisation through endocytosis, both of which are established pathways for intraneuronal Aβ cytotoxicity. This concept led to the hypothesis that, in a similar process, RAGE may function as a pathological receptor in the early stages of glaucoma, when Aβ oligomers are most toxic to RGGs, and later in the course of the disease, when a higher

concentration of Aβ is present. Other underlying mechanisms may also be activated and contribute to the RGC loss.

Chapter 1 of this thesis (the literature review) covered the basics of why glaucoma may be classified as a neurodegenerative disease, its links with AD and mechanisms that may lead to RGC loss. The role of RAGE in AD and its expression in the retina during the pathological process was also presented. The chapter concluded that, based on a growing body of evidence showing that, in AD, RAGE can act as a receptor that magnifies Aβ cytotoxicity and given the striking underlying physiological and pathological similarities between glaucoma and AD, a similar cascade of events may occur in glaucoma that ultimately lead to RGC loss. This led to further experiments to explore the role of RAGE and its ligand Aβ in an established mouse model of AOH (experimental glaucoma).

To test this hypothesis and to determine whether RAGE and Aβ mediate RGC loss, AOH was induced in genetically modified C57BL/6 mice (RAGE knockout or RAGE$^{-/-}$) and C57BL/6 WT control mice. This model is also known as the retinal ischemia–reperfusion model. This model was chosen based on the pathological consequences of the procedure, which closely mimic clinical neurodegeneration in the retina. More specifically, the inner retina is particularly vulnerable in this model and manifests as RGC loss via retinal neurodegeneration as the most salient feature of this model.

The first set of experiments in this thesis (Chapter 3) showed that, following AOH, both RAGE$^{-/-}$ and WT mice exhibited RGC loss; however, significantly more RGCs were lost in WT than in RAGE$^{-/-}$ mice. A non-significant change in retinal structure and function, as assessed by OCT and ERG, confirmed the resilience of RGCs in RAGE$^{-/-}$ mice

to an immediate and acute elevation of IOP. The changes in RAGE and Aβ level in response to AOH was then explored. Higher RAGE expression and increased Aβ deposition was observed in the GCL of WT AOH mice. By contrast, only a weak signal for Aβ was observed in RAGE$^{-/-}$ AOH mice. Interestingly, co-localisation of RAGE and Aβ in the GCL of WT AOH was seen; this observation confirmed RAGE–Aβ binding following AOH.

This thesis research next examined whether RAGE–Aβ activation mediates RGC loss via apoptosis. The caspase family members are all well-known mediators of RGC apoptosis and caspase 3, in particular, is activated downstream of both the intrinsic and extrinsic pathways. Immunoblotting showed an increase in caspase 3 activity in WT AOH and RAGE$^{-/-}$ AOH retinas, but significantly greater caspase 3 activation was observed in the WT compared with the RAGE$^{-/-}$ AOH retinas. Remarkably, co-localisation of RAGE–Aβ and caspase 3–Aβ was observed in the GCL of WT AOH retinas. This observation further supports the notion that RAGE–Aβ binding is involved in RGC loss via apoptosis.

To determine the specificity of Aβ in mediating RGC loss through binding to RAGE, exogenous Aβ oligomers were injected into the vitreous of the eye to determine whether this would accelerate RGC loss in WT but not RAGE$^{-/-}$ mice (Chapter 3). The $A\beta_{1-42}$ isoform was chosen for injection based on previous studies showing that this particular isoform is has the most potent neurotoxicity to RGCs. The animals were euthanised at two time points after Aβ injection (72 h and 1 week) to determine whether RGC loss is time dependent. WT control mice exhibited significant loss of RGCs, retinal structure and function in compared with RAGE$^{-/-}$ mice, 1 week after Aβ injection. Immunofluorescence

images showed a time-dependent accumulation of RAGE and Aβ in the GCL of WT mice. The immunoreactivity of caspase 3 was greatest in the WT 1 week after injection. Together, these results suggest that RAGE–Aβ binding is a time-dependent process that ultimately leads to RGC loss via apoptosis.

In summary, the results presented here demonstrate, for the first time, that the RAGE–Aβ axis is actively involved in RGC loss following glaucomatous injury. These findings provide new insight into how RAGE–Aβ binding can amplify the critical effects of Aβ on several signalling molecules that mediate RGC loss via the apoptotic pathway. These results also demonstrate that RAGE expression increases and remains elevated as long as Aβ is present. This could result in production of a positive feedback loop through which RAGE initiates and perpetuates Aβ neuronal toxicity. Collectively, these results establish that RAGE-mediated endocytosis leads to Aβ internalisation in RGCs and ultimately neuronal Aβ cytotoxicity.

5.2. Limitations and future directions

This thesis research has used a rodent model for neurodegenerative glaucomatous pathology to identify the potential mechanisms linking RAGE and its ligand Aβ to accelerated RGC loss following acute IOP elevation. This study was based on an acute model and further studies, particularly using transgenically modified acute and/or chronic models of glaucoma (e.g. DBA/2J), should be completed before extrapolating the findings to a pharmacological target. Although this acute model differs from chronic conditions in timeline and aetiological origin, it provides a sound platform for evaluating the underlying causes of retinal neurodegeneration in glaucoma. Complementary tests

including in vivo behavioural studies such as orientation tests [183], maze tests [184], and optokinetic tests [185] which measure visual performance in mice eye can be also useful for analysing retinal dysfunction.

A limitation of the current study was the short timeframe chosen post Aβ injection. The first timepoint (i.e. 72hrs) was chosen based on current available evidence reported by Guo *et al.* [6]. However, as we did not observe a significant RGC loss at this timepoint, therefore animal euthanasia was extended to 1 week post Aβ injection which showed a significant RGC loss in WT mice. Ideally, to investigate time-dependent Aβ regulation of RGC loss, animal survival should be extended up to a month.

The compelling findings from this study suggest that inhibiting RAGE activity in glaucoma may lead to successful attenuation of RGC loss. I propose two potential approaches to achieve this. First, experiments could be conducted using animal models of acute and chronic glaucoma and administering FPS-ZM1, a BBB-permeant, non-toxic, tertiary amide, high-affinity and multimodal blocker of RAGE to determine its specificity and efficacy in reducing RGC loss. Second, experiments could examine the effects of supplementation with the soluble isoform of RAGE, sRAGE, in an animal model of glaucoma. sRAGE is known to increase blood flow and reduce neuroinflammation and tertiary amide levels by acting as a decoy receptor that sequesters the Aβ and prevents it from interacting with RAGE. Interestingly, sRAGE may also be a possible biomarker for glaucoma. Detectable levels of sRAGE in human plasma have been linked to a number of chronic conditions including diabetes and AD. It would be interesting to study plasma sRAGE levels in a glaucoma vs non-glaucoma group to determine whether sRAGE also plays a role in glaucoma.

The studies described in this thesis demonstrate that the RAGE–Aβ mediates RGC loss via the apoptotic pathway. However, the underlying mechanistic link between RAGE-mediated signalling pathways and Aβ neurotoxicity needs further investigation. Previous studies have shown that RAGE–Aβ binding activates p38 MAPK, which leads to intracellular accumulation and, ultimately, Aβ-induced neuronal loss in the brain. The MAPKs are proposed as a primary candidate for RAGE-mediated signal transduction because both p38 and JNK have been implicated in the neurotoxic effects of Aβ [186]. By using selective inhibitors of JNK and p38 MAPK, it would be interesting to study the downstream effects of Aβ on RGCs in glaucoma.

In conclusion, a combination of studies are required to understand fully the role of RAGE–Aβ interaction in mediating RGC loss in glaucoma. These include:

1. studying the RAGE–Aβ axis in a chronic mouse model and in larger animals
2. determining the efficacy of RAGE inhibitors in protecting RGCs in glaucoma
3. determining the underlying mechanism for RAGE–Aβ-induced cellular perturbations.

Appendix — Supplementary results

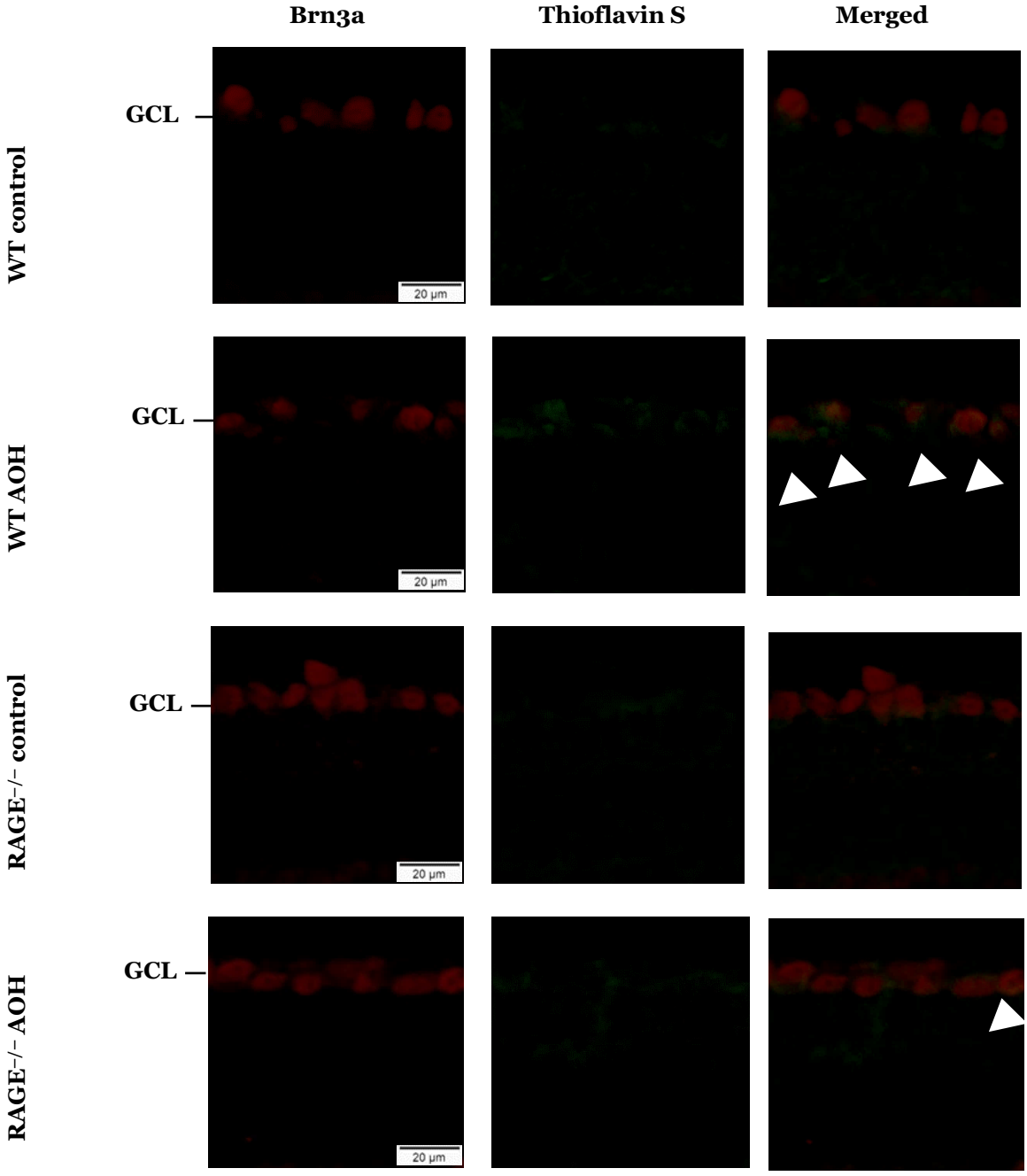

Figure 26. Immunostaining of WT and RAGE$^{-/-}$ retinas using Brn3a antibody. Brn3a (red) was used as a specific marker of RGCs. Following Brn3a immunostaining, retinas were stained with thioflavin S (green) for Aβ labelling (n=3).

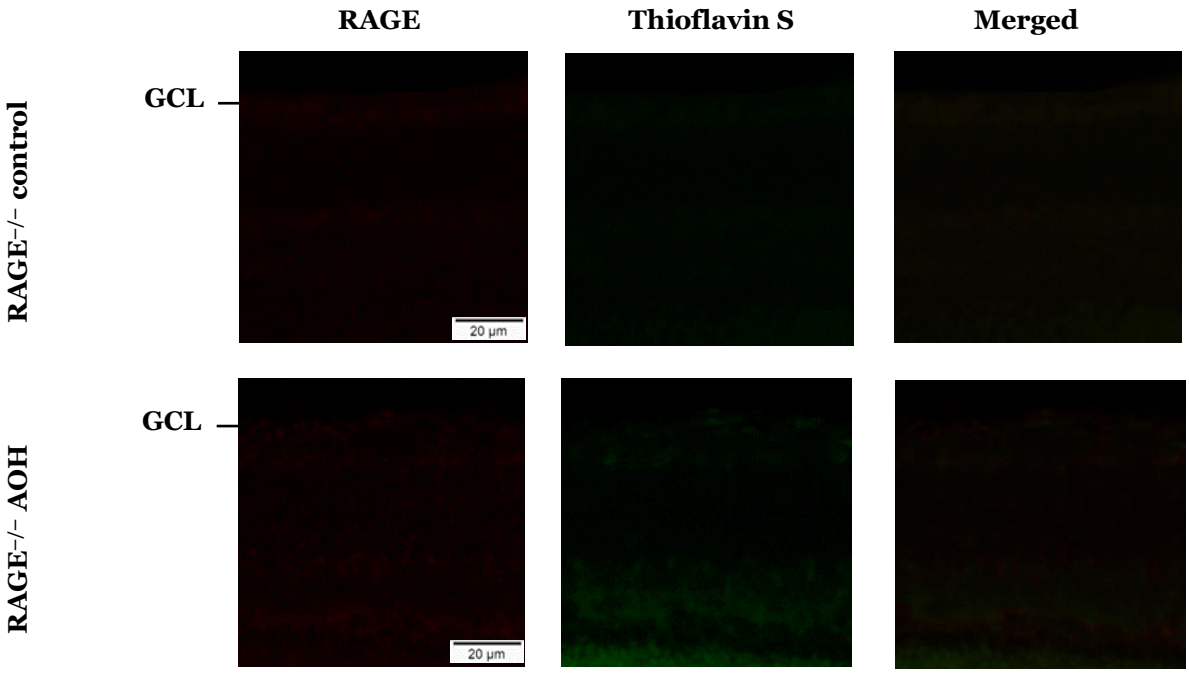

Figure 27. Immunostaining of RAGE antibody in RAGE−/− retinas. Immunostaining of RAGE retinas was performed along with immunostaining of WT retinas, as discussed in Chapter 2. Unsurprisingly, no RAGE signal was observed in RAGE−/− tissues. RAGE antibody (red channel) and thioflavin S (green channel) were used for labelling RAGE and Aβ, respectively (n=3).

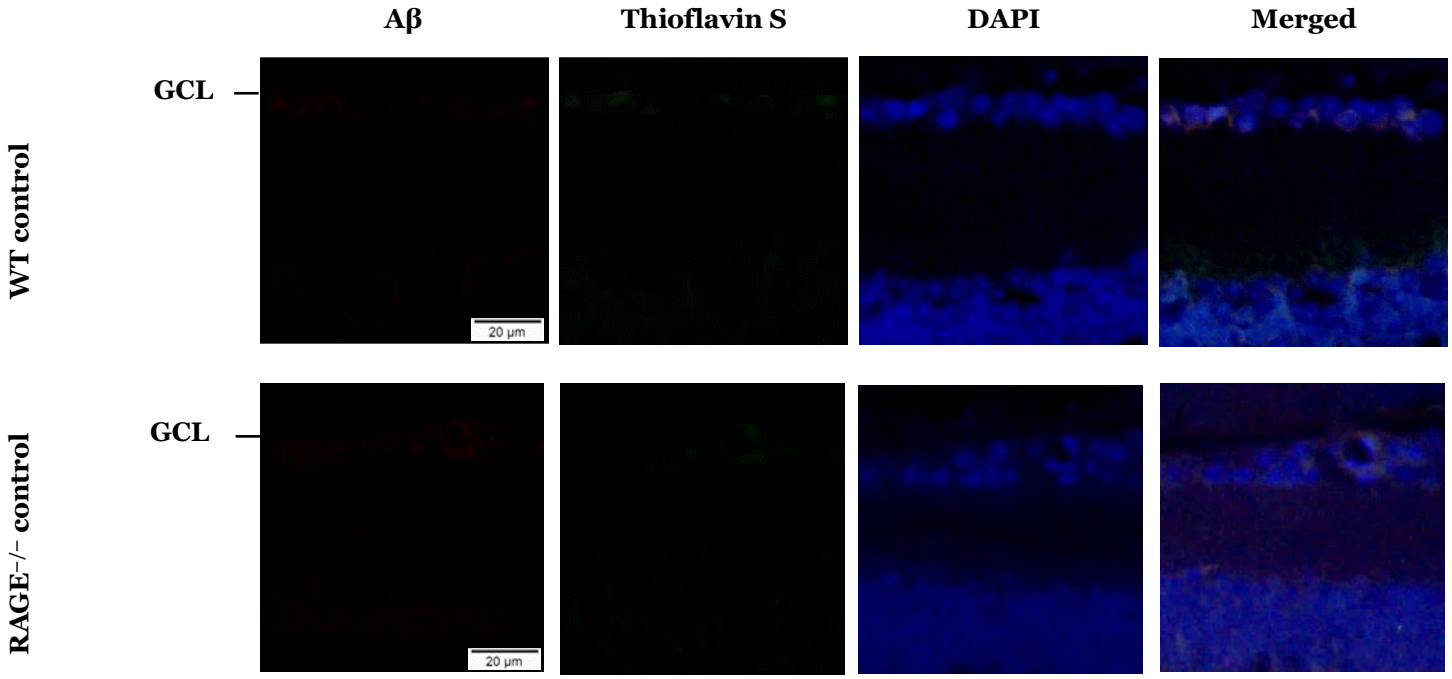

Figure 28. Immunostaining of Aβ in WT control and RAGE$^{-/-}$control retinas. Immunostaining of control retinas from WT and RAGE$^{-/-}$ mice was performed along with immunostaining of AOH retinas using Aβ antibody (red channel) followed by thioflavin S (green channel) staining. DAPI was used for nuclei labelling (n=3).

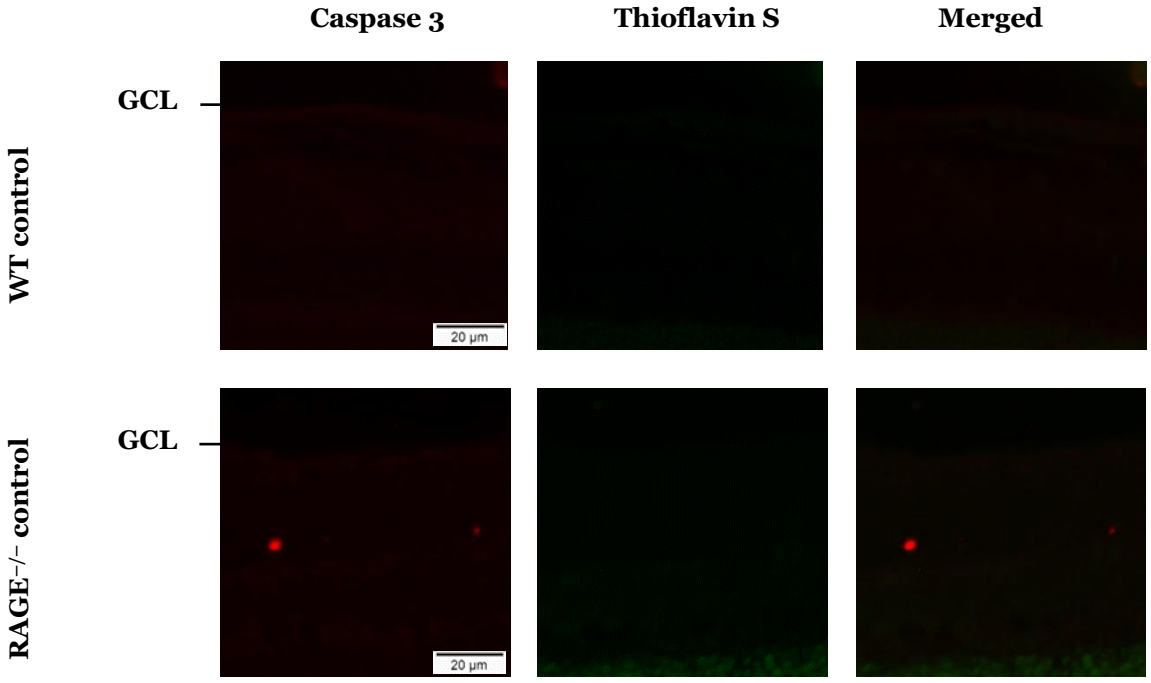

Figure 29. Immunostaining of caspase 3 antibody in WT control and RAGE$^{-/-}$ control retinas. Immunostaining of control retinas using caspase 3 antibody in WT and RAGE$^{-/-}$ mice was performed along with immunostaining of AOH retinas. Thioflavin S (green channel) staining was used for Aβ labelling. DAPI was used for nuclei labelling (n=3).

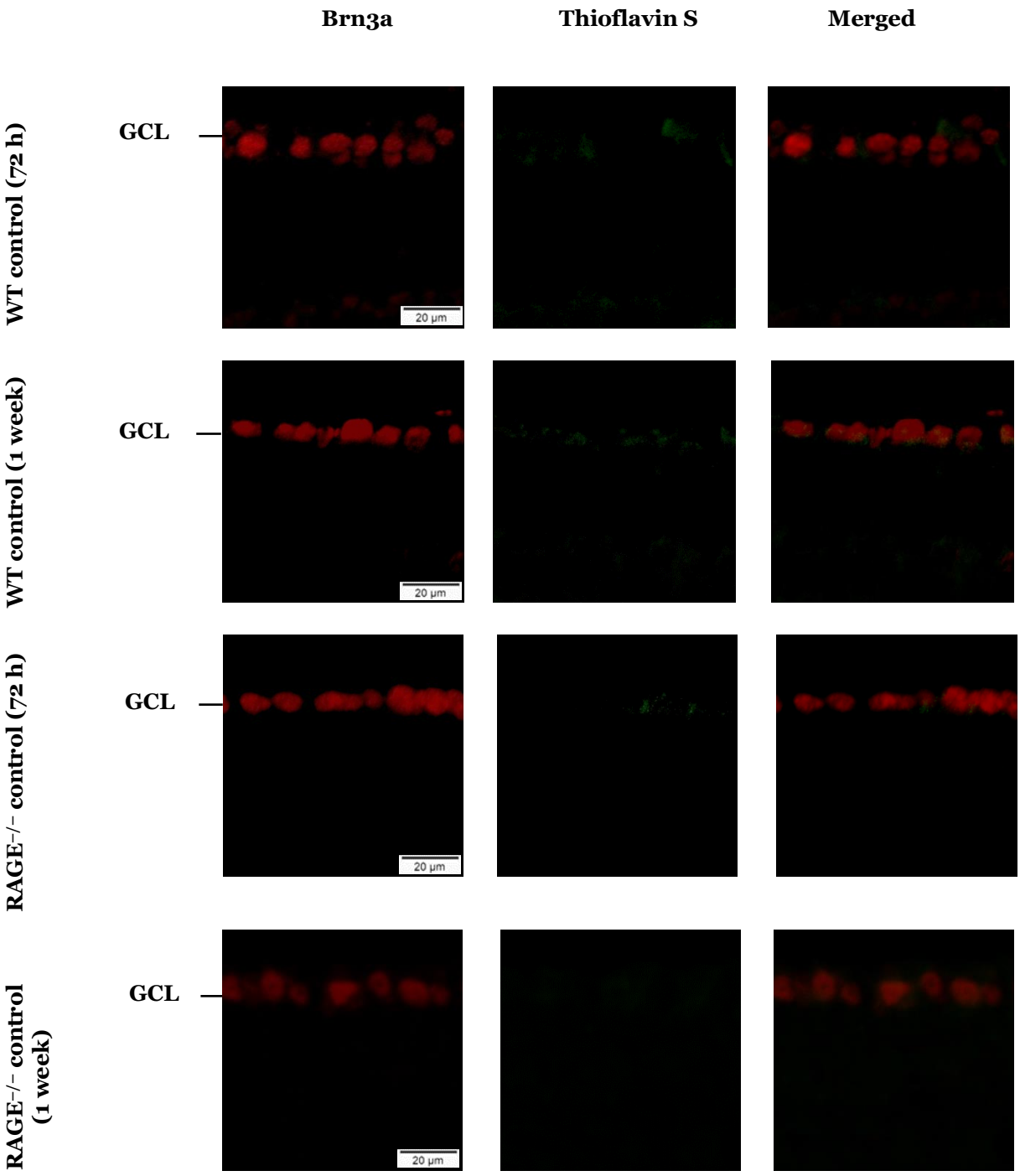

Figure 30. Immunostaining of Brn3a antibody in control retinas. Immunostaining of control retinas from WT and RAGE-/- mice was performed along with immunostaining of injected retinas using Brn3a antibody (red). Brn3a was used as a specific marker of RGCs. Following Brn3a immunostaining, thioflavin S staining (green channel) was used for Aβ immunostaining (n=3).

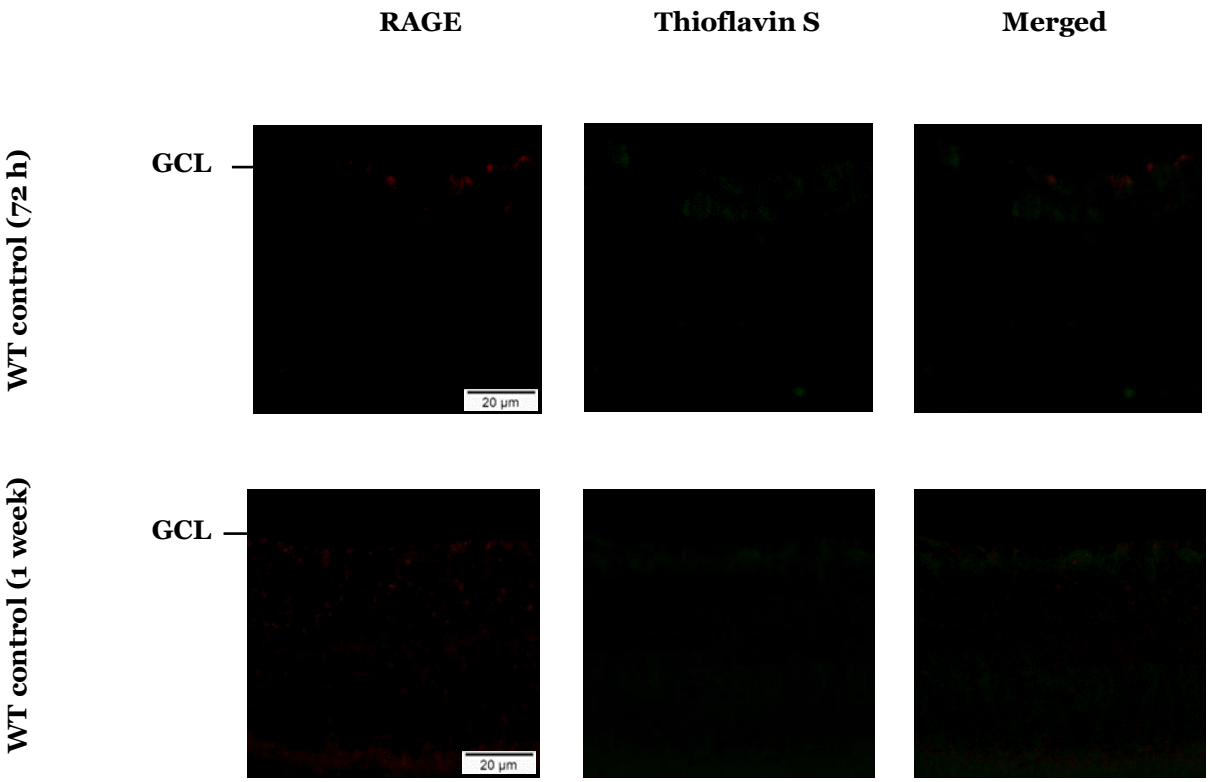

Figure 31. Immunostaining of RAGE antibody in WT control retinas. Immunostaining of WT control retinas was performed along with immunostaining of injected retinas using RAGE antibody (red channel). The tissues, were then subjected to thioflavin S (green channel) staining for Aβ labelling (n=3).

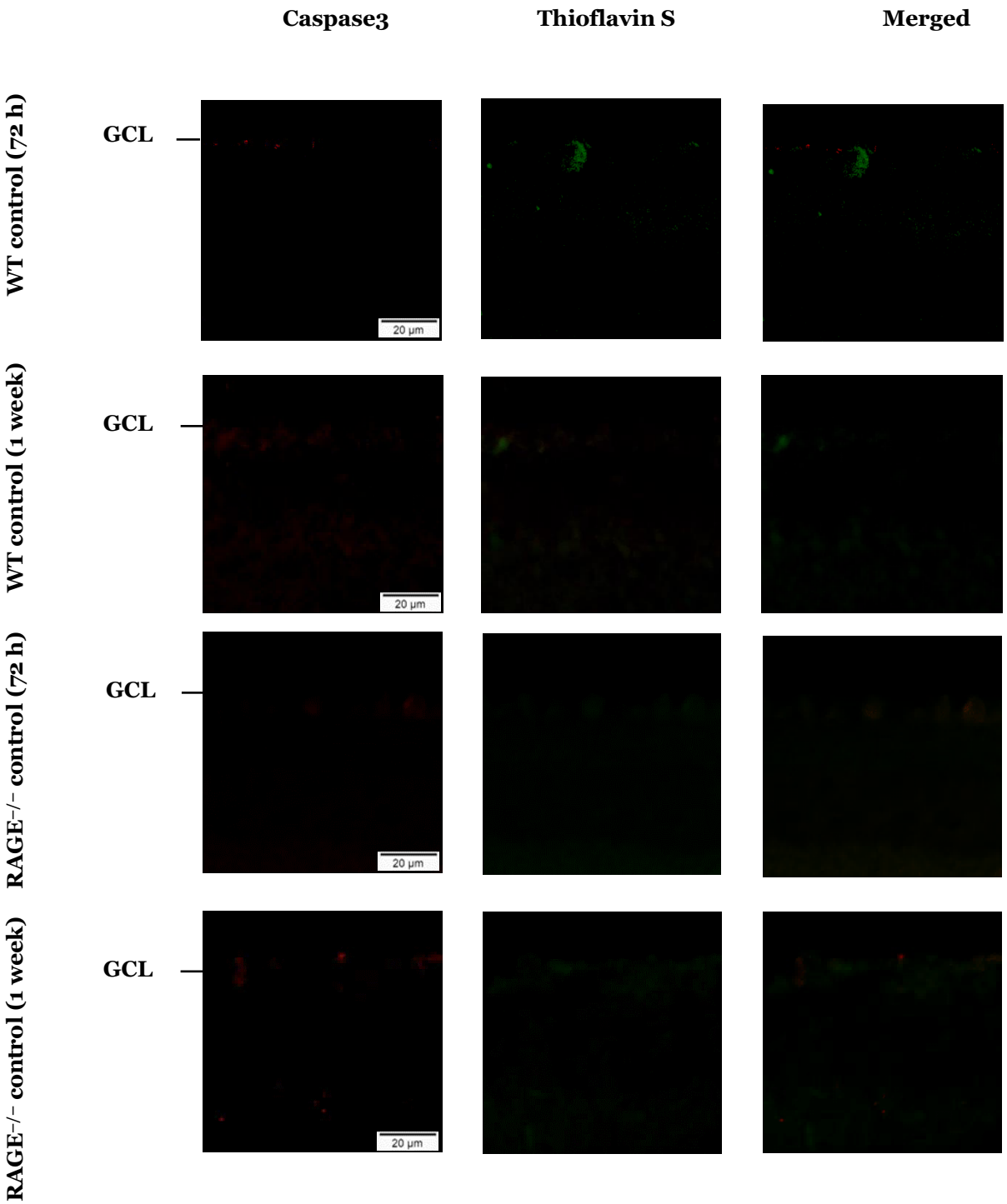

Figure 32. Immunostaining of caspase 3 antibody in control retinas. Immunostaining of WT control and RAGE $^{-/-}$ control retinas was performed along with immunostaining of injected retinas using caspase 3 antibody (red channel). The tissues were then subjected to thioflavin S (green channel) staining for Aβ labelling (n=3).

References

[1] S. Keel *et al.*, "Prevalence of glaucoma in the Australian National Eye Health Survey," *Br. J. Ophthalmol.*, Apr. 2018.

[2] B. R. LaHood, J. Erceg, T. H. Bevin, and G. Sanderson, "High rate of incidental glaucoma detection in New Zealand," *N. Z. Med. J.*, vol. 129, no. 1446, pp. 33–37, Dec. 2016.

[3] E. Y. H. Wong *et al.*, "Detection of undiagnosed glaucoma by eye health professionals.," *Ophthalmology*, vol. 111, no. 8, pp. 1508–1514, Aug. 2004.

[4] J. Qu, D. Wang, and C. L. Grosskreutz, "Mechanisms of Retinal Ganglion Cell Injury and Defense in Glaucoma," *Exp. Eye Res.*, vol. 91, no. 1, pp. 48–53, Jul. 2010.

[5] R. Susanna Jr, C. G. De Moraes, G. A. Cioffi, and R. Ritch, "Why Do People (Still) Go Blind from Glaucoma?," *Transl. Vis. Sci. Technol.*, vol. 4, no. 2, p. 1, Mar. 2015.

[6] L. Guo *et al.*, "Targeting amyloid-β in glaucoma treatment," *Proc. Natl. Acad. Sci.*, vol. 104, no. 33, p. 13444 LP-13449, Aug. 2007.

[7] K. Tsuruma, Y. Tanaka, M. Shimazawa, and H. Hara, "Induction of amyloid precursor protein by the neurotoxic peptide, amyloid-beta 25–35, causes retinal ganglion cell death," *J. Neurochem.*, vol. 113, no. 6, pp. 1545–1554, Jun. 2010.

[8] A. Ning, J. Cui, E. To, K. H. Ashe, and J. Matsubara, "Amyloid-beta deposits lead to retinal degeneration in a mouse model of Alzheimer disease.," *Invest. Ophthalmol. Vis. Sci.*, vol. 49, no. 11, pp. 5136–5143, Nov. 2008.

[9] Kolb H, Fernandez E, Nelson R, *The Organization of the Retina and Visual System*. 1995.

[10] P. Mitchell, W. Smith, K. Attebo, and P. R. Healey, "Prevalence of open-angle glaucoma in Australia. The Blue Mountains Eye Study.," *Ophthalmology*, vol. 103, no. 10, pp. 1661–1669, Oct. 1996.

[11] Y. Shiose, "Intraocular pressure: new perspectives.," *Surv. Ophthalmol.*, vol. 34, no. 6, pp. 413–435, 1990.

[12] A. Heijl, M. C. Leske, B. Bengtsson, L. Hyman, B. Bengtsson, and M. Hussein, "Reduction of intraocular pressure and glaucoma progression: results from the Early Manifest Glaucoma Trial.," *Arch. Ophthalmol. (Chicago, Ill. 1960)*, vol. 120, no. 10, pp. 1268–1279, Oct. 2002.

[13] E. Rom, "Sensory stimulation for lowering intraocular pressure, improving blood flow to the optic nerve and neuroprotection in primary open-angle glaucoma," *Acupunct. Med.*, vol. 31, no. 4, p. 416 LP-- 421, Dec. 2013.

[14] K. Wang *et al.*, "Intraocular pressure-lowering efficacy and safety of bimatoprost 0.03% therapy for primary open-angle glaucoma and ocular hypertension patients in China," *BMC Ophthalmol.*, vol. 14, no. 1, p. 21, 2014.

[15] Ş. Cornel, T. C. Mihaela, I. D. Adriana, B. Mehdi, and D. S. Algerino, "NOVELTIES IN MEDICAL TREATMENT OF GLAUCOMA ," *Rom. J. Ophthalmol.*, vol. 59, no. 2, pp. 78–87, Apr. 2015.

[16] D. R. Anderson, "Collaborative normal tension glaucoma study.," *Curr. Opin. Ophthalmol.*, vol. 14, no. 2, pp. 86–90, Apr. 2003.

[17] "The Advanced Glaucoma Intervention Study (AGIS): 7. The relationship between control of intraocular pressure and visual field deterioration.The AGIS Investigators.," *Am. J. Ophthalmol.*, vol. 130, no. 4, pp. 429–440, Oct. 2000.

[18] A. Sommer *et al.*, "Relationship between intraocular pressure and primary open angle glaucoma among white and black Americans. The Baltimore Eye Survey.," *Arch. Ophthalmol. (Chicago, Ill. 1960)*, vol. 109, no. 8, pp. 1090–1095, Aug. 1991.

[19] T. E. D. P. R. Group, "Prevalence of Open-Angle Glaucoma Among Adults in the United States," *Arch. Ophthalmol.*, vol. 122, no. 4, pp. 532–538, Apr. 2004.

[20] H. A. Quigley and A. T. Broman, "The number of people with glaucoma worldwide in 2010 and 2020," *Br. J. Ophthalmol.*, vol. 90, no. 3, pp. 262–267, Mar. 2006.

[21] C. W. McMonnies, "Glaucoma history and risk factors," *J. Optom.*, vol. 10, no. 2, pp. 71–78, 2017.

[22] Pl. O. N. E. (Drugs with T. A. S. R. Glaucoma Australia (Glaucoma brochure), British Medical Journal (Glaucoma), PLoS ONE (Clinical management outcomes of childhood glaucoma suspects), Scientific Reports (Fluctuation in systolic blood pressure), Lions Eye Institute (Glaucoma), Optometry Aust and Meta-Analysis), "Glaucoma." 2017.

[23] R. C. Tripathi, S. K. Parapuram, B. J. Tripathi, Y. Zhong, and K. V Chalam, "Corticosteroids and glaucoma risk.," *Drugs Aging*, vol. 15, no. 6, pp. 439–450, Dec. 1999.

[24] H. A. Quigley, E. M. Addicks, W. R. Green, and A. E. Maumenee, "Optic nerve damage in human glaucoma. II. The site of injury and susceptibility to damage.," *Arch. Ophthalmol. (Chicago, Ill. 1960)*, vol. 99, no. 4, pp. 635–649, Apr. 1981.

[25] R. N. Weinreb, T. Aung, and F. A. Medeiros, "The Pathophysiology and Treatment of Glaucoma: A Review," *JAMA*, vol. 311, no. 18, pp. 1901–1911, May 2014.

[26] H. A. Quigley *et al.*, "Retrograde axonal transport of BDNF in retinal ganglion cells is blocked by acute IOP elevation in rats.," *Invest. Ophthalmol. Vis. Sci.*, vol. 41, no. 11, pp. 3460–3466, Oct. 2000.

[27] A. J. Tatham, R. N. Weinreb, L. M. Zangwill, J. M. Liebmann, C. A. Girkin, and F. A. Medeiros, "The relationship between cup-to-disc ratio and estimated number of retinal ganglion cells," *Invest. Ophthalmol. Vis. Sci.*, vol. 54, no. 5, pp. 3205–3214, May 2013.

[28] A. London, I. Benhar, and M. Schwartz, "The retina as a window to the brain-from eye research to CNS disorders.," *Nat. Rev. Neurol.*, vol. 9, no. 1, pp. 44–53, Jan. 2013.

[29] H. Yao, T. Wang, J. Deng, D. Liu, X. Li, and J. Deng, "The development of blood-retinal barrier during the interaction of astrocytes with vascular wall cells," *Neural Regen. Res.*, vol. 9, no. 10, pp. 1047–1054, May 2014.

[30] M. Campbell and P. Humphries, "The blood-retina barrier: tight junctions and barrier modulation.," *Adv. Exp. Med. Biol.*, vol. 763, pp. 70–84, 2012.

[31] S. Banerjee and M. A. Bhat, "Neuron-glial interactions in blood-brain barrier formation.," *Annu. Rev. Neurosci.*, vol. 30, pp. 235–258, 2007.

[32] N. Gupta, L.-C. Ang, L. Noel de Tilly, L. Bidaisee, and Y. H. Yucel, "Human glaucoma and neural degeneration in intracranial optic nerve, lateral geniculate nucleus, and visual cortex.," *Br. J. Ophthalmol.*, vol. 90, no. 6, pp. 674–678, Jun. 2006.

[33] N. Gupta, G. Greenberg, L. N. de Tilly, B. Gray, M. Polemidiotis, and Y. H. Yücel, "Atrophy of the lateral geniculate nucleus in human glaucoma detected by magnetic resonance imaging," *Br. J. Ophthalmol.*, vol. 93, no. 1, pp. 56–60, Jan. 2009.

[34] Y. Ou, D. S. Grossman, P. P. Lee, and F. A. Sloan, "Glaucoma, Alzheimer's Disease and Other Dementia: A Longitudinal Analysis," *Ophthalmic Epidemiol.*, vol. 19, no. 5, pp. 285–292, Oct. 2012.

[35] A. U. Bayer, F. Ferrari, and C. Erb, "High occurrence rate of glaucoma among patients with Alzheimer's disease.," *Eur. Neurol.*, vol. 47, no. 3, pp. 165–168, 2002.

[36] C.-W. Su, C.-C. Lin, C.-H. Kao, and H.-Y. Chen, "Association Between Glaucoma and the Risk of Dementia," *Medicine (Baltimore).*, vol. 95, no. 7, p. e2833, Feb. 2016.

[37] C. Criscuolo, C. Fabiani, E. Cerri, and L. Domenici, "Synaptic Dysfunction in Alzheimer's Disease and Glaucoma: From Common Degenerative Mechanisms Toward Neuroprotection," *Front. Cell. Neurosci.*, vol. 11, p. 53, Feb. 2017.

[38] N. Origlia, C. Criscuolo, O. Arancio, S. S. Yan, and L. Domenici, "RAGE Inhibition in Microglia Prevents Ischemia-Dependent Synaptic Dysfunction in an Amyloid-Enriched Environment," *J. Neurosci.*, vol. 34, no. 26, p. 8749 LP-8760, Jun. 2014.

[39] A. A. Sadun and C. J. Bassi, "Optic nerve damage in Alzheimer's disease.," *Ophthalmology*, vol. 97, no. 1, pp. 9–17, Jan. 1990.

[40] E. Abramov, I. Dolev, H. Fogel, G. D. Ciccotosto, E. Ruff, and I. Slutsky, "Amyloid-beta as a positive endogenous regulator of release probability at hippocampal synapses.," *Nat. Neurosci.*, vol. 12, no. 12, pp. 1567–1576, Dec. 2009.

[41] D. Puzzo and O. Arancio, "Amyloid-beta peptide: Dr. Jekyll or Mr. Hyde?," *J. Alzheimers. Dis.*, vol. 33 Suppl 1, pp. S111--20, 2013.

[42] J. E. Morley and S. A. Farr, "The role of amyloid-beta in the regulation of memory.," *Biochem. Pharmacol.*, vol. 88, no. 4, pp. 479–485, Apr. 2014.

[43] S. J. Soscia *et al.*, "The Alzheimer's disease-associated amyloid beta-protein is an antimicrobial peptide.," *PLoS One*, vol. 5, no. 3, p. e9505, Mar. 2010.

[44] Z. Wang, L. Yang, and H. Zheng, "Role of APP and Abeta in synaptic physiology.," *Curr. Alzheimer Res.*, vol. 9, no. 2, pp. 217–226, Feb. 2012.

[45] D. J. Selkoe, "Preventing Alzheimer's disease.," *Science*, vol. 337, no. 6101, pp. 1488–1492, Sep. 2012.

[46] K. Pauwels *et al.*, "Structural basis for increased toxicity of pathological abeta42:abeta40 ratios in Alzheimer disease.," *J. Biol. Chem.*, vol. 287, no. 8, pp. 5650–5660, Feb. 2012.

[47] C. Carvalho, P. S. Katz, S. Dutta, P. V. G. Katakam, P. I. Moreira, and D. W. Busija, "Increased Susceptibility to Amyloid-β Toxicity in Rat Brain Microvascular Endothelial Cells under Hyperglycemic Conditions," *J. Alzheimers. Dis.*, vol. 38, no. 1, pp. 75–83, 2014.

[48] M. Gralle and S. T. Ferreira, "Structure and functions of the human amyloid precursor protein: The whole is more than the sum of its parts," *Prog. Neurobiol.*, vol. 82, no. 1, pp. 11–32, May 2007.

[49] I. Benilova, E. Karran, and B. De Strooper, "The toxic Abeta oligomer and Alzheimer's disease: an emperor in need of clothes.," *Nat. Neurosci.*, vol. 15, no. 3, pp. 349–357, Jan.

2012.

[50] C. Haass and D. J. Selkoe, “Soluble protein oligomers in neurodegeneration: lessons from the Alzheimer’s amyloid beta-peptide.,” *Nat. Rev. Mol. Cell Biol.*, vol. 8, no. 2, pp. 101–112, Feb. 2007.

[51] R. J. O’Brien and P. C. Wong, “Amyloid precursor protein processing and Alzheimer’s disease.,” *Annu. Rev. Neurosci.*, vol. 34, pp. 185–204, 2011.

[52] R. Deane *et al.*, “RAGE mediates amyloid-$β$ peptide transport across the blood-brain barrier and accumulation in brain,” *Nat. Med.*, vol. 9, no. 7, pp. 907–913, Jul. 2003.

[53] □ B, “Caspase activation and amyloid precursor protein cleavage in rat ocular hypertension.,” *Invest. Ophthalmol. Vis. Sci.*, vol. 43, no. 4, pp. 1077–1087, Apr. 2002.

[54] D. Goldblum, A. Kipfer-Kauer, G.-M. Sarra, S. Wolf, and B. E. Frueh, “Distribution of amyloid precursor protein and amyloid-beta immunoreactivity in DBA/2J glaucomatous mouse retinas.,” *Invest. Ophthalmol. Vis. Sci.*, vol. 48, no. 11, pp. 5085–5090, Nov. 2007.

[55] A. Kipfer-Kauer, S. J. McKinnon, B. E. Frueh, and D. Goldblum, “Distribution of Amyloid Precursor Protein and Amyloid-β in Ocular Hypertensive C57BL/6 Mouse Eyes,” *Curr. Eye Res.*, vol. 35, no. 9, pp. 828–834, Sep. 2010.

[56] X.-S. Mi *et al.*, “Protection of Retinal Ganglion Cells and Retinal Vasculature by Lycium Barbarum Polysaccharides in a Mouse Model of Acute Ocular Hypertension,” *PLoS One*, vol. 7, no. 10, p. e45469, Oct. 2012.

[57] K. Sugaya *et al.*, “Three genes in the human MHC class III region near the junction with the class II: gene for receptor of advanced glycosylation end products, PBX2 homeobox gene and a notch homolog, human counterpart of mouse mammary tumor gene int-3.,” *Genomics*, vol. 23, no. 2, pp. 408–419, Sep. 1994.

[58] M. Neeper *et al.*, “Cloning and expression of a cell surface receptor for advanced glycosylation end products of proteins.,” *J. Biol. Chem.*, vol. 267, no. 21, pp. 14998–15004, Jul. 1992.

[59] J. Qin, R. Goswami, S. Dawson, and G. Dawson, “Expression of the Receptor for Advanced Glycation End Products in Oligodendrocytes in Response to Oxidative Stress,” *J. Neurosci. Res.*, vol. 86, no. 11, pp. 2414–2422, Aug. 2008.

[60] S. Mukhopadhyay and T. K. Mukherjee, “Bridging advanced glycation end product, receptor for advanced glycation end product and nitric oxide with hormonal replacement/estrogen therapy in healthy versus diabetic postmenopausal women: a perspective.,” *Biochim. Biophys. Acta*, vol. 1745, no. 2, pp. 145–155, Sep. 2005.

[61] H. J. Huttunen, J. Kuja-Panula, G. Sorci, A. L. Agneletti, R. Donato, and H. Rauvala, “Coregulation of neurite outgrowth and cell survival by amphoterin and S100 proteins through receptor for advanced glycation end products (RAGE) activation.,” *J. Biol. Chem.*, vol. 275, no. 51, pp. 40096–40105, Dec. 2000.

[62] C. Ott, K. Jacobs, E. Haucke, A. Navarrete Santos, T. Grune, and A. Simm, “Role of advanced glycation end products in cellular signaling.,” *Redox Biol.*, vol. 2, pp. 411–429, 2014.

[63] A. Schmidt, B. Kuhla, K. Bigl, G. Munch, and T. Arendt, “Cell cycle related signaling in Neuro2a cells proceeds via the receptor for advanced glycation end products.,” *J. Neural*

Transm., vol. 114, no. 11, pp. 1413–1424, 2007.

[64] M. He *et al.*, "Receptor for advanced glycation end products binds to phosphatidylserine and assists in the clearance of apoptotic cells.," *EMBO Rep.*, vol. 12, no. 4, pp. 358–364, Apr. 2011.

[65] T. Chavakis *et al.*, "The pattern recognition receptor (RAGE) is a counterreceptor for leukocyte integrins: a novel pathway for inflammatory cell recruitment.," *J. Exp. Med.*, vol. 198, no. 10, pp. 1507–1515, Nov. 2003.

[66] G. Fritz, "RAGE: a single receptor fits multiple ligands.," *Trends Biochem. Sci.*, vol. 36, no. 12, pp. 625–632, Dec. 2011.

[67] A. M. Schmidt, S. Du Yan, S. F. Yan, and D. M. Stern, "The multiligand receptor RAGE as a progression factor amplifying immune and inflammatory responses," *J. Clin. Invest.*, vol. 108, no. 7, pp. 949–955, Oct. 2001.

[68] L. Sessa *et al.*, "The receptor for advanced glycation end-products (RAGE) is only present in mammals, and belongs to a family of cell adhesion molecules (CAMs).," *PLoS One*, vol. 9, no. 1, p. e86903, 2014.

[69] I. Gonzalez, J. Romero, B. L. Rodriguez, R. Perez-Castro, and A. Rojas, "The immunobiology of the receptor of advanced glycation end-products: trends and challenges.," *Immunobiology*, vol. 218, no. 5, pp. 790–797, May 2013.

[70] B. I. Hudson *et al.*, "Identification, classification, and expression of RAGE gene splice variants.," *FASEB J.*, vol. 22, no. 5, pp. 1572–1580, May 2008.

[71] J. Li and A. M. Schmidt, "Characterization and functional analysis of the promoter of RAGE, the receptor for advanced glycation end products.," *J. Biol. Chem.*, vol. 272, no. 26, pp. 16498–16506, Jun. 1997.

[72] J. Li, X. Qu, and A. M. Schmidt, "Sp1-binding elements in the promoter of RAGE are essential for amphoterin-mediated gene expression in cultured neuroblastoma cells.," *J. Biol. Chem.*, vol. 273, no. 47, pp. 30870–30878, Nov. 1998.

[73] K. Kierdorf and G. Fritz, "RAGE regulation and signaling in inflammation and beyond.," *J. Leukoc. Biol.*, vol. 94, no. 1, pp. 55–68, Jul. 2013.

[74] L. J. Sparvero *et al.*, "RAGE (Receptor for Advanced Glycation Endproducts), RAGE ligands, and their role in cancer and inflammation.," *J. Transl. Med.*, vol. 7, p. 17, Mar. 2009.

[75] G. R. Barile and A. M. Schmidt, "RAGE and its ligands in retinal disease.," *Curr. Mol. Med.*, vol. 7, no. 8, pp. 758–765, Dec. 2007.

[76] Z. Cai *et al.*, "Role of RAGE in Alzheimer's Disease.," *Cell. Mol. Neurobiol.*, vol. 36, no. 4, pp. 483–495, May 2016.

[77] M. Almasieh, A. M. Wilson, B. Morquette, J. L. Cueva Vargas, and A. Di Polo, "The molecular basis of retinal ganglion cell death in glaucoma.," *Prog. Retin. Eye Res.*, vol. 31, no. 2, pp. 152–181, Mar. 2012.

[78] S. Du Yan *et al.*, "RAGE and amyloid-β peptide neurotoxicity in Alzheimer's disease," *Nature*, vol. 382, no. 6593, pp. 685–691, Aug. 1996.

[79] R. Deane, R. D. Bell, A. Sagare, and B. V Zlokovic, "Clearance of amyloid-β peptide across

the blood-brain barrier: Implication for therapies in Alzheimer's disease," *CNS Neurol. Disord. Drug Targets*, vol. 8, no. 1, pp. 16–30, Mar. 2009.

[80] A. Mohamed and E. Posse de Chaves, "Aβ internalization by neurons and glia," *Int. J. Alzheimers. Dis.*, vol. 2011, p. 127984, Feb. 2011.

[81] S.-Y. Kook, H. Seok Hong, M. Moon, and I. Mook-Jung, "Disruption of blood-brain barrier in Alzheimer disease pathogenesis.," *Tissue barriers*, vol. 1, no. 2, p. e23993, Apr. 2013.

[82] I. G. Onyango, J. B. Tuttle, and J. P. Bennett Jr., "Altered intracellular signaling and reduced viability of Alzheimer's disease neuronal cybrids is reproduced by $β$-amyloid peptide acting through receptor for advanced glycation end products (RAGE)," *Mol. Cell. Neurosci.*, vol. 29, no. 2, pp. 333–343, Jun. 2005.

[83] F. Fang *et al.*, "RAGE mediates Abeta accumulation in a mouse model of Alzheimer's disease via modulation of beta- and gamma-secretase activity.," *Hum. Mol. Genet.*, vol. 27, no. 6, pp. 1002–1014, Mar. 2018.

[84] K. Takuma *et al.*, "RAGE-mediated signaling contributes to intraneuronal transport of amyloid-beta and neuronal dysfunction.," *Proc. Natl. Acad. Sci. U. S. A.*, vol. 106, no. 47, pp. 20021–20026, Nov. 2009.

[85] M. Nita and A. Grzybowski, "The Role of the Reactive Oxygen Species and Oxidative Stress in the Pathomechanism of the Age-Related Ocular Diseases and Other Pathologies of the Anterior and Posterior Eye Segments in Adults.," *Oxid. Med. Cell. Longev.*, vol. 2016, p. 3164734, 2016.

[86] S. Du Yan *et al.*, "Non-enzymatically glycated tau in Alzheimer's disease induces neuronal oxidant stress resulting in cytokine gene expression and release of amyloid $β$-peptide," *Nat. Med.*, vol. 1, no. 7, pp. 693–699, Jul. 1995.

[87] K. Hensley *et al.*, "A model for beta-amyloid aggregation and neurotoxicity based on free radical generation by the peptide: relevance to Alzheimer disease.," *Proc. Natl. Acad. Sci. U. S. A.*, vol. 91, no. 8, pp. 3270–3274, Apr. 1994.

[88] M.-P. Wautier, O. Chappey, S. Corda, D. M. Stern, A. M. Schmidt, and J.-L. Wautier, "Activation of NADPH oxidase by AGE links oxidant stress to altered gene expression via RAGE," *Am. J. Physiol. Metab.*, vol. 280, no. 5, pp. E685--E694, May 2001.

[89] S. Askarova, X. Yang, W. Sheng, G. Y. Sun, and J. C.-M. Lee, "Role of Aβ-receptor for advanced glycation endproducts interaction in oxidative stress and cytosolic phospholipase A2 activation in astrocytes and cerebral endothelial cells.," *Neuroscience*, vol. 199, pp. 375–85, Dec. 2011.

[90] F. Fang *et al.*, "RAGE-dependent signaling in microglia contributes to neuroinflammation, A accumulation, and impaired learning/memory in a mouse model of Alzheimer's disease," *FASEB J.*, vol. 24, no. 4, pp. 1043–1055, Apr. 2010.

[91] C. Bonaiuto, P. P. McDonald, F. Rossi, and M. A. Cassatella, "Activation of nuclear factor-kappa B by beta-amyloid peptides and interferon-gamma in murine microglia.," *J. Neuroimmunol.*, vol. 77, no. 1, pp. 51–56, Jul. 1997.

[92] J. C. Tobon-Velasco, E. Cuevas, and M. A. Torres-Ramos, "Receptor for AGEs (RAGE) as Mediator of NF-kB Pathway Activation in Neuroinflammation and Oxidative Stress."

[93] R. Deane *et al.*, "A multimodal RAGE-specific inhibitor reduces amyloid beta-mediated

brain disorder in a mouse model of Alzheimer disease.," *J. Clin. Invest.*, vol. 122, no. 4, pp. 1377–1392, Apr. 2012.

[94] E. Emanuele *et al.*, "Circulating Levels of Soluble Receptor for Advanced Glycation End Products in Alzheimer Disease and Vascular Dementia," *Arch. Neurol.*, vol. 62, no. 11, p. 1734, Nov. 2005.

[95] X.-Y. Xu *et al.*, "Plasma levels of soluble receptor for advanced glycation end products in Alzheimer's disease," *Int. J. Neurosci.*, vol. 127, no. 5, pp. 454–458, May 2017.

[96] G. Tezel, C. Luo, and X. Yang, "Accelerated Aging in Glaucoma: Immunohistochemical Assessment of Advanced Glycation End Products in the Human Retina and Optic Nerve Head," *Investig. Opthalmology Vis. Sci.*, vol. 48, no. 3, p. 1201, Mar. 2007.

[97] Y. Kaji *et al.*, "Inhibition of Diabetic Leukostasis and Blood-Retinal Barrier Breakdown with a Soluble Form of a Receptor for Advanced Glycation End Products," *Investig. Opthalmology Vis. Sci.*, vol. 48, no. 2, p. 858, Feb. 2007.

[98] K. A. Howes *et al.*, "Receptor for Advanced Glycation End Products and Age-Related Macular Degeneration," *Investig. Opthalmology Vis. Sci.*, vol. 45, no. 10, p. 3713, Oct. 2004.

[99] M. Banevicius, A. Vilkeviciute, L. Kriauciuniene, R. Liutkeviciene, and V. P. Deltuva, "The Association Between Variants of Receptor for Advanced Glycation End Products (RAGE) Gene Polymorphisms and Age-Related Macular Degeneration," *Med. Sci. Monit.*, vol. 24, pp. 190–199, Jan. 2018.

[100] J. A. Ratnayaka, L. C. Serpell, and A. J. Lotery, "Dementia of the eye: the role of amyloid beta in retinal degeneration," *Eye*, vol. 29, no. 8, pp. 1013–1026, Aug. 2015.

[101] K. Ohno-Matsui, "Parallel findings in age-related macular degeneration and Alzheimer's disease.," *Prog. Retin. Eye Res.*, vol. 30, no. 4, pp. 217–238, Jul. 2011.

[102] J. Wang, K. Ohno-Matsui, and I. Morita, "Elevated amyloid beta production in senescent retinal pigment epithelium, a possible mechanism of subretinal deposition of amyloid beta in age-related macular degeneration.," *Biochem. Biophys. Res. Commun.*, vol. 423, no. 1, pp. 73–78, Jun. 2012.

[103] R. T. Liu *et al.*, "Inflammatory mediators induced by amyloid-beta in the retina and RPE in vivo: implications for inflammasome activation in age-related macular degeneration.," *Invest. Ophthalmol. Vis. Sci.*, vol. 54, no. 3, pp. 2225–2237, Mar. 2013.

[104] K. H. Kurji *et al.*, "Microarray analysis identifies changes in inflammatory gene expression in response to amyloid-beta stimulation of cultured human retinal pigment epithelial cells.," *Invest. Ophthalmol. Vis. Sci.*, vol. 51, no. 2, pp. 1151–1163, Feb. 2010.

[105] M. P. Lambert *et al.*, "Diffusible, nonfibrillar ligands derived from Abeta1-42 are potent central nervous system neurotoxins.," *Proc. Natl. Acad. Sci. U. S. A.*, vol. 95, no. 11, pp. 6448–6453, May 1998.

[106] J. M. Mc Donald *et al.*, "The presence of sodium dodecyl sulphate-stable Abeta dimers is strongly associated with Alzheimer-type dementia.," *Brain*, vol. 133, no. Pt 5, pp. 1328–1341, May 2010.

[107] C. A. McLean *et al.*, "Soluble pool of Abeta amyloid as a determinant of severity of neurodegeneration in Alzheimer's disease.," *Ann. Neurol.*, vol. 46, no. 6, pp. 860–866, Dec.

1999.

[108] D. H. Anderson, K. C. Talaga, A. J. Rivest, E. Barron, G. S. Hageman, and L. V Johnson, "Characterization of beta amyloid assemblies in drusen: the deposits associated with aging and age-related macular degeneration.," *Exp. Eye Res.*, vol. 78, no. 2, pp. 243–256, Feb. 2004.

[109] Y. Yamada *et al.*, "The expression of advanced glycation endproduct receptors in rpe cells associated with basal deposits in human maculas," *Exp. Eye Res.*, vol. 82, no. 5, pp. 840–848, May 2006.

[110] S. W. Park *et al.*, "RAGE mediated intracellular Aβ uptake contributes to the breakdown of tight junction in retinal pigment epithelium," *Oncotarget*, vol. 6, no. 34, pp. 35263–35273, Nov. 2015.

[111] W. Zhang, H. Liu, M. Al-Shabrawey, R. W. Caldwell, and R. B. Caldwell, "Inflammation and diabetic retinal microvascular complications," *J. Cardiovasc. Dis. Res.*, vol. 2, no. 2, pp. 96–103, 2011.

[112] A. T. Tsegay, "Review on Early Neurodegenerative Changes in Diabetic Retinopathy," *Neuro Ophthalmol. Vis. Neurosci.*, vol. 1, no. 1, pp. 13–17, Dec. 2014.

[113] G. Tezel and M. B. Wax, "Increased production of tumor necrosis factor-alpha by glial cells exposed to simulated ischemia or elevated hydrostatic pressure induces apoptosis in cocultured retinal ganglion cells.," *J. Neurosci.*, vol. 20, no. 23, pp. 8693–8700, Dec. 2000.

[114] G. Tezel and M. B. Wax, "Glial modulation of retinal ganglion cell death in glaucoma.," *J. Glaucoma*, vol. 12, no. 1, pp. 63–68, Feb. 2003.

[115] G. Tezel, L. Y. Li, R. V Patil, and M. B. Wax, "TNF-alpha and TNF-alpha receptor-1 in the retina of normal and glaucomatous eyes.," *Invest. Ophthalmol. Vis. Sci.*, vol. 42, no. 8, pp. 1787–1794, Jul. 2001.

[116] A. H. Neufeld, M. R. Hernandez, and M. Gonzalez, "Nitric oxide synthase in the human glaucomatous optic nerve head.," *Arch. Ophthalmol. (Chicago, Ill. 1960)*, vol. 115, no. 4, pp. 497–503, Apr. 1997.

[117] J. Yang, P. Yang, G. Tezel, R. V Patil, M. R. Hernandez, and M. B. Wax, "Induction of HLA-DR Expression in Human Lamina Cribrosa Astrocytes by Cytokines and Simulated Ischemia," *Invest. Ophthalmol. Vis. Sci.*, vol. 42, no. 2, pp. 365–371, Feb. 2001.

[118] G. R. Howell *et al.*, "Axons of retinal ganglion cells are insulted in the optic nerve early in DBA/2J glaucoma," *J. Cell Biol.*, vol. 179, no. 7, pp. 1523–1537, Dec. 2007.

[119] A. Ebneter, R. J. Casson, J. P. M. Wood, and G. Chidlow, "Microglial activation in the visual pathway in experimental glaucoma: spatiotemporal characterization and correlation with axonal injury.," *Invest. Ophthalmol. Vis. Sci.*, vol. 51, no. 12, pp. 6448–6460, Dec. 2010.

[120] C. E. Mac Nair, C. L. Schlamp, A. D. Montgomery, V. I. Shestopalov, and R. W. Nickells, "Retinal glial responses to optic nerve crush are attenuated in Bax-deficient mice and modulated by purinergic signaling pathways," *J. Neuroinflammation*, vol. 13, no. 1, p. 93, 2016.

[121] A. I. Ramirez *et al.*, "The Role of Microglia in Retinal Neurodegeneration: Alzheimer's Disease, Parkinson, and Glaucoma," *Front. Aging Neurosci.*, vol. 9, p. 214, Jul. 2017.

[122] G. Tezel, "TNF-alpha signaling in glaucomatous neurodegeneration.," *Prog. Brain Res.*,

vol. 173, pp. 409–421, 2008.

[123] G. Dvoriantchikova, E. Hernandez, J. Grant, A. R. C. Santos, H. Yang, and D. Ivanov, "The High-Mobility Group Box-1 Nuclear Factor Mediates Retinal Injury after Ischemia Reperfusion," *Investig. Opthalmology Vis. Sci.*, vol. 52, no. 10, p. 7187, Sep. 2011.

[124] A. Goldin, J. A. Beckman, A. M. Schmidt, and M. A. Creager, "Advanced glycation end products: sparking the development of diabetic vascular injury.," *Circulation*, vol. 114, no. 6, pp. 597–605, Aug. 2006.

[125] M. F. Cordeiro *et al.*, "Real-time imaging of single nerve cell apoptosis in retinal neurodegeneration.," *Proc. Natl. Acad. Sci. U. S. A.*, vol. 101, no. 36, pp. 13352–13356, Sep. 2004.

[126] L. Guo, S. E. Moss, R. A. Alexander, R. R. Ali, F. W. Fitzke, and M. F. Cordeiro, "Retinal ganglion cell apoptosis in glaucoma is related to intraocular pressure and IOP-induced effects on extracellular matrix.," *Invest. Ophthalmol. Vis. Sci.*, vol. 46, no. 1, pp. 175–182, Jan. 2005.

[127] R. D. Fechtner and R. N. Weinreb, "Mechanisms of optic nerve damage in primary open angle glaucoma.," *Surv. Ophthalmol.*, vol. 39, no. 1, pp. 23–42, 1994.

[128] A. C. Gauthier and J. Liu, "Epigenetics and Signaling Pathways in Glaucoma.," *Biomed Res. Int.*, vol. 2017, p. 5712341, 2017.

[129] C. M. McDowell, H. E. Tebow, R. J. Wordinger, and A. F. Clark, "Smad3 is necessary for transforming growth factor-beta2 induced ocular hypertension in mice," *Exp. Eye Res.*, vol. 116, pp. 419–423, Nov. 2013.

[130] C. L. Pervan, "Smad-independent TGF-beta2 signaling pathways in human trabecular meshwork cells.," *Exp. Eye Res.*, vol. 158, pp. 137–145, May 2017.

[131] D. Jia *et al.*, "RAGE-mediated extracellular matrix proteins accumulation exacerbates HySu-induced pulmonary hypertension.," *Cardiovasc. Res.*, vol. 113, no. 6, pp. 586–597, May 2017.

[132] C. Casola *et al.*, "S100 alone has the same destructive effect on retinal ganglion cells as in combination with HSP 27 in an autoimmune glaucoma model.," *J. Mol. Neurosci.*, vol. 56, no. 1, pp. 228–236, May 2015.

[133] H. B. Rajamohamedsait and E. M. Sigurdsson, "Histological Staining of Amyloid and Pre-Amyloid Peptides and Proteins in Mouse Tissue," *Methods Mol. Biol.*, vol. 849, p. 10.1007/978--1--61779--551--0_28, 2012.

[134] M. Fa, I. J. Orozco, Y. I. Francis, F. Saeed, Y. Gong, and O. Arancio, "Preparation of Oligomeric β-amyloid(1-42) and Induction of Synaptic Plasticity Impairment on Hippocampal Slices," *J. Vis. Exp.*, no. 41, p. 1884, Jul. 2010.

[135] S. M. Saszik, J. G. Robson, and L. J. Frishman, "The scotopic threshold response of the dark-adapted electroretinogram of the mouse," *J. Physiol.*, vol. 543, no. Pt 3, pp. 899–916, Sep. 2002.

[136] D. H. Stephen J Ryan, *Retina.* .

[137] J. G. Fujimoto, "Optical coherence tomography for ultrahigh resolution in vivo imaging," *Nat. Biotechnol.*, vol. 21, p. 1361, Oct. 2003.

[138] M. D. Fischer *et al.*, "Noninvasive, In Vivo Assessment of Mouse Retinal Structure Using Optical Coherence Tomography," *PLoS One*, vol. 4, no. 10, p. e7507, Oct. 2009.

[139] J. Juranek, R. Ray, M. Banach, and V. Rai, "Receptor for advanced glycation end-products in neurodegenerative diseases.," *Rev. Neurosci.*, vol. 26, no. 6, pp. 691–698, 2015.

[140] L. F. Lue *et al.*, "Involvement of microglial receptor for advanced glycation endproducts (RAGE) in Alzheimer's disease: identification of a cellular activation mechanism.," *Exp. Neurol.*, vol. 171, no. 1, pp. 29–45, Sep. 2001.

[141] S. D. Yan *et al.*, "Non-enzymatically glycated tau in Alzheimer's disease induces neuronal oxidant stress resulting in cytokine gene expression and release of amyloid beta-peptide.," *Nat. Med.*, vol. 1, no. 7, pp. 693–699, Jul. 1995.

[142] R. Ray, J. K. Juranek, and V. Rai, "RAGE axis in neuroinflammation, neurodegeneration and its emerging role in the pathogenesis of amyotrophic lateral sclerosis.," *Neurosci. Biobehav. Rev.*, vol. 62, pp. 48–55, Mar. 2016.

[143] M. Son *et al.*, "Protection against RAGE-mediated neuronal cell death by sRAGE-secreting human mesenchymal stem cells in 5xFAD transgenic mouse model.," *Brain. Behav. Immun.*, vol. 66, pp. 347–358, Nov. 2017.

[144] N. Takahashi *et al.*, "Necrostatin-1 analogues: critical issues on the specificity, activity and in vivo use in experimental disease models.," *Cell Death Dis.*, vol. 3, p. e437, Nov. 2012.

[145] G. Dvoriantchikova, A. Degterev, and D. Ivanov, "Retinal ganglion cell (RGC) programmed necrosis contributes to ischemia-reperfusion-induced retinal damage.," *Exp. Eye Res.*, vol. 123, pp. 1–7, Jun. 2014.

[146] S. Gao, K. Andreeva, and N. G. F. Cooper, "Ischemia-reperfusion injury of the retina is linked to necroptosis via the ERK1/2-RIP3 pathway.," *Mol. Vis.*, vol. 20, pp. 1374–1387, 2014.

[147] M. Adachi, K. Takahashi, M. Nishikawa, H. Miki, and M. Uyama, "High intraocular pressure-induced ischemia and reperfusion injury in the optic nerve and retina in rats.," *Graefes Arch. Clin. Exp. Ophthalmol.*, vol. 234, no. 7, pp. 445–451, Jul. 1996.

[148] B. Fortune *et al.*, "Selective Ganglion Cell Functional Loss in Rats with Experimental Glaucoma," *Invest. Ophthalmol. Vis. Sci.*, vol. 45, no. 6, pp. 1854–1862, Jun. 2004.

[149] S. Arai-Gaun, N. Katai, T. Kikuchi, T. Kurokawa, K. Ohta, and N. Yoshimura, "Heme oxygenase-1 induced in muller cells plays a protective role in retinal ischemia-reperfusion injury in rats.," *Invest. Ophthalmol. Vis. Sci.*, vol. 45, no. 11, pp. 4226–4232, Nov. 2004.

[150] A. Al-Mujaini, U. K. Wali, and S. Azeem, "Optical Coherence Tomography: Clinical Applications in Medical Practice," *Oman Med. J.*, vol. 28, no. 2, pp. 86–91, Mar. 2013.

[151] I. Soto, M. E. Pease, J. L. Son, X. Shi, H. A. Quigley, and N. Marsh-Armstrong, "Retinal Ganglion Cell Loss in a Rat Ocular Hypertension Model Is Sectorial and Involves Early Optic Nerve Axon Loss," *Invest. Ophthalmol. Vis. Sci.*, vol. 52, no. 1, pp. 434–441, Jan. 2011.

[152] B. Mead and S. Tomarev, "Evaluating retinal ganglion cell loss and dysfunction.," *Exp. Eye Res.*, vol. 151, pp. 96–106, Oct. 2016.

[153] B. J. Smith, X. Wang, B. C. Chauhan, P. D. Cote, and F. Tremblay, "Contribution of retinal ganglion cells to the mouse electroretinogram.," *Doc. Ophthalmol.*, vol. 128, no. 3, pp. 155–

168, Jun. 2014.

[154] M. J. Pérez de Lara *et al.*, "Assessment of inner retina dysfunction and progressive ganglion cell loss in a mouse model of glaucoma," *Exp. Eye Res.*, vol. 122, pp. 40–49, 2014.

[155] V. Porciatti, "Electrophysiological assessment of retinal ganglion cell function," *Exp. Eye Res.*, vol. 141, pp. 164–170, 2015.

[156] G. Tezel, "Applying proteomics to research for optic nerve regeneration in glaucoma: what's on the horizon?," *Expert Rev. Proteomics*, pp. 1–3, Sep. 2016.

[157] B. Mead *et al.*, "Mesenchymal stromal cell-mediated neuroprotection and functional preservation of retinal ganglion cells in a rodent model of glaucoma.," *Cytotherapy*, vol. 18, no. 4, pp. 487–496, Apr. 2016.

[158] Q. Zhang *et al.*, "Melanopsin-expressing retinal ganglion cell loss and behavioral analysis in the Thy1-CFP-DBA/2J mouse model of glaucoma.," *Sci. China. Life Sci.*, vol. 56, no. 8, pp. 720–730, Aug. 2013.

[159] Z. Puyang, H.-Q. Gong, S.-G. He, J. B. Troy, X. Liu, and P.-J. Liang, "Different functional susceptibilities of mouse retinal ganglion cell subtypes to optic nerve crush injury.," *Exp. Eye Res.*, vol. 162, pp. 97–103, Sep. 2017.

[160] M. C. Crair and C. A. Mason, "Reconnecting Eye to Brain," *J. Neurosci.*, vol. 36, no. 42, pp. 10707–10722, Oct. 2016.

[161] O. S. Dhande and A. D. Huberman, "Retinal ganglion cell maps in the brain: implications for visual processing.," *Curr. Opin. Neurobiol.*, vol. 24, no. 1, pp. 133–142, Feb. 2014.

[162] T. Baden, P. Berens, K. Franke, M. Roman Roson, M. Bethge, and T. Euler, "The functional diversity of retinal ganglion cells in the mouse.," *Nature*, vol. 529, no. 7586, pp. 345–350, Jan. 2016.

[163] X. Duan, M. Qiao, F. Bei, I.-J. Kim, Z. He, and J. R. Sanes, "Subtype-specific regeneration of retinal ganglion cells following axotomy: effects of osteopontin and mTOR signaling.," *Neuron*, vol. 85, no. 6, pp. 1244–1256, Mar. 2015.

[164] H. Levkovitch-Verbin, "Chapter 2 - Retinal ganglion cell apoptotic pathway in glaucoma: Initiating and downstream mechanisms," in *New Trends in Basic and Clinical Research of Glaucoma: A Neurodegenerative Disease of the Visual System, Part A*, vol. 220, G. Bagetta and C. B. T.-P. in B. R. Nucci, Eds. Elsevier, 2015, pp. 37–57.

[165] S. W. Park *et al.*, "RAGE mediated intracellular A$β$ uptake contributes to the breakdown of tight junction in retinal pigment epithelium," *Oncotarget*, vol. 6, no. 34, pp. 35263–35273, Nov. 2015.

[166] J. Wang, C. Zhu, Y. Xu, B. Liu, M. Wang, and K. Wu, "Development and expression of amyloid-beta peptide 42 in retinal ganglion cells in rats.," *Anat. Rec. (Hoboken).*, vol. 294, no. 8, pp. 1401–1405, Aug. 2011.

[167] P. J. Morin *et al.*, "Amyloid precursor protein is synthesized by retinal ganglion cells, rapidly transported to the optic nerve plasma membrane and nerve terminals, and metabolized.," *J. Neurochem.*, vol. 61, no. 2, pp. 464–473, Aug. 1993.

[168] K. U. Loffler, D. P. Edward, and M. O. Tso, "Immunoreactivity against tau, amyloid precursor protein, and beta-amyloid in the human retina.," *Invest. Ophthalmol. Vis. Sci.*, vol. 36, no. 1, pp. 24–31, Jan. 1995.

[169] Y. Ito *et al.*, "Induction of amyloid-β(1-42) in the retina and optic nerve head of chronic ocular hypertensive monkeys," *Mol. Vis.*, vol. 18, p. 2647–xxx, Oct. 2012.

[170] V. Dinet *et al.*, "APP involvement in retinogenesis of mice.," *Acta Neuropathol.*, vol. 121, no. 3, pp. 351–363, Mar. 2011.

[171] L. V Johnson, W. P. Leitner, A. J. Rivest, M. K. Staples, M. J. Radeke, and D. H. Anderson, "The Alzheimer's A$β$-peptide is deposited at sites of complement activation in pathologic deposits associated with aging and age-related macular degeneration," *Proc. Natl. Acad. Sci. U. S. A.*, vol. 99, no. 18, pp. 11830–11835, Sep. 2002.

[172] T. Yoshida *et al.*, "The potential role of amyloid β in the pathogenesis of age-related macular degeneration," *J. Clin. Invest.*, vol. 115, no. 10, pp. 2793–2800, Oct. 2005.

[173] A. Prakasam *et al.*, "Differential Accumulation of Secreted APP Metabolites in Ocular Fluids," *J. Alzheimer's Dis.*, vol. 20, no. 4, pp. 1243–1253, 2010.

[174] S. K. Singh, S. Srivastav, A. K. Yadav, S. Srikrishna, and G. Perry, "Overview of Alzheimer's Disease and Some Therapeutic Approaches Targeting A$β$ by Using Several Synthetic and Herbal Compounds," *Oxid. Med. Cell. Longev.*, vol. 2016, p. 7361613, Dec. 2016.

[175] S. Jin *et al.*, "Amyloid-β(1–42) Aggregation Initiates Its Cellular Uptake and Cytotoxicity ," *J. Biol. Chem.*, vol. 291, no. 37, pp. 19590–19606, Sep. 2016.

[176] S. Du Yan *et al.*, "RAGE and amyloid-$β$ peptide neurotoxicity in Alzheimer's disease," *Nature*, vol. 382, no. 6593, pp. 685–691, Aug. 1996.

[177] E. Lana *et al.*, "Perforin Promotes Amyloid Beta Internalisation in Neurons.," *Mol. Neurobiol.*, vol. 54, no. 2, pp. 874–887, Mar. 2017.

[178] G. Kheiri, M. Dolatshahi, F. Rahmani, and N. Rezaei, "Role of p38/MAPKs in Alzheimer's disease: implications for amyloid beta toxicity targeted therapy.," *Rev. Neurosci.*, May 2018.

[179] J. Ji *et al.*, "Effects of elevated intraocular pressure on mouse retinal ganglion cells.," *Vision Res.*, vol. 45, no. 2, pp. 169–179, Jan. 2005.

[180] S. J. McKinnon; D. M. Lehman; L.A. Kerrigan-Baumrind; C. A. Merges; M. E. Pease; D. F. Kerrigan; N. L. Ransom; N. G. Tahzib; H. A. Reitsamer; H. Levkovitch-Verbin; H. A. Quigley; D. J. Zack J. Zack, "Caspase Activation and Amyloid Precursor Protein Cleavage in Rat Ocular Hypertension," *Invest. Ophthalmol. Vis. Sci.*, vol. 43, no. 4, pp. 1077–1087, Apr. 2002.

[181] H. S. Kim and C. K. Park, "Retinal ganglion cell death is delayed by activation of retinal intrinsic cell survival program.," *Brain Res.*, vol. 1057, no. 1–2, pp. 17–28, Sep. 2005.

[182] S. Yoneda, H. Hara, A. Hirata, M. Fukushima, Y. Inomata, and H. Tanihara, "Vitreous fluid levels of beta-amyloid((1-42)) and tau in patients with retinal diseases.," *Jpn. J. Ophthalmol.*, vol. 49, no. 2, pp. 106–108, 2005.

[183] L. Hetherington, M. Benn, P. J. Coffey, and R. D. Lund, "Sensory capacity of the royal college of surgeons rat.," *Invest. Ophthalmol. Vis. Sci.*, vol. 41, no. 12, pp. 3979–3983, Nov. 2000.

[184] P. J. Coffey *et al.*, "Long-term preservation of cortically dependent visual function in RCS rats by transplantation.," *Nat. Neurosci.*, vol. 5, no. 1, pp. 53–56, Jan. 2002.

[185] C. Schmucker, M. Seeliger, P. Humphries, M. Biel, and F. Schaeffel, “Grating acuity at different luminances in wild-type mice and in mice lacking rod or cone function.,” *Invest. Ophthalmol. Vis. Sci.*, vol. 46, no. 1, pp. 398–407, Jan. 2005.

[186] Q. Wang, D. M. Walsh, M. J. Rowan, D. J. Selkoe, and R. Anwyl, “Block of long-term potentiation by naturally secreted and synthetic amyloid beta-peptide in hippocampal slices is mediated via activation of the kinases c-Jun N-terminal kinase, cyclin-dependent kinase 5, and p38 mitogen-activated protein kinase as well a,” *J. Neurosci.*, vol. 24, no. 13, pp. 3370–3378, Mar. 2004.